Bax interacts with VDAC-ANT mitchondrial intermembrane contact sites during apoptosis: implications for a mechanism of outer mitochondrial membrane permeabilisation.

A thesis submitted for the degree of

Doctor of Philosophy

by

Helen Emma Barksby

Department of Biochemistry and Molecular Biology

University College London

ProQuest LLC
789 East Eisenhower Parkway
P.O. Box 1346
Ann Arbor, MI 48106-1346

Acknowledgements

After writing this thesis I have suddenly realised how many people I need to thank. The PhD experience has been a long and difficult journey. These are the people that have kept me sane and focussed.

Firstly I am indebted to my supervisor Prof. Martin Crompton for his guidance throughout the course of the research and in writing this thesis. Thanks to Michaela Capano for her technical advice about transfections and fluorescence microscopy and Dr. John Ward for the plasmids containing Bax and Bcl-X_L.

I would like to thank my friends and colleagues in the lab for their company and making the PhD more enjoyable-Michaela, Audrey, Yanmin, Nick and Veronica. I especially want to thank Ayesha, Hilary and Suki for being there through the good and the bad.

Thanks to Nikki and Everton for their friendship and providing me with a fun and happy home for 3 years.

Since moving to Newcastle many friends have supported me through the task of writing my thesis, thanks Rachel, Tanya, Maria, Jon and Jenny. I am especially grateful to Penny for reading my thesis, for her positive attitude and for helping me reach the end!

Finally I would like to thank mum, dad and Daniel for their unfailing support through my many years of education.

For Anne and Daniel

Abstract

The Bcl-2 family of proteins regulates the mitochondrial apoptotic pathway and consists of both pro- and anti-apoptotic members. Bax-α is present in the cytosol of healthy cells. Apoptotic stimuli induce the translocation of Bax-α to the mitochondria leading to the permeabilisation of the outer mitochondrial membrane (OMM) and the release of downstream pro-apoptotic proteins from the intermembrane space (IMS). The mechanism by which Bax permeabilises the OMM remains unclear. Recent evidence suggests Bax alone might be sufficient to permeabilise the OMM. However, other models indicate the involvement of the mitochondrial permeability transition pore complex or the voltage-dependent anion channel (VDAC) present in the OMM. In this study Bax and C-terminally truncated Bax were expressed as GST-fusion proteins and were immobilised on agarose-GSH. The binding of mitochondrial membrane proteins that might be involved in the Bax mediated release of proteins from the IMS was investigated. The results showed that VDAC and the adenine nucleotide translocase (ANT) were retained by GST-Bax. Exogenous cyclophilin D (Cyp D) was added in the presence of VDAC and ANT and was also retained indicating that Bax interacts with the components of the permeability transition pore complex. The anti-apoptotic Bcl-2 protein Bcl-X_L was expressed with a hexahistidine tag at its N-terminus. This was used to investigate its effects on Bax interaction with VDAC and ANT. The ANT ligands atractyloside and bongkrekic acid which promote and inhibit apoptosis respectively were shown to change the relative amounts of VDAC and ANT that bind GST-Bax. Apoptotic cell death has been identified in cardiomyocytes subjected to ischaemia. In this investigation cardiomyocytes transfected with GFP-Bax were treated with cyanide to simulate ischaemia and GFP-Bax translocation was observed using fluorescence microscopy. GFP-Bax co-immunoprecipitated with VDAC and ANT after translocation to mitochondria but not with Cyp D. The implications of these findings are discussed in this thesis.

Table of Contents

Chapter 2: Materials and Methods

Chapter 3: Expression of Bax, C-terminally truncated Bax and Bcl-X_L as Fusion Proteins in *E.coli*

Chapter 4: Interactions of Bax and BaxΔc with a junctional mitochondrial membrane complex

Chapter 7: Discussion

Figures

Tables

Abbreviations

AIF	apoptosis inducing factor
ANT	adenine nucleotide translocase
Apaf-1	apoptosis activating protease activating factor-1
BA	bongkrekic acid
BCA	bicinchoninic acid
BH	bcl-2 homology
BSA	bovine serum albumin
CAD	caspase activated DNase
CARD	caspase activation and recruitment domain
Caspases	cysteine-dependent-aspartate-directed proteases
CHAPS	3-[(3-cholamidopropyl)dimethylammonio}-1-1propane-sulfonate
CSA	cyclosporin A
Cyp D	cyclophilin D
DAPPAC	diaminopentanepentamminecobalt
DED	death effector domain
DISC	death inducing signalling complex
DMSO	dimethylsulfoxide
DTT	DL-dithiothreitol
E. coli	*Escherichia coli*
EDTA	ethylene diamine-N,N,N'-tetraacetic acid
EGTA	ethylene glycol-O,-O'-bis(2-amino-ethyl)-N,N,N',N'-tetraacetic acid
Endo G	endonuclease G
ER	endoplasmic reticulum
FADD	Fas-associated death domain
F.S.D	full scale deflection
GFP	green fluorescent protein
GSH	glutathione (reduced)
GST	glutathione-s-transferase
HEPES	4-(2-hydroxyethyl)-1-piperazinepropanesulfonic acid
IAP	inhibitor of apoptosis protein

IMM	inner mitochondrial membrane
IMS	intermembrane space
IP_3	inositol-3 phosphate
IPTG	isopropyl thiogalactoside
Kb	kilobases
kDa.	kilodaltons
LB	Luria Bertani
mCSA	N-methyl-Val-4-cyclosporin
MES	2-(N-morpholino)ethanesulfonic acid
MPT	mitochondrial permeability transition
NTA	nitrilotriacetic acid
OD	optical density
OMM	outer mitochondrial membrane
PCD	programmed cell death
PMSF	phenyl methyl sulphonyl fluoride
RFP	red fluorescent protein
ROS	reactive oxygen species
SAED	sulfosuccinimidyl 2-(7-azido-4-methylcoumarin-acetamido) ethyl-1,3-dithiopropionate
SDS-PAGE	sodium dodecyl sulphate polyacrylamide gel electrophoresis
SERCA	sarco-endoplasmic Ca^{2+} ATPase
SR	sacroplasmic reticulum
TCA	tricarboxcylic acid cycle
TEMED	N, N, N', N'-tetramethylethylene-diamine
TNFR	tumour necrosis factor receptor
Tris	tris(hydroxymethyl)aminoethane
VDAC	voltage dependent anion channel

Chapter 1: Introduction

[1.1] Background

Apoptosis is an evolutionarily conserved cell suicide program that is essential for development and maintenance of tissue homeostasis in multicellular organisms. This form of cell death differs from necrosis which is considered to be accidental and is the result of lethal cell injury. Apoptotic cell death has many important physiological functions including the termination of immune responses and eliminating viral-infected cells. In addition, defects in the pathways leading to apoptosis have been implicated in the pathology of various diseases such as neurological disorders, heart disease and cancer. The identification of pro-apoptotic proteins within the IMS has established the important role mitochondria play in the apoptotic process. For example, the release of cytochrome c from the IMS leads to apoptosome formation and activation of pro-caspase 9 which in turn activates downstream pro-caspases leading to the cleavage of structural cellular proteins and chromatin. SMAC/Diablo, also present in the IMS, deregulates the inhibitor of apoptosis proteins (IAPs). Pro- and anti-apoptotic Bcl-2 proteins regulate the permeabilisation of the OMM. However, the mechanism responsible for the release of proteins from the IMS remains unclear.

This introduction focuses on the main events that occur during apoptosis, in particular how mitochondria are recruited by the Bcl-2 proteins into apoptotic pathways and how they are involved in bringing about the destruction of the cell.

[1.2] Apoptosis

In 1972, Kerr and co-workers (Kerr et al., 1972) coined the term "apoptosis" to describe cell death during which cells shared the same morphological features such as shrinkage of the cell away from its neighbours, plasma membrane blebbing, cytoplasmic and nuclear condensation and preservation of the structure of organelles including mitochondria until the last stages of programmed cell death (PCD). Different types of cells undergoing PCD share these changes suggesting a common conserved pathway. These features were distinct from those observed when cells underwent necrotic cell death, where cells swell and chromatin appears diffuse or finely clumped. Apoptotic cells are gradually phagocytosed by neighbouring cells or macrophages whilst necrotic cells lyse, releasing their contents into the extracellular space and thus eliciting an inflammatory response by the tissue (Wyllie et al., 1980).

[1.3] The Apoptotic cascade

The pathways leading to apoptotic cell death are intricate and precisely ordered. Apoptosis is initiated by intracellular or extracellular signals followed by the activation of a cascade of proteolytic enzymes, in particular a group of cysteine proteases known as caspases (*c*ysteine-dependent *asp*artate-directed prote*ases*) (Wolf & Green, 1999, Wang & Lenardo, 2000) are involved in apoptosis. These enzymes initiate the process, propagate or amplify the signal, or attack cellular structures to cause their collapse as a result of activation of different apoptotic pathways. The extrinsic pathway is activated

by the ligation of death receptors leading to the rapid activation of upstream (initiator) and downstream (effector) caspases, and the mitochondria are initially bypassed (Lui et al., 1997, Scaffidi et al., 1998, Scaffidi et al., 1999) allowing cells to respond directly to the immediate environment. The death receptors belong to the TNF receptor (TNFR) superfamily and are single transmembrane spanning proteins with cysteine-rich domains in the extracellular region (Hofmann et al., 1999, Locksley et al., 2001). An example of this type of receptor is the Fas receptor (CD95) (Huang et al., 1996), which is triggered by the Fas ligand and signals through the *Fas-as*sociated *DD* adaptor protein (FADD). The intrinsic pathway of PCD is driven by organelles, particularly the mitochondria, which detect and respond to unfavourable changes in the internal environment. Organelles other than mitochondria may initiate apoptosis (Ferri & Kroemer, 2001). Nuclear damage may be sufficient to induce cell death, Golgi dysfunction may activate caspase-2 and caspase-12 can be selectively activated in response to ER stress which can be the result of accumulation of unfolded proteins in the ER or inhibition of the ER-Golgi transport (Oyadomari et al., 2002). Figure **[1.1]** outlines the control of apoptosis through the extrinsic and intrinsic pathways. Activation of these pathways leads to the activation of downstream effector caspases which are required to dismantle cellular components. Cross-talk between the extrinsic and intrinsic pathways does occur for example, the release of cytochrome c from mitochondria can occur when either of these pathways is activated in mammalian cells (Goldstein et al., 2000) and death-receptor mediated activation of caspase-8 can lead to cleavage of the Bcl-2 protein Bid which is involved in the mitochondrial pathway (Kuwana et al., 1998).

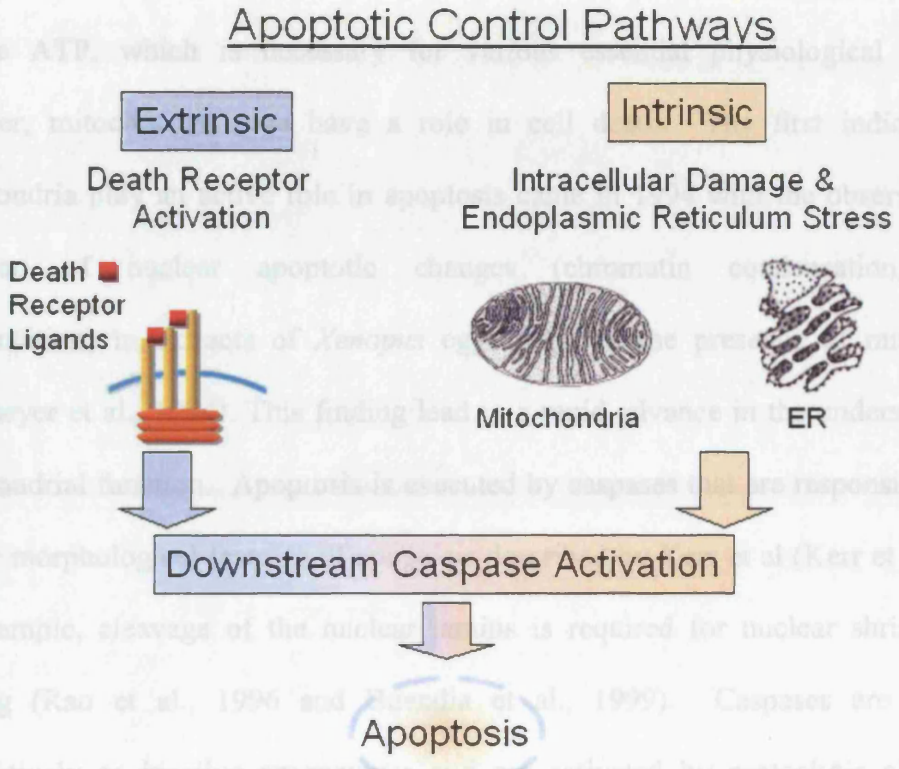

Figure [1.1] Control of apoptotic pathways. There are two principal pathways that lead to caspase activation and cell death. The extrinsic pathway is triggered by ligation of the cell surface death receptors and allows the cell to respond directly to the immediate environment. Cell death can also occur via the intrinsic pathway driven by organelles particularly the mitochondria or in response to ER stress (P. Lovat, personal communication).

[1.4] Mitochondria and Apoptosis

Mitochondria are often referred to as the "powerhouses" of cells; their function is to produce ATP, which is necessary for various essential physiological processes. However, mitochondria also have a role in cell death. The first indication that mitochondria play an active role in apoptosis came in 1994 with the observation that induction of nuclear apoptotic changes (chromatin condensation, nuclear fragmentation) in extracts of *Xenopus* eggs required the presence of mitochondria (Newmeyer et al., 1994). This finding lead to a rapid advance in the understanding of mitochondrial function. Apoptosis is executed by caspases that are responsible for the distinct morphological features of apoptosis described by Kerr et al (Kerr et al., 1972). For example, cleavage of the nuclear lamins is required for nuclear shrinkage and budding (Rao et al., 1996 and Buendia et al., 1999). Caspases are expressed constitutively as inactive proenzymes and are activated by proteolytic cleavage to generate large (p20) and small (p10) subunits. These enzymes can be grouped structurally and functionally into two classes (Earnshaw et al., 1999). Class I are the initiator caspases that contain long prodomains with either a *cas*pase *r*ecruitment *d*omain (CARD) or a *d*eath *e*ffector *d*omain (DED) and are mutually cleaved after aggregation into complexes, a process mediated by adaptor proteins. These caspases then cleave and activate class II, the effector caspases, which have short prodomains. Caspases-2, -9, -8 and -10 are apoptosis initiators and cleave and activate apoptosis effectors caspases-3, -6 and -7. The domain structures of the principal caspases are shown in figure **[1.2]**.

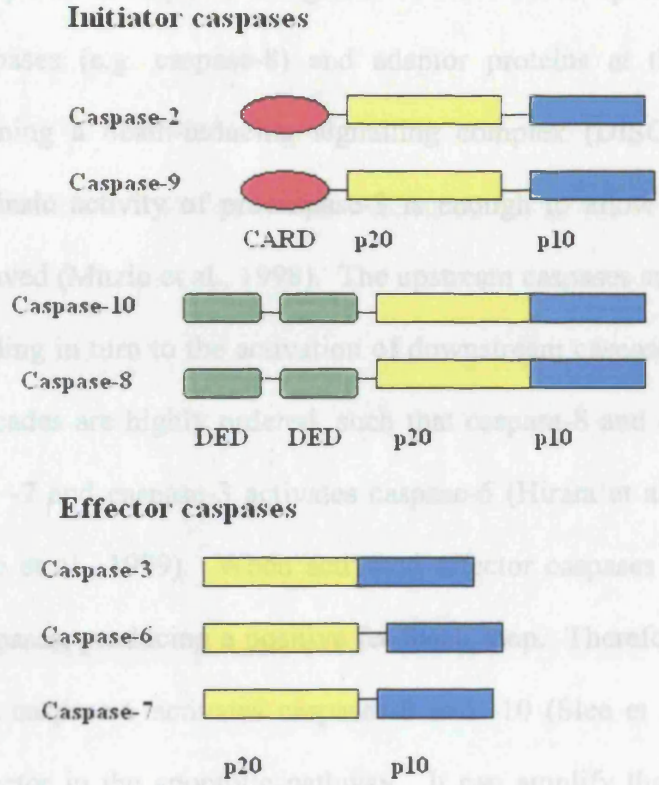

Figure [1.2] Caspases are the executioners of the apoptotic response. The domain structure of the principal caspases involved in apoptosis. Caspases are activated by cleavage to generate a large (p20) and small (p10) subunit. Initiator caspases contain a long prodomain with either a CARD (pink) or DED (green) domain. These domains interact with complementary domains on adaptor proteins that serve to cluster the initiator caspases and facilitate autoproteolysis.

Apoptosis in response to ligation of the death receptors leads to assembly of upstream caspases (e.g. caspase-8) and adaptor proteins at the plasma membrane receptor, forming a death-inducing signalling complex (DISC). It is thought that the low intrinsic activity of procaspase-8 is enough to allow some of the proenzymes to be cleaved (Muzio et al., 1998). The upstream caspases are processed to their active forms leading in turn to the activation of downstream caspases. Studies indicate that caspase cascades are highly ordered, such that caspase-8 and -9 cleave and activate caspase-3 and -7 and caspase-3 activates caspase-6 (Hirata et al., 1998, Takahashi et al., 1999, Slee et al., 1999). When activated effector caspases can activate remaining initiator caspases, producing a positive feedback loop. Therefore caspase-3 activates caspase-2 and caspase-6 activates caspases-8 and -10 (Slee et al., 1999). Caspase-3 is a key effector in the apoptotic pathway. It can amplify the signal from upstream caspases (e.g. by cleaving procaspase-8) and can cleave caspase-activated DNase (CAD) (Enari et al., 1998) which is responsible for the chromatin degradation in apoptotic cells and can be detected as a 180bp nucleosomal ladder on agarose gels. This DNase exists in non-apoptotic cells as an inactive complex with an inhibitory subunit and is known as ICAD (Nagata, 2000, Lui et al., 1997). Other caspase substrates include structural proteins, such as fodrin and vimentin which are cleaved by caspase-3 (Janicke et al., 1998, Slee et al., 2001) and nuclear lamins A and B which are cleaved by caspase-6 (Slee et al., 2001). Mitochondria can be recruited into the apoptotic pathway by caspase-8 (Luo et al., 1998, Li et al., 1998). Figure **[1.3]** shows that caspase-8 cleaves the Bcl-2 family protein Bid to a produce a 15 kDa carboxyl-terminal truncated Bid

fragment (tBid) that translocates from the cytosol to mitochondria (see section **[1.5]** for the Bcl-2 family proteins).

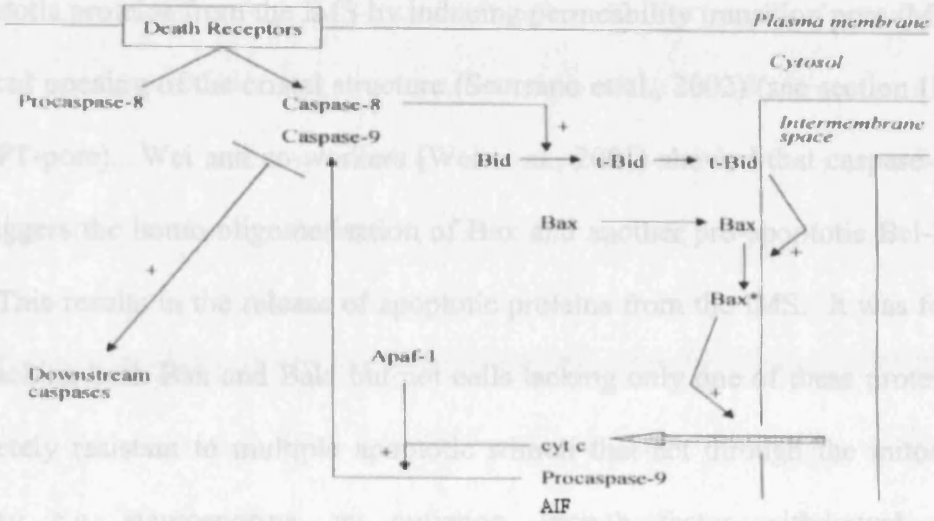

Figure [1.3] Mitochondria are recruited into the apoptotic pathway by the Bcl-2 family proteins Bax and Bid. Proteins Bax and Bid translocate from the cytosol to the mitochondrial outer membrane when cells receive an apoptotic stimulus. Bid is processed by caspase-8 to a truncated form (t-Bid) before translocation to the outer mitochondrial membrane where it can process Bax. The activated Bax then causes the release of apoptosis-inducing factor (AIF), procaspase-9, cytochrome c, and other intermembrane space proteins into the cytosol.

Bid is thought to have two functions. One in promoting conformational changes in Bax, a Bcl-2 pro-apoptotic protein that also translocates from the cytosol to mitochondria

during apoptosis. These Bid-induced conformational changes in Bax are required for the membrane insertion of its hydrophobic C-terminal domain anchor and oligomerisation (Desagher et al., 1999, Wei et al., 2001). The other function of Bid is to bring about mitochondrial membrane restructuring to ease the egress of pro-apoptototic proteins from the IMS by inducing permeability transition pore (MPT-pore) mediated opening of the cristal structure (Scorrano et al., 2002) (see section **[1.8.3]** for the MPT-pore). Wei and co-workers (Wei et al., 2001) showed that caspase-activated Bid triggers the homo-oligomerisation of Bax and another pro-apoptotic Bcl-2 protein Bak. This results in the release of apoptotic proteins from the IMS. It was found that cells lacking both Bax and Bak, but not cells lacking only one of these proteins, were completely resistant to multiple apoptotic stimuli that act through the mitochondrial pathway e.g. staurosporine, uv radiation, growth factor withdrawal, and the endoplasmic reticulum stress stimulus thapsigargin. Therefore, it was concluded that Bax or Bak are essential for the mitochondrial intrinsic pathway involvement in apoptosis.

[1.5] The Bcl-2 family of proteins

The Bcl-2 proteins are key regulators of apoptosis. Bcl-2 was the first discovered as a proto-oncogene found at breakpoints of t (14;18) chromosomal translocations in B-cell lymphomas (Tsujimoto et al., 1985). In this condition neoplastic cell expansion can be attributed primarily to failed PCD rather than rapid cell division. Gene transfection studies showed that overexpression of Bcl-2 significantly prolongs cell survival in the

presence of classical apoptotic stimuli such as lymphokine deprivation from haematopoietic cells and glucocorticoid treatment of thymocytes. Conversely, antisense mediated suppression of Bcl-2 expression was demonstrated to induce or accelerate cell death (Reed, 1990). Since then other proteins belonging to this family have been found. Some are anti-apoptotic such as Bcl-X_L while others for example, Bax are pro-apoptotic. The precise functions of most of the Bcl-2 proteins have not been elucidated. A principal site of action of the Bcl-2 family proteins is the mitochondrion where they regulate the release of apoptogenic, proteins for example, cytochrome c from the IMS (section **[1.7.3]**). The proteins can be classified into three functional groups (Adams & Cory, 1998). Members of the first group, such as Bcl-2 and Bcl-X_L, are characterised by four short conserved Bcl-2 homology (BH) domains (BH1-4). They also possess a C-terminal hydrophobic tail, which localises the proteins to the outer surface of mitochondria, the ER and the nuclear membranes (Krajewski et al., 1993, Gonzalez-Garcia et al., 1994, Lithgow et al., 1994). All members of this group possess anti-apoptotic activity. Group II consists of proteins with pro-apoptotic activities for example, Bax and Bak. Their overall structure is similar to group I proteins containing the hydrophobic tail but not the BH4 domain at the N-terminus. The third group of Bcl-2 family members which, consists of a large and diverse group of proteins whose only common feature is the presence of the 12-16 amino acid BH3 domain (Figure **[1.4]** and Table **[1.1]**).

One characteristic of the Bcl-2 family of proteins is that they are capable of forming homo- and heterodimers. In a landmark study by Oltvai and co-workers (Oltvai et al.,

1993) it was shown that Bax co-immunoprecipitates with Bcl-2 from RL7 cells (human B-cell line which produces high levels of Bcl-2). Their work also showed that Bax forms homodimers and heterodimers *in vivo*. Another important finding from this study was that the intracellular ratio of Bax to Bcl-2 is an important indicator of whether or not a cell will live or die. If Bcl-2 predominates the cells survive whereas if Bax is more abundant cell death occurs (Oltvai et al., 1993).

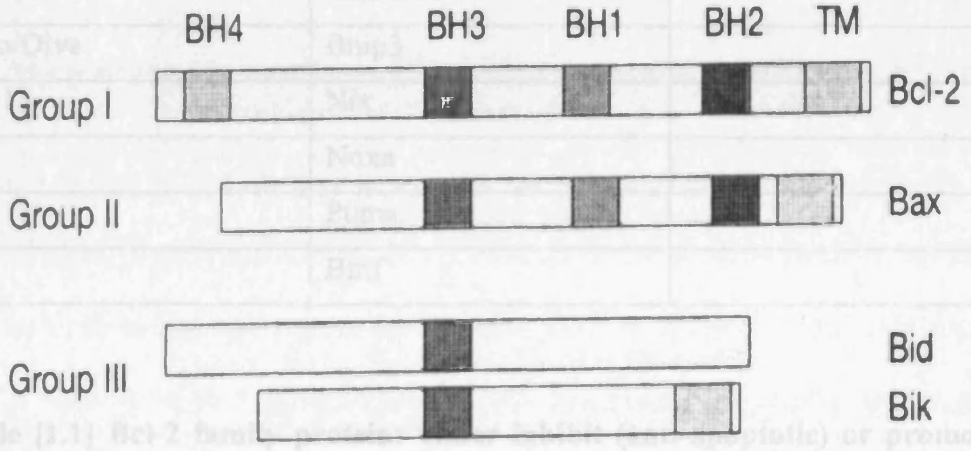

Figure [1.4] The Bcl-2 family of proteins can be classified into 3 functional groups. Members of group I have four short, conserved Bcl-2 homology (BH) domains (BH1-4). They also possess a C-terminal hydrophobic domain (TM). These proteins include Bcl-2 and Bcl-X_L. Group II proteins have a similar structure to group I except for the N-terminal BH4 domain. The group members are pro-apoptotic such as Bax and Bak. Group III proteins contain the BH3 domain. These proteins may share little sequence similarity to the other two groups except for this BH3 domain. Members of this group can be either pro- or anti-apoptotic. (Diagram taken from Hengartner, 2000).

Anti-apoptotic	**Pro-apoptotic**	
	BH3 domain-only	**Multi-domain**
Bcl-2f	Bid	Bax
Bcl-X_L	Bad	Bak
Bcl-w	Bik/Nbk	Bok
Mcl-1	Hrk	Bcl-X_S
A1/Bfl	Bim/Bod	
Boo/Diva	Bnip3	
Nrl13	Nix	
	Noxa	
	Puma	
	Bmf	

Table [1.1] Bcl-2 family proteins either inhibit (anti-apoptotic) or promote (pro-apoptotic) apoptosis. Most of the anti-apoptotic proteins contain all four BH domains. The pro-apoptotic proteins can be divided into two groups: the BH3 domain-only proteins which share little sequence similarity except for their BH3 domains and the multi-domain proteins which contain BH 1,2 and 3 domains.

[1.6] Bcl-X_L-an anti-apoptotic protein

Boise and co-workers found the gene encoding Bcl-X_L (Boise et al., 1993). They showed that Bcl-X_L could function as a Bcl-2-independent regulator of programmed cell death. Alternative splicing results in two distinct Bcl-X mRNAs. The protein

product of the larger mRNA (Bcl-X_L) was similar in size and structure to Bcl-2 (Bcl-X_L is 27 kDa and Bcl-2 is 26 kDa). When stably transfected into an interleukin-3 (IL-3)-dependent cell line, it inhibited cell death upon growth factor withdrawal to the same degree as Bcl-2. The smaller mRNA (Bcl-X_S) encodes a protein that inhibits the ability of Bcl-2 to enhance the survival of growth factor-deprived cells. *In vivo*, Bcl-X_S is expressed in cells that undergo a high rate of turnover, such as developing lymphocytes. In contrast, Bcl-X_L is present in tissues that contain long-lived post-mitotic cells, for example the adult brain.

Bcl-X_L functions antagonistically to pro-apoptotic Bcl-2 proteins, for example Bax (section **[1.7.3]**). Studies have shown that Bcl-X_L prevents the loss of OMM integrity by preventing hyperpolarisation of the OMM and mitochondrial swelling in response to apoptotic stimuli such as staurosporine and IL-3 withdrawal (Vander Heiden et al., 1997). The same study also showed that overexpression of Bcl-X_L in Jurket T cells undergoing apoptosis prevents cell death.

[1.7] Bax a pro-apoptotic protein

Oltvai and co-workers first identified Bax as a protein that could form heterodimers with Bcl-2 (Oltvai et al., 1993). Their findings suggested a model for the control of programmed cell death in which the ratio of Bcl-2 to Bax determined cell survival or death following an apoptotic stimulus. *In situ* hybridisation was used to map the human

bax gene to chromosome 19q 13.3-13.4 (Apte et al., 1995). Oltvai and co-workers (Oltvai et al., 1993) described six different bax mRNA transcripts produced by alternative splicing. Bax-α is a 579 bp transcript that codes for a 21 kDa protein, which has a C-terminal transmembrane domain. Most studies relating to Bax function and apoptosis have focused on this splice variant. The amino acid sequence of Bax-α, BH domains and the C-terminal transmembrane domain are shown in figure **[1.5].** The beta mRNA transcript is 657 bp and contains a larger version of exon 6 which contains a termination codon. Bax-β is a 24 kDa protein that lacks the C-terminus and hence the transmembrane anchor. The bax-γ mRNA transcript is 126 bp and consists of exons 1 and 3. The Bax-γ protein is only 4.5 kDa and results from premature termination in exon 3 due to a translational frameshift (Ovalti et al., 1993). The bax-δ mRNA is a 433 bp transcript that is missing exon 3 but retains the same translational frame. The Bax-δ protein retains the transmembrane anchor (Apte et al., 1995). The bax-ε transcript contains an additional exon (exon 5) in addition to the same exons as bax-α whilst bax-σ contains the same exons as bax-α except that it contains a 3' truncated exon 7. Figure **[1.6]** shows 9 different bax transcripts produced from the bax gene. The functions of these different splice variants are not known. More recently three other splice variants have been identified. Zhou and co-workers (Zhou et al., 1998) identified bax-ω whilst screening human hippocampal cDNA for brain-specific homologues of bax. They found a 28 kDa protein that lacks the C-terminal transmembrane anchor. The Bax-ω is identical to Bax-α through the region of the protein encoded by exons 1 to 6, after exon 6 Bax-ω is generated as a result of the splice donor site at the 3'end of exon 6 joining to a site 49 bases pairs 5' to the Bax-α acceptor site on exon 7. Bax-κ

contains an insert between exons 1 and 2, and an initiation at an alternative start site in exon 2 produces a protein that lacks the N-terminal ART domain that regulates pro-apoptotic function, and deletion of this region produces a protein with increased apoptotic activity (Jin et al., 2001). Cartron and co-workers (Cartron et al., 2002) identified a form of Bax designated Bax-ψ. Bax-ψ is a N-terminal truncated form of Bax that results from a partial deletion of exon 1 of the bax gene. Bax-ψ has also been found to be present in normal tissues. This form of the protein localises to mitochondria and was found to be a more powerful inducer of apoptosis than Bax-α. The expression of Bax-ψ in glioblastomas compared with Bax-α correlated with longer survival in patients with brain tumours (Cartron et al., 2002).

The bax promoter region contains 4 motifs with homology to consensus p53-binding sites. Co-transfection assays using p53 deficient tumour cell lines showed that bax is a primary response gene for p53 and is involved in a p53 regulated pathway for induction of apoptosis (Miyashita and Reed, 1995)

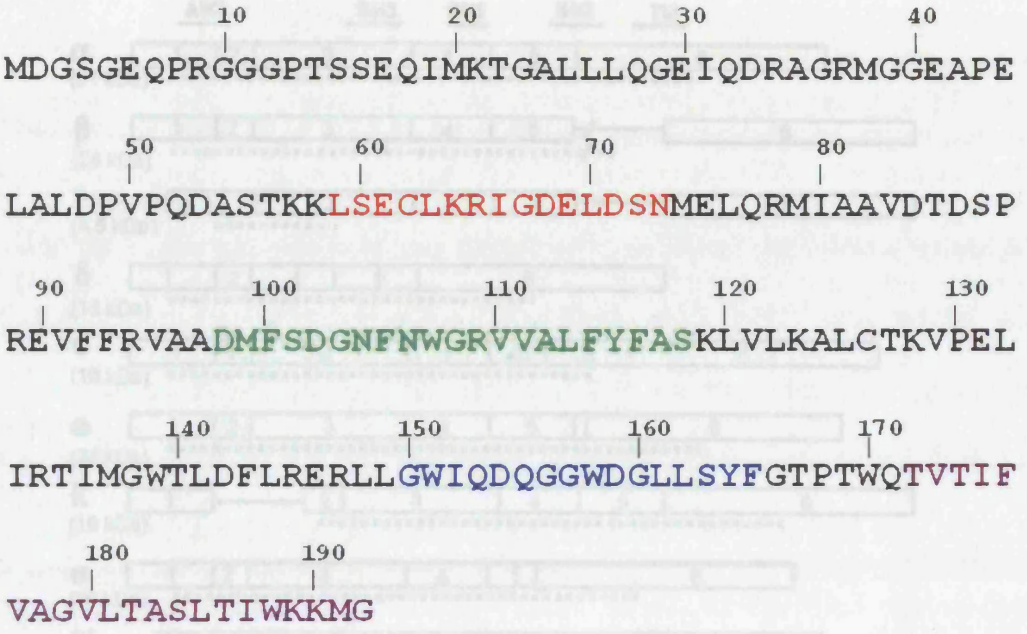

Figure [1.5] Primary sequence of Bax-α. Bax-α consists of 192 amino acids. The BH3 domain is shown in red and contains amino acids 59 to 73. This domain is essential for oligomerisation with anti-apoptotic Bcl-2 proteins e.g. Bcl-2 and Bcl-X_L or with other Bax molecules. The BH1 and BH2 domains are shown in green and blue respectively. The C-terminal transmembrane anchor inserts into the outer mitochondrial membrane (shown in purple).

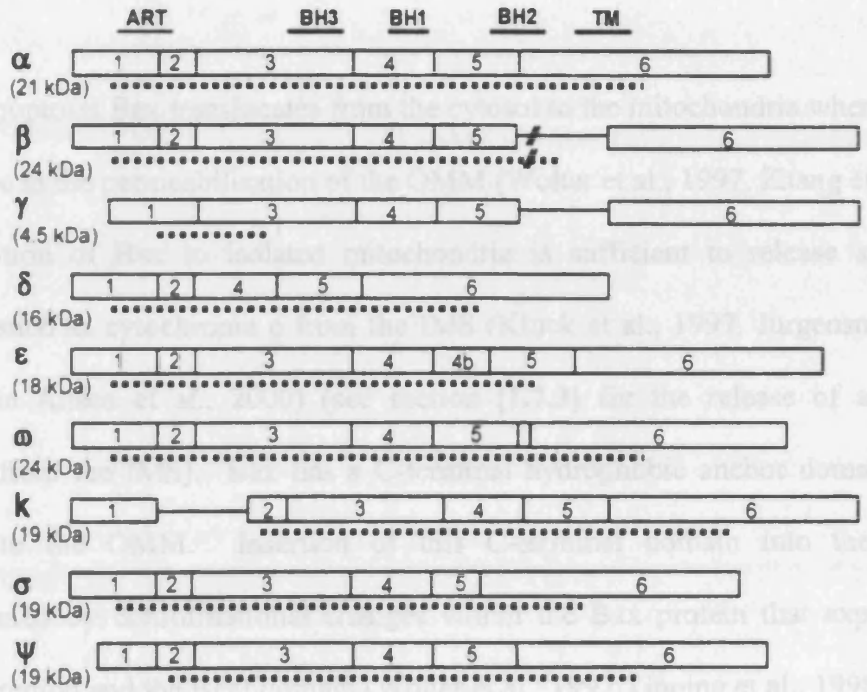

Figure [1.6] Splice variants of bax. The bax gene contains 6 different exons from which 9 different transcripts can be produced. Exons are numbered within the boxes and the domains of Bax-α are shown within the above boxes. The dotted line indicates the length of the translated region (diagram taken from Clerk et al., 2003)

[1.7.1] Translocation and homo-oligomerisation of Bax during apoptosis

During apoptosis Bax translocates from the cytosol to the mitochondria where it plays a major role in the permeabilisation of the OMM (Wolter et al., 1997, Zhang et al., 1998). The addition of Bax to isolated mitochondria is sufficient to release apoptogenic proteins such as cytochrome c from the IMS (Kluck et al., 1997, Jurgensmeier et al., 1998, von Ahsen et al., 2000) (see section **[1.7.3]** for the release of apoptogenic proteins from the IMS). Bax has a C-terminal hydrophobic anchor domain that can insert into the OMM. Insertion of this C-terminal domain into the OMM is accompanied by conformational changes within the Bax protein that expose the N-terminal region and the BH3 domain (Wolter et al., 1997, Goping et al., 1998, Desagher et al., 1999). These changes are thought to lead to dimerisation, possibly mediated by the exposed BH3 domain (Wang et al., 1998, Antonsson et al., 2001). Higher Bax oligomers have also been described. In particular, Bax complexes (4-mers and 12 mers) were isolated from apoptotic cells (Antonsson et al., 2001, Gross et al., 1998). More recently very large Bax aggregates, containing thousands of Bax molecules have been detected in close proximity to mitochondria during apoptosis (Nechushtan et al., 2001, Capano & Crompton, 2002). Capano & Crompton (Capano & Crompton, 2002) showed that the translocation of Bax, with green fluorescent protein (GFP) present at the N-terminus of Bax, was biphasic. When apoptosis was initially induced by the addition of staurosporine to GFP-Bax transfected cardiomyocytes, there was little evidence of Bax association with mitochondria. After one to three hours incubation with staurosporine the association of GFP-Bax with mitochondria was clearly

discernible. GFP-Bax aggregates were visible after four to five hours of incubation with staurosporine and after seven to nine hours the mitochondria began to break up and disappear. The function of these large Bax aggregates is not clear. In the same study it was shown that cardiomyocytes were transfected with both GFP-Bax and cytochrome c with a red fluorescent protein tag (RFP). Before the induction of apoptosis with staurosporine, the RFP-Bax was localised to the IMS. After two hours of exposure to staurosporine the RFP-cytochrome c distribution became more diffuse indicating that RFP-cytochrome c was released from the IMS into the cytosol. At this stage it was found that RFP-cytochrome c release from the IMS was complete. It was concluded that cytochrome c release occurs in the first phase of GFP-Bax translocation to mitochondria when only a small proportion of the GFP-Bax is co-localised with the mitochondria. Therefore these results indicate that the formation of large Bax aggregates occurs after cytochrome c release from the IMS and this higher Bax structure is not required for the permeabilisation of the OMM to pro-apoptotic proteins in the IMS.

[1.7.2] Bax and detergent-induced conformational changes and oligomerisation

In vitro studies using recombinant Bax and isolated mitochondria have shown that it is the Bax oligomers, (4- 12mers) which are biologically active rather than the monomeric form in that only detergent-oligomerised Bax was able to induce cytochrome c release from isolated mitochondria whereas monomeric Bax could not (Antonsson et al., 2000). The conformational changes leading to the exposure of the N-terminal region and BH3

domain that take place when the C-terminal hydrophobic domain of Bax inserts into the OMM during apoptosis and which are necessary for oligomerisation to take place can be induced *in vitro* by the incubating Bax with nonionic detergents (Hsu & Youle, 1997). The degree to which the N-terminal region exposure and oligomerisation takes place is dependent upon the detergent used. Nonidet P-40 and Triton-X100 both strongly induced heterodimerisation of Bax with Bcl-X_L and homodimerisation in Bax present in protein extracts derived from non-apoptotic thymocytes. Whereas Tween 20 induced heterodimerisation with Bcl-X_L but not homodimerisation. The nonionic detergent CHAPS was unable to induce conformational changes leading to Bax oligomerisation (Hsu & Youle, 1998).

[1.7.3] *Bax and the release of apoptogenic proteins from the IMS*

Bax mediates the release of apoptogenic proteins from the IMS. The first to be recognised was cytochrome c (Lui et al., 1996). Addition of Bax to isolated mitochondria is sufficient to induce the release of cytochrome c. (Eskes et al., 1998, Jurgenmeier et al., 1998, Luo et al., 1998 and Desagher et al., 1999). Cytochrome c release is almost a universal feature of apoptotic cell death. However, in some cases, it is a very late event, for example, apoptosis induced by death receptors bypassing the mitochondrial pathway (Scaffidi et al, 1998). In this case cell death is almost insensitive to protection by Bcl-X_L. Goldstein and co-workers (Goldstein et al., 2000) transfected HeLa cells with a recombinant plasmid containing cytochrome c-GFP. They found that the release of cytochrome c-GFP from the IMS always precedes the

exposure of phosphatidylserine and loss of plasma membrane integrity that are characteristics that appear in the later stages of apoptotic cell death. Cytochrome c-GFP release was found to be complete after 5 minutes and was shown to be independent of the type and strength of the stimulus and was also shown to be temperature independent over the range 24°C-37°C. Released cytochrome c binds to the cytosolic adaptor protein apoptosis activating protease activating factor-1 (Apaf-1) and dATP together they activate pro-caspase-9. Apaf-1 contains multiple domains that facilitate protein-protein interactions including a N-terminal CARD, a nucleotide-binding domain and a series of 12 or 13 WD-40 repeats at the C-terminus. The binding of cytochrome c to the WD-40 domain increases the affinity of Apaf-1 for dATP/ATP, and the binding of dATP/ATP promotes the oligomerisation of Apaf-1 into a high-molecular weight complex, the apoptosome (Jiang & Wang, 2000). Interactions between Apaf-1, cytochrome c, and pro-caspase-9 are not transient and this complex forms the active enzyme. The apoptosome is a large complex (700 kDa) and may involve other proteins e.g. heat shock protein-70 (Cain et al., 1999, Cain et al., 2000, Beere et al., 2000). Caspase-9 activates effector caspases e.g. caspase-3 and this cleaves ICAD that results in chromatin degradation (Zou et al., 1999). Procaspase-2, 3 and 9 are also released from the IMS (Zou et al., 1999, Susin et al., 1999a) During apoptosis a variety of pro-apoptotic proteins are released from the IMS in addition to cytochrome c. Smac /Diablo (Du et al., 2000, Verhagen et al., 2000) and HtrA2/Omi (Suzuki et al., 2001, Hegde et al., 2002, Verhagen et al., 2002) both potentiate caspase activation by binding to inhibitors of apoptosis proteins (IAPs) and blocking their caspase inhibitory activity. Apoptosis inducing factor (AIF) (Susin et al., 1999b) and

endonuclease G (Endo G) (Li et al., 2001) are also released from the IMS. During apoptosis both AIF and Endo G translocate from the IMS to the nucleus. AIF induces chromatin condensation and large-scale DNA fragmentation (50 kbp) (Susin et al., 1999b). Endo G catalyses both high molecular weight DNA cleavage and oligonucleosomal DNA breakdown in a sequential manner. In addition Endo G cooperates with exonuclease and DNase I to facilitate DNA processing (Widlak et al., 2001). Whether pro-apoptotic Bcl-2 proteins release all apoptogenic factors from the IMS and the temporal sequence of their release remain unclear. Recently it was reported that Bax-mediated mitochondrial permeabilisation does not directly induce AIF release and that AIF release occurs downstream of cytochrome c release (Arnoult et al., 2002). A subsequent study by the same group showed that OMM permeabilisation induced by Bax resulted in the release of cytochrome c, Smac/Diablo and HtrA2/Omi but subsequent caspase activation is required to induce translocation of Endo G and AIF into the cytosol from the IMS (Arnoult et al., 2003).

[1.8] Molecular mechanisms of OMM permeabilisation by Bax

[1.8.1] Bax only models for OMM permeabilisation

The mechanism by which Bax induces permeabilisation of the OMM has been the focus of much research and still remains controversial. One hypothesis put forward is that Bax is able to form channels in the OMM through which pro-apoptotic proteins can pass. NMR studies have shown that Bcl-X_L and Bax are structurally similar to the

diptheria toxin and the bacterial colicins (Muchmore et al., 1996, Suzuki et al., 2000). These observations have inspired several studies showing that these proteins exhibit ion channel activities in synthetic bilayers. In most cases, the channel activities were recorded at a non-physiological pH and it was questionable as to whether these channels would be large enough to allow the passage of cytochrome c (Minn et al., 1997, Antonsson et al., 1997). However, Bax tetramers were shown to form a channel large enough to allow the release of cytochrome c from liposomes (Saito et al., 2000). In addition, Bax was isolated as high molecular weight oligomers (96 kDa and 260 kDa) from mitochondrial membranes of apoptotic HeLa cells and it was prosposed that Bax oligomers might constitute the structural entirety of the cytochrome c-conducting channel in the OMM (Antonsson et al., 2001). Other studies had implicated the OMM protein the voltage-dependent anion channel (VDAC) in the Bax-induced permeabilisation of the OMM, however in this study VDAC did not co-elute with the Bax oligomers from the OMM of apoptotic cells. More recently, it was shown that Bid, Bax and lipids cooperate to form openings in the OMM through which apoptogenic proteins can pass into the cytosol (Kuwana et al., 2002). In this study the apoptotic process of protein release from the IMS and its control by Bax/Bid was reconstituted using isolated OMM and protein-free liposomes. The results showed that Bax and Bid interact directly with the OMM. VDAC which has been implicated in Bax-induced permeabilisation of the OMM (see section **[1.8.2]**) and other mitochondrial membrane proteins are not required for permeabilisation of the OMM to take place. Permeabilisation of liposomes by Bax was found to be dependent on the amount of the lipid cardiolipin. Previous studies have shown that cardiolipin is also required for the

membrane targeting of Bid (Lutter et al., 2000). Other studies have shown that the ability of detergent-oligomerised Bax to produce pores in lipid membranes was affected by the addition of lipids that can alter the intrinsic curvature of the membrane whereas the lipids had little effect on Bax binding or insertion into the membrane (Basanez et al., 2002). Kuwana and co-workers suggested that cardiolipin might increase the local stress curvature of the OMM sensitising it to Bax-induced pore formation (Kuwana et al., 2003).

[1.8.2] Bax regulates OMM permeabilisation through its interaction with VDAC

Voltage-dependent anion channels (VDACs) are pore-forming proteins found in the OMM of all eukaryotes (Schein et al., 1976). These protein, vary in size from 30-32 kDa, are capable of forming channels with a diameter of 2.5-3nm in planar phospholipid bilayers (Granville & Gottlieb, 2003). VDACs play a role in the regulated flux of metabolites across the OMM. The gating of the channel depends upon the transmembrane potential. VDACs are "open" at low transmembrane potentials, with a preference for anions such as phosphate, chloride, and adenine nucleotides. At higher transmembrane potentials, VDACs are in a "closed" conformation and are slightly more selective for cation (Manella et al., 1992). Two isoforms of VDAC have been identified in rats and humans (Blachly-Dyson et al., 1993). Previous studies have shown that it is the more abundant isoform VDAC-1 that interacts with ANT to form contact sites (see section **[1.8.4]**) between the IMM and the OMM (Brdiczka et al., 1998). However, more recently it has been shown that the low abundance isoform

VDAC-2 inhibits the activation of the pro-apoptotic Bcl-2 protein Bak. VDAC-2 interacts specifically with inactive monomeric Bak. Cells deficient in VDAC-2 but not VDAC-1 exhibited enhanced Bak oligomerisation and were more susceptible to apoptotic cell death (Cheng et al., 2003).

Another hypothesis put forward is that Bax induces OMM permeabilisation through its interaction with the OMM protein VDAC. Shimizu and co-workers demonstrated that the addition of recombinant Bax to VDAC liposomes enhanced sucrose uptake but uptake of sucrose into liposomes incorporating Bax without VDAC was low indicating that the Bax-enhanced sucrose uptake by VDAC liposomes was mediated not by a putative Bax channel but by the effect of Bax on VDAC (Shimizu et al., 1999). Further work by the same group showed that Bax and VDAC are capable of forming a large pore that was permeable to cytochrome c (Shimizu et al., 2000). However, this pore was not wide enough to allow the efflux of proteins larger than cytochrome c. The anti-apoptotic protein Bcl-X_L can also interact directly with VDAC (Shimizu et al., 1999). Studies have shown that Bax and Bcl-X_L function antagonistically to each other, Bcl-X_L closes VDACs whereas Bax opens them (Shimizu et al., 2000).

An alternative hypothesis concerning the role of VDAC in OMM permeabilisation was put forward by Vander Heiden and co-workers (Vander Heiden et al., 1999) in which VDAC closure causes a defect in ATP/ADP exchange, inhibition of the F_1 F_0-ATPase, hyperpolerisation of the IMM followed by a loss of OMM integrity and cytochrome c release. The change in mitochondrial membrane potential may result from a failure of

the VDAC in the OMM bound to ANT in the IMM (see section **[1.8.4]** for intermembrane junctional complexes) to mediate ATP/ADP exchange. Contrary to Shimizu and co-workers, Vander Heiden found that Bcl-2/Bcl-X_L expression prevented VDAC closure and the subsequent build up of ATP and creatine phosphate in the IMS leading to secondary mitochondrial dysfunction and cytochrome c release (Vander Heiden et al., 1999). Furthermore Bcl-X_L permitted growth factor-deprived cells to maintain sufficient mitochondrial ATP/ADP exchange to sustain coupled respiration and that mitochondrial adenylate transport was under active regulation.

More recently, it was shown that Bid and not Bax regulates VDACs (Rostovtseva et al., 2004). This study contradicts previous work by Shimizu and co-workers that demonstrated Bid induces cytochrome c release but not as a result a direct interaction with VDAC (Shimizu et al., 1999, Shimizu et al., 2001). Rostovtsera and co-workers (Rostovtseva et al., 2004) studied the effects of Bax and Bid on the properties of VDACs reconstituted into planar phospholipid membranes. Full-length recombinant Bax in the monomeric and detergent-induced oligomeric forms were used. Recombinant Bid was activated by cleavage with caspase-8. They showed that the addition of Bax had no effect on VDAC and it was concluded that Bax does not induce cytochrome c release by acting on VDAC. In contrast they showed that cleaved Bid induces the closure of VDACs and it was proposed that the Bid-induced reduction of the permeability of VDACs might interfere with metabolite exchange between mitochondria and cytosol leading to an accumulation of products of mitochondrial

activity within the IMS, generation of an osmotic gradient, and matrix swelling followed by the rupture of the OMM.

[1.8.3] Bax interacts with ANT to induce cytochrome c release

ANT is a homodimer consisting of 32 kDa subunits in the IMM. One of its functions is to catalyse the one to one exchange of cytosolic ADP against matrix ATP across the IMM (Fiore et al., 1998 and references therein). Immunological and molecular biological techniques have shown there are three isoforms in humans and two in rat (Doerner et al., 1997). A study of the distribution of the isoforms in rat showed that ANT-1 is found predominantly in the skeletal muscle, heart and brain whereas ANT-2 is found predominantly in the kidney, spleen and liver (Dorner et al., 1999). In a recent study by Brdiczka and co-workers ANT isoforms were found to have different distributions in the IMM and have different affinities for the matrix protein cyclophilin D (Cyp D) (see section **[1.8.5]** for the MPT-pore) (Vyssokikh et al., 2001). They found that the cristae contained ANT-2 only and both isoforms were found in the peripheral inner membrane. In addition, ANT-1 was found to have a higher affinity for Cyp D.

Previous studies have also implicated ANT in the release of apoptogenic proteins from the IMS. Bax and ANT coimmunoprecipitated from tissue extracts derived from rat brain, mouse liver and human HT-29 colon cancer cells (Marzo et al., 1998b). Other work shows that Bax and ANT interact to form a non-specific pore and Bcl-2 suppresses pore-formation (Brenner et al., 2000, Jacotot et al., 2001). In addition Bax

and Bcl-2 also influence the enzymatic activity of ANT as an ADP/ATP antiporter (Belzacq et al., 2003). Recent data has shown that α-helices –5 and –6 of Bax were shown to mediate the insertion of Bax into the OMM (Heimlich et al., 2004) and therefore it is possible that Bax inserted into the OMM may interact directly with ANT in the IMM.

[1.8.4] Bax interacts with intermembrane junctional complexes to bring about permeabilisation of the OMM

Regions of contact between the OMM and IMM were first observed using electron microscopy (Hackenbrock, 1968). When mitochondria are suspended in hypertonic media the matrix space enclosed by the IMM shrinks in size and pulls away from the OMM, but regions of contact between the OMM and IMM remain. It is estimated that isolated rat liver mitochondria, for example, contain about 100 intermembrane contact sites per mitochondrion (Reichert & Neupert, 2002). Contact sites are formed by interactions between IMM and OMM proteins and participate in various functions. These include the translocation of newly synthsised proteins into mitochondria, mitochondrial fission/fusion events, metabolic transfer, and interaction with Bcl-2 proteins during apoptosis. Certain contact sites are held together quite strongly and resist sonication and mitochondrial subfractionation. In this way membrane fractions of intermediate density between the inner and outer membranes have been isolated on density gradients. The composition of these intermediate-density fractions is thought to reflect the composition of certain types of contact sites. VDAC and ANT have been

shown to be components of contact sites (Brdiczka, 1991). Other proteins that have been localised to these regions include hexokinase (Kottke et al., 1988), creatine kinase (Papadopoulos et al., 1999, West et al., 2001), the peripheral benzodiazapine receptor (PBR) which regulates the transfer of cholesterol from the OMM to the IMM, Cyp D in the matrix binds ANT in the contact sites and can form the mitochondrial permeability transition pore (MPT) complex (Crompton et al., 1998) (see section **[1.8.4]**) and Bcl-2 proteins (De Jong et al., 1994, Crompton et al., 2002). In addition contact sites have been shown to contain a high proportion of cardiolipin (Ardail et al., 1990). Whether all components reside in the same contact site is not known. Perhaps the two membrane components, VDAC (OMM) and ANT (IMM) establish a junctional complex holding the membranes together and the proteins associate with the complex depending on the function to be executed. Recent studies have shown that the binding of hexokinase II to VDAC present in contact sites can inhibit Bax-induced cytochrome c release and apoptosis (Pastorino et al., 2002). How exactly this is achieved is not clear. However, hexokinase II is thought to bind VDAC as a tetramer (Xie & Wilson, 1990), which would have a molecular weight of 400 kDa. Therefore, it may sterically hinder Bax binding to VDAC. How mitochondrial contact sites play a role in the permeabilisation of the OMM is not clear. Hexokinase II binding stablises contact sites (Pastorino & Hoek, 2003) and Bax binding displaces hexokinase II promoting disruption of the contact site complex and facilitating the release of intermembrane pro-apoptotic factors, e.g. cytochrome c, through a VDAC-associated channel.

[1.8.5] Bax interacts with the MPT-pore to induce permeabilisation of the OMM

Another way in which intermembrane contact sites may play a role in the Bax-induced permeabilisation of the OMM is via the formation of the MPT-pore. In the late 1970s certain permeability properties of the IMM induced by the presence of Ca^{2+} were proposed to be due to the presence of a transmembrane channel or pore (Hunter & Haworth, 1979). Further studies have shown that high inorganic phosphate and high matrix calcium levels cause the free permeation of low molecular weight solutes (below 1500 Da) across the IMM (Al Nasser and Crompton, 1986). In reconstituted systems, Ca^{2+} alone is sufficient to deform purified ANT into a non-specific pore. This occurs reversibly. However, the time required for pore formation and its reversal (minutes) (Brustovetsky & Klingenberg, 1996, Brustrovetsky et al., 2002) is considerably slower than Ca^{2+}-induced pore opening and its reversal in intact mitochondria (seconds) (Crompton & Costi, 1988). This data together with the finding that the Cyp D ligand, cyclosporin A (CSA), inhibits MPT-pore opening in intact mitochondria (Crompton et al., 1988) provided evidence for Cyp D as a component of the MPT-pore. The components of the pore have now been elucidated. Woodfield and co-workers demonstrated that ANT and Cyp D play a role in MPT (Woodfield et al., 1998). In another study by Crompton and co-workers, VDAC was also implicated in MPT (Crompton et al., 1998). It was found that GST-Cyp D attached to a glutathione-agarose matrix specifically retained VDAC and ANT. Therefore, a model was proposed where Cyp D recruits ANT in the inner membrane, which binds VDAC in the outer membrane at the contact sites between the two membranes (Crompton et al.,

1998). Cyp D, like other cellular cyclophilin isoforms, is a peptidyl-prolyl cis/trans isomerase (PPIase) that catalyses the interconversion of cis and trans isomers of bonds preceding proline in a peptide chain. The Cyp D isoform is a 21 kDa nuclear encoded protein that contains a N-terminal presequence that targets the protein to the mitochondria (Bergsma et al., 1991). Later it was shown that Cyp D is present in the mitochondrial matrix (Johnson et al., 1999). It is thought agents which trigger MPT-pore opening do so by causing Cyp D to bind to ANT, for example, oxidative stress (Halestrap et al., 1997) and Ca^{2+} (Halestrap and Davidson, 1990). The physiological role of pore remains unclear. It is thought that the MPT-pore plays a role in the pathogenesis of ischaemic/reperfusion type injury (reviewed in Crompton, 1999). MPT-pore opening has been detected *in vivo* during myocardial reperfusion injury associated with tissue Ca^{2+} overload and oxidative stress (Griffiths & Halestrap, 1995) and oxidant stress (hydroperoxide) induced injury in hepatocytes (Nieminen et al., 1995). The MPT- pore inhibitor CSA was shown to provide protection against hydroperoxide-induced injury in heart and liver cells (Pastorino et al., 1993, Nazareth et al., 1991, Griffiths & Halestrap, 1993). In cell death involving cardiomyocytes, e.g. myocardial infarction in humans, both necrosis and apoptosis have been observed (Veinot et al., 1997). Apoptosis was considered the predominant form of cell death in the border zone between noninfarcted areas and the more severely compromised tissue (Veinot et al., 1997).

With regard to the role of the PT-pore in Bax-induced permeabilisation of the OMM, the results from various studies have been contradictory. It was hypothesised that Bax

may interact with the MPT-pore to induce pore-opening that would lead to expansion of the mitochondrial matrix and subsequent rupture of the OMM (Loeffler & Kroemer, 2000). The MPT-pore inhibitor CSA has also been shown to inhibit apoptosis in a variety of cells under a range of stimuli. However, Cyp D is one of several cyclophilin isoforms which bind CSA with similar affinities e.g. cyclophilin-A (cytosol), cyclophilin-B (endoplasmic reticulum). The selective suppression of Cyp A using antisense RNA in a neuronal cell line mimicks the capacity of CSA to block apoptosis induced by staurosporine, NO and other stimuli (Capano et al., 2002b). In other studies using isolated mitochondria the target for CSA can only be Cyp D since this is the only cyclophilin that is present in mitochondria (Connern & Halestrap, 1992, Crompton, 2003). Bax-induced cytochrome c release from isolated mitochondria, in the presence of Ca^{2+} was suppressed by CSA (Narita et al., 1998) but in the absence of calcium it was not (von Ahsen et al., 2000). A more recent report has shown that t-Bid–induced cytochrome c release from isolated mitochondria was inhibited by CSA (Scorrano et al., 2002). Electron microscopy studies revealed that the narrow tubular junctions connecting the lumen of the cristae with the intermembrane space opened up under the influence of tBid facilitating the cytochrome c diffusion out of the lumen to the outer membrane. This study showed that the cytochrome c associated with the IMM would need to pass through these junctions to gain access to the OMM, from where it would be released into the cytosol. Other studies using isolated mitochondria have shown MPT is not involved in the Bax-induced permeabilisation of the OMM. Doran & Halestrap (Doran & Halestrap, 2000) reported that Bax dimers were present in Percoll-purified rat liver mitochondria and can induce the release of cytochrome c from the

mitochondria. They showed this process occurs rapidly and without the concomitant loss of adenylate kinase indicating that a specific mechanism is involved and therefore rupture of the OMM does not occur. They found that dextran which maintains contact sites between the OMM and the IMM inhibited cytochrome c release suggesting that contact sites may play a role in the regulation of cytochrome c release. In addition their results showed that the MPT-pore inhibitor, CSA, did not prevent the release of cytochrome c and it was concluded that MPT was not involved in cytochrome c release. Another study showed that the addition of Bax to rat heart mitochondria lead to the uncoupling and inhibition of respiration without MPT occurring (Appaix et al., 2002). The effects of full-length and C-terminally truncated Bax on respiration rate, membrane potential, MgATPase activity and the kinetics of the regulation of respiration were studied in isolated rat heart mitochondria and permeabilised cardiomyocytes. It was concluded that full-length Bax affects the OMM and the IMM in three different ways. The first is by causing the opening of pores in the OMM. The second is by inhibiting some segments of the respiratory chain and the third by uncoupling the IMM by increasing proton leak without opening of the MPT-pore. Their results showed that the MPT-pore inhibitor CSA prevented none of these Bax-induced effects.

Different mechanisms for the release of apoptogenic proteins from the IMS may operate depending on the pathology involved. The MPT-pore may be a more relevant mechanism in conditions such as ischaemia/reperfusion injury when there are rises in intracellular Ca^{2+} levels and reactive oxygen species (ROS), which activate MPT. However, the question remains unanswered as to whether the rupture of the OMM and

release of apoptogenic proteins is mediated by Bax binding to MPT-pores or whether induction of the MPT by Ca^{2+} is sufficient to cause lysis of the OMM and the release of proteins from the IMS. In neurodegenerative disorders such as strokes, the glutamate receptors are overstimulated leading to prolonged increases in cytosolic Ca^{2+}which can lead to the release of cytochrome c (Sugawara et al., 1999). A later study showed that this calcium-induced cytochrome c release from CNS mitochondria was the result of MPT and rupture of the OMM (Bustrovetsky et al., 2002). However, this study did not investigate whether or not Bax or any other Bcl-2 protein played a role in the permeabilisation of the OMM. In another study Cao and co-workers (Cao et al., 2001) demonstrated that Bax translocates from the cytosol to the mitochondria in rat neurons after transient cerebral ischaemia. This study showed that the ANT ligand, bongkrekic acid, prevented the co-immunoprecipitation of Bax and ANT and Bax triggered pro-caspase-9 release from the IMS of isolated brain mitochondria. These results clearly showed that Bax participated in apoptosis in ischaemic rat neurons but the role the MPT might play in this process was not investigated.

[1.8.6] Bax-induced permeabilisation of the OMM and mitochondrial fission/fusion

Mitochondria are capable of forming interconnected networks which are regulated by a dynamic balance of organelle fusion and fission (Mozdy & Shaw, 2003; Scott et al., 2003). Recent studies have suggested that these processes are involved in the regulation of apoptosis. In mammalian cells in the early stages apoptosis the mitochondrial network is destroyed (Frank et al., 2001; Karbowski & Youle, 2003). The precise mechanism by which apoptotic fragmentation of the mitochondria occurs is

not known, however, it is thought to be dependent on the activation or fission (Frank et al., 2001; Breckenridge et al., 2003) or an inhibition of fusion (Karbowski et al., 2004) or perhaps a combination of both. During apoptosis Bax and Bak translocate to the mitochondria and co-localise with proteins involved in mitochondrial dynamics (Frank et al., 2001; Breckenridge et al., 2003), for example, Drp 1 (Smirnova et al., 1998) which is a dynamin-related GTPase involved in fission and Mfn which is involved in fusion (Ishihara et al., 2003, Santel & Fuller, 2001). One explanation as to how the mitochondrial fusion/fission balance affects apoptosis is that fission and fusion events alter the mitochondrial lipid composition that can influence apoptosis. It has been reported that cardiolipin is required for Bax mediated permeabilisation of liposomes (Kuwana et al., 2002) and for the functioning of tBid (Lutter et al., 2000). Changes in mitochondrial dynamics may alter the cardiolipin content of the OMM making it more susceptible to Bax-induced permeabilisation.

[1.9] Apoptosis and ischaemia in cardiomyocytes

Cardiomyocytes are contractile cells of the heart that are terminally differentiated. Although recently it was shown that a subpopulation of cardiomyocytes might re-enter the cell cycle (Anversa et al., 2002), it is unlikely that this is sufficient to compensate for any substantial loss of these cells. Therefore cardiomyocyte cell death as a result of ischaemic/reperfusion injury, for example, has a significant impact on cardiac function. One of the main insults that are thought to lead to cell death is oxidative stress. Reactive oxygen species (ROS) are produced in the ischaemic heart (Vanden Hoek et

al., 1997, Becker et al., 1999) and these are substantially increased following reperfusion (Ferrari et al., 1998). *In vivo* ROS can be produced by inflammatory cells (Duilio et al., 2001) but in cardiomyocytes subjected to simulated ischaemia mitochondria are the main source (Becker et al., 1999). Recently a correlation between increased ROS production and cardiomyocyte apoptosis has been reported (Qin et al., 2003). Ischaemic/reperfusion injury can result in cell death by either necrosis or apoptosis. In addition, cardiomyocyte cell death sharing features of apoptosis and necrosis has been reported (Leist & Jaattela, 2001). The opening of MPT-pores is a key event in ischaemic/reperfusion injury (reviewed in Halestrap et al., 2004) and can lead to necrotic cell death or apoptosis. Under normal physiological conditions MPT-pores are closed and the IMM is permeable to a few selected metabolites and ions. However under pathological conditions which give rise to increased intramitochondrial calcium and ROS, the MPT-pores open and this has two major consequences. Firstly, although small molecular weight solutes move freely across the IMM, proteins are retained within the matrix and as a result exert a colloidal osmotic pressure that causes mitochondria to swell. The unfolding of the cristae allows the matrix to expand without rupture of the IMM, the OMM breaks and this will lead to the release of proteins from the IMS. Secondly the IMM becomes freely permeable to protons. This uncouples oxidative phosphorylation, causing the proton-translocating ATPase to reverse direction and actively hydrolyse ATP. Under such conditions, intracellular ATP concentrations rapidly decline, leading to the disruption of ionic and metabolic homeostasis and the activation degradative enzymes such as phospholipases, nuclease, and proteases. These changes cause irreversible damage and lead to necrotic cell death (Halestrap et al.,

2004). However, if the pathological insult is less severe and MPT-pore opening is transient, ATP levels may be maintained and the cells may recover. Another outcome, apoptotic cell death may occur if MTP-pore opening occurs in some of the mitochondria within a cell but not others so that ATP levels are maintained but rupture of the OMM occurs resulting in the release of apoptogenic proteins from the IMS. The role that Bax plays in apoptosis occurring under these conditions has not been fully investigated. Previous *in vitro* studies by Pastorino and co-workers showed that Bax was capable of inducing MPT in isolated mitochondria in the presence of calcium (Pastorino et al., 1999). Therefore it is possible that Bax and Ca^{2+} may act synergistically to induce the release of apoptogenic proteins from the IMS in ischaemic/anoxic-induced apoptosis.

The work in this thesis is aimed at determining which mitochondrial membrane proteins interact with Bax during apoptosis. In particular *in vitro* studies with GST-Bax were used to determine whether or not Bax could interact with reconstituted components of the MPT-pore complex, VDAC, ANT and Cyp D. Only then could the MPT-pore complex be implicated as a mechanism for Bax-induced permeabilisation of the OMM. Rat cardiomyocytes were transfected with GFP-Bax and treated with sodium cyanide to induce simulated ischaemia. A time-course of GFP-Bax translocation from the cytosol to the mitochondria was observed in single cardiomyocytes using fluorescence microscopy. Other work presented in this thesis focuses on a novel method used in an attempt to identify the mitochondrial calcium uniporter protein responsible for the transport of Ca^{2+} across the IMM.

The specific aims of each of the results chapters are:

Chapter 3:

To obtain pure recombinant GST or His_6-tagged full-length Bax, C-terminally truncated Bax (BaxΔc) and Bcl-X_L

Chapter 4:

To show that the GST-tagged Bax proteins were biologically active by inducing cytochrome c release from isolated mitochondria.

To examine Bax interaction with the mitochondrial membrane proteins VDAC and ANT *in vitro*.

To find out if Bax-VDAC-ANT interactions were affected by the removal of the hydrophobic C-terminus of Bax.

To examine the effects of different detergents on VDAC/ANT binding to Bax

To examine the effects of Bcl-X_L, atractyloside and bongkrekate on VDAC/ANT binding to Bax

Chapter 5

To examine GFP-Bax translocation from the cytosol to mitochondria in single primary rat cardiomyocytes during apoptosis induced by sodium cyanide using fluorescence microscopy

To determine whether VDAC, ANT and Cyp D co-immunoprecipitate with GFP-Bax localised to mitochondria in rat cardiomyocytes treated with sodium cyanide

Chapter 6

To identify the calcium uniporter in rat liver mitochondria

Chapter 2: Materials and Methods

[2.1] Materials

The Hanks balanced salt solution used in the preparation of the rat cardiomyocytes was obtained from Gibco-BRL and the M199 medium used for the culture of the rat cardiomyocytes was produced by Sigma. Plasmids pQE-31 and pQE-60 contained human bax and 3' truncated baxΔc (which lacks the nucleotide sequences coding for the C-terminal 22 amino acids) respectively. Bax was ligated into the *Bam HI* and *Sac I* sites. BaxΔc was ligated into the *Nco I* and *Bgl II* sites. Human bcl-X_L was ligated into the *Bam HI* and *Bgl II* sites of pQE-60. The full-length recombinant Bax protein contains the hexahisitidine tag at the N-terminus. BaxΔc and Bcl-X_L contain the tag at the C-terminus. These plasmids were obtained from Dr. John Ward, Department of Biochemistry and Molecular Biology, UCL. The GFP-Bax construct was a gift from Michela Capano in this laboratory (Capano & Crompton, 2002). Full-length bax cDNA was ligated into the *Hind*III and *EcoR*I restriction sites of pEGFP-C3. The pGEX-3X plasmid containing cyp D (rat) cDNA was produced by Dr. Sukaina Virji in this laboratory (Crompton et al., 1998). The cyp D lacked the pre-sequence encoding the mitochondrial targeting sequence and was ligated into the *BamHI* and *EcoRI*.

The nucleotide triphosphates (dNTP), primers and pfu polymerase were obtained from Pharmacia Biotech, and the DMSO, ethidium bromide and markers for agarose gel electrophoresis (phage λ digested with *Pst I*) were from Sigma. The pGEX-3X was from Amersham Pharmacia. Restriction enzymes and the T_4 ligase were from New

England Biolabs. The pQE-31 and pQE-60 plasmids were produced by Qiagen and the pEGF-C3 plasmid was obtained from Clonetech.

Lipofectamine 2000 reagent was obtained from Life Technologies, Paisley, Scotland. The Nonidet-P40, agarose-glutathione (GSH), reduced GSH, protease inhibitor cocktail and imidazole were obtained from Sigma. Columns used for GST-Bax purification were from Pierce. The nitrilotriacetic acid (NTA) column (5ml) and the anion-exchange column, Mono Q HR 5/5 (1ml), were obtained from Amersham Pharmacia. The BCA protein assay reagents were supplied by Pierce. SDS-PAGE was carried out using the SE 250-Mighty Small II Slab Gel Electrophoresis unit, Hoeffer Scientific Instruments, San Francisco. Nitrocellulose sheets were obtained from Schleicher and Schuell, Dassel, Germany. Enhanced chemiluminescence reagents (ECL) were obtained from Amersham Pharmacia and X-ray film from Fujifilm. Anti-human antibodies to Bax (monoclonal)(6A7), Bcl-X_L (polyclonal) and cytochrome c (monoclonal) (clone 7H8.2C12) were obtained from Pharmingen, CA. Anti-human monoclonal VDAC antibody clone 31HL was obtained from Calbiochem. Anti-rat polyclonal antibody was raised against the peptide YDEIKKYV, corresponding to the C-terminus of rat ANT-1. The polyclonal anti-Cyp D antibody was raised against the peptide CSDGGARGANSSSQNP, corresponding to the amino acids 1-16 after cleavage of the mitochondrial targeting sequence. Both of these antibodies were produced by Dr. Veronica Doyle in the laboratory. The secondary antibodies were both polyclonal. An anti-mouse IgG conjugated with horse-radish peroxidase was used to detect the primary monoclonal antibodies and this was from Calbiochem. An anti-rabbit IgG conjugated with horse-radish peroxidase was used to detect the primary

polyclonal antibodies ANT and CypD. Anti-GFP monoclonal antibody (clone 1E4) was obtained from MBL laboratories, Nagoya, Japan. Factor Xa used to cleave GST-Bax was obtained from Amersham Biosciences. MitoTracker red used for fluorescence microscopy was supplied by Molecular Probes. The atractyloside was obtained from Sigma and the bongkrekic acid from Calbiochem.

[2.2] Cell culture and transfection

Primary cultures of cardiomyocytes were prepared from 14 day-old Sprague-Dawley rats and seeded on to laminin-coated glass coverslips according to the method used by Doyle et al. (Doyle et al., 1999). Briefly, rats were sacrificed by cervical dislocation and their hearts removed, chopped finely and incubated with 5ml of Hanks balanced salt solution containing 0.8mg/ml collagenase II, 20μg/ml DNase II, 20units/ml penicillin, 20μg/ml streptomyocin, 1mM taurine, 40μM $CaCl_2$ for 15 minutes at 35°C. The procedure was repeated 3 times, each time with fresh medium. After gentle centrifugation, cells (approximately 10^7) were resuspended in M199 culture medium containing 20units/ml penicillin, 20μg/ml streptomyocin, 2μg/ml vitamin B_{12}, and 10% v/v fetal calf serum. The cells were then subsequently seeded onto laminin-treated glass coverslips at a density of $5x10^5$ cells/ 0.5ml and incubated in an atmosphere of CO_2/ air (1:19) at 37°C. After 3 hours, 1μM cytosine arabinoside was added to limit the growth of fibroblasts (Tanaka et al., 1994). Cells were transfected with pEGFP-C3-bax after 2 days of culture, replacing the medium with fresh culture media after 5 hours incubation. Optimum transfection was obtained with 1μg of plasmid DNA and 3μl of

Lipofectamine per coverslip. Cells were used for fluorescence microcopy 1-2 days after transfection.

[2.3] Subcloning bax and baxΔc into pGEX

[2.3.1] PCR to obtain bax and baxΔc

PCR was used to amplify bax and baxΔc present in the pQE-31 and pQE-60 plasmid, respectively. Each 50µl reaction contained: 2ng of template DNA, 10pmol of each primer, 1µmol of dNTP, 5µl of 10x buffer, 2.5 units of pfu polymerase and 5% w/v DMSO. The complete reaction mix minus polymerase was preheated to 99°C for 3 minutes before addition of the polymerase and subjection to the following PCR protocol: denaturation for 1 minute at 95°C, annealing for 1 minute at 65°C and elongation for 1 minute 30 seconds at 72°C. This cycle was repeated 28 times followed by a final elongation step at 72°C for 5 minutes. The primers were designed to be complementary to the 5' and the 3' termini of bax and baxΔc. The forward primers contained a *Sma I/ Xma I* site and the reverse primer an *EcoRI* site to enable the PCR product to be ligated into the pGEX-3X vector.

The primer sequences used were:

bax forward primer- **5'**-TGACC**CCGGG**ATGGACGGGTCCGGGGAGCA **3'**

baxΔc reverse primer-**5'**- TGAC**GAATTC**TTACTGCCAAGTGGGGCGTCCAA **3'**

bax reverse primer-**5'**- CGCTCA**GAATTC**TCAGCCCATCTTCTTCCACATG **3'**

The restriction sites within the primers are shown in bold.

[2.3.2] Ligation into pGEX-3X

The plasmid vector pGEX-3X contained the *gst* (glutathione-s-transferase) gene between the transcriptional start site and a multiple cloning site, enabling a *gst* gene fusion to be created after ligation with the PCR product. The PCR products and pGEX-3X were digested with *Eco RI* and *Xma I.* The latter is an isoschizomer of *Sma I* producing "sticky ends", which increases the efficiency of the ligation reaction compared to a blunt end ligation if *Sma I* was used. The digest (20μl) contained: PCR product and pGEX-3X (3:1), *Xma I* buffer, 20 units of *Xma I* and 20 units of *Eco RI.* Digests were incubated at 37°C for 2 hours. The digested pGEX-3X (10% 0f each digest) was analysed by agarose gel electrophoresis. Gels contained TAE buffer (100mM Tris-acetate, 10mM EDTA, pH 8.0) and ethidium bromide (1μg/ml) was added to molten gels to allow the DNA to be visualised under uv light. Samples were prepared for electrophoresis by the addition of 10x sample loading buffer containing 5% glycerol, 100mM Na_2 EDTA, 1% w/v SDS and 0.1% bromophenol blue. The DNA was approximately quantified by comparison with known amounts of phage λ DNA cut with *Pst I.* Digests were denatured with phenol/chloroform (1:1). The upper phase was collected and 0.5μl of glycogen solution was added to facilitate pellet identification. Ethanol (3 volumes) was added and the tubes were stored at -60°C for 30 minutes to precipitate the DNA. The DNA and the glycogen were subsequently pelleted at 10 000 rpm for 15 minutes, before removal of the ethanol and washing in 70 % ethanol with final suspension in 4μl of water. The DNA was ligated by addition of 1μl of 10x buffer, 1μl of T4 ligase (10 units) and 4μl of water and incubated at 16°C overnight.

[2.3.3] Transforming E. coli with recombinant bax – pGEX-3X plasmids

The ligation mix derived as described above (7µl) was used to transform *E.coli* XL-blue competent cells. A 300µl aliquot of these cells was thawed on ice, the ligation mix was added and the cells were kept on ice for 40 minutes. This was followed by a 10-minute incubation at 37°C for 1 hour Luria Bertani (LB) broth (1ml) was mixed with the cells and the incubation extended for a further 1 hour. The cells were plated on LB-agar plates containing 100µg/ml ampicillin and grown overnight.

[2.3.4] Screening transformants

The plasmid DNA from the positive transformants was prepared using a Qiagen miniprep kit followed by digestion with the restriction enzymes *Xma I* and *Eco RI* to cut out the bax inserts. The digested DNA was analysed by agarose gel electrophoresis. Recombinant plasmids were sequenced to check for errors that may have occurred during the amplification of bax.

[2.4] Expression of recombinant proteins

[2.4.1] Expression of GST-Bax and GST-BaxΔc

For expression of GST-BaxΔc, a single colony was inoculated into 10 ml of LB medium containing 100µg/ml of ampicillin and was left to grow at 37°C overnight. This was subsequently used to inoculate 100ml of fresh LB medium, 100µg/ml ampicillin. The cells were grown to an OD_{600nm} of 0.8 and induced with 0.2mM IPTG and grown for a further 3 hours before harvesting. For GST-Bax expression, a single

colony was inoculated into 100ml of Terrific broth (TB) containing 100μg/ml of ampicillin. This medium contained: 12g peptone, 24g yeast extract, 4ml glycerol, 0.17M K_2PO_4 and 0.72M KH_2PO_4. The culture was grown at 37°C overnight and expression was induced by the addition of 10μM IPTG with cells being cultured for 24 hours at 22°C before harvesting. To obtain the recombinant protein, cells were resuspended in buffer (20ml) containing 50mM HEPES, 50mM NaCl, 0.5mM EDTA, 5mM DTT, 10μl/ ml protease inhibitor cocktail, 1mM PMSF, 1% Nonidet P-40 detergent, pH 7.3. Cells were lysed in this solution by intermittent sonication (20 secs on/ 20 secs off) for a total of 6 minutes. The lysate was then centrifuged at 10000 rpm for 5 minutes to pellet the bacterial membranes.

[2.4.2] Expression of GST-Cyp D and GST

A single colony of XL-blue *E. coli* transformed with pGEX-3X-*cyp D* was inoculated into 10ml of LB medium containing 100μg/ml of ampicillin and was left to grow at 37°C overnight. Fresh LB medium (10ml) containing 100μg/ml of ampicillin was inoculated with 1ml of the overnight culture. Cells were grown to an OD_{600nm} of 0.6 and GST-Cyp D expression was induced with 0.4mM IPTG and then grown for a further 3 hours before harvesting. The expression of GST was performed in the same way using XL-blue cells transformed with pGEX-3X.

[2.4.3] Expression of hexahistidine-tagged Bax, BaxΔc and Bcl-X_L

Expression was carried out as described for the GST-Bax proteins except 1 litre of culture was used instead of 100ml and the cells were induced with 1mM IPTG.

[2.4.4] Purification of GST-tagged proteins

The GST-tagged proteins were purified using a column (0.5ml) consisting of an agarose-bead matrix that had been chemically cross-linked to glutathione after expoxy-activation via sulphur atoms and a 12-atom spacer. The bacterial cell lysate was applied to a column pre-equilibrated with sonication buffer followed by washing with 5 column-volumes of the same buffer. The GST-tagged protein was eluted with 0.5ml of 50mM HEPES, 50mM GSH, 50mM NaCl.

[2.4.5] Cleavage of GST-Bax

The pGEX-3X plasmid (see figure [3.6]) encodes a factor Xa protease recognition site between gst and multiple cloning sites. This enables the cleavage of the fusion protein in a single digestion step. The factor Xa solution was prepared using cold water (4°C) to give a final concentration of 1U/µl. The cleavage of the fusion protein was performed whilst GST-Bax was bound to the glutathione-agarose matrix. The matrix was washed with 10 bed volumes of factor Xa cleavage buffer containing 50mM Tris-HCl, pH 7.5, 150mM NaCl, 1mM $CaCl_2$. For each ml of glutathione-agarose 50µl of factor Xa solution was added to 950µl of cleavage buffer. The glutathione-agarose was incubated with the factor Xa for 24 hours at 4°C with gentle agitation. Bax was obtained in the supernatant from the glutathione-agarose by centrifugation at 5000 rpm for 5 minutes.

[2.4.6] Purification of hexahistidine-tagged BaxΔc and Bcl-X_L

A pre-packed (5ml) NTA column attached to an FPLC system was chelated with Ni^{2+} ions ($NiCl_2$ solution, 200mM) to produce an affinity matrix that bound the hexahistidine-tag. The bacterial lysate containing BaxΔc-His_6 or His_6-Bcl-X_L was applied to the column. After washing with 5 volumes (25ml) of buffer containing 50mM HEPES, 50mM NaCl, pH 7.3, 0.5% Nonidet-P-40, bacterial protease inhibitor cocktail (10µl/ml), the bound proteins were eluted with a two-step imidazole gradient: 50-150mM over 8ml then 0.15 to 1M over the next 8ml. The eluate from the Ni^{2+}-NTA column containing BaxΔc-His_6 was diluted 25x in buffer containing 50mM MES, 50mM NaCl, pH 6.0 and applied to a Mono Q HR 5/5 FPLC anion-exchange column equilibrated with the same buffer. A NaCl gradient (50-500mM) was used to elute the bound proteins. Fractions containing the BaxΔc-His_6 protein were either dialysed against 50mM HEPES, 100mM NaCl, 30% glycerol w/v, pH 7.3 or were concentrated in centricon 30 tubes and diluted with the above buffer. These samples were stored at -60°C. The eluate from the Ni^{2+}-NTA column containing His_6-Bcl-X_L was diluted 25x in buffer containing 50mM HEPES, 50mM NaCl, pH 7.3 and applied to the Mono Q column equilibrated with the same buffer. A NaCl gradient (50-500mM) was used to elute the bound proteins. The fractions containing Bcl-X_L were stored in 30% glycerol at -60°C

[2.5] Separation of proteins by Sodium Dodecyl Sulphate-Polyacrylamide Gel Electophoresis (SDS-PAGE)

[2.5.1] Reagents for SDS-PAGE

The reagents for SDS-PAGE were prepared as follows: acrylamide solution was made by dissolving 48g of acrylamide, 1.5g of N, N'-methylene-bis-acrylamide in water to give a final volume of 100ml. The gel buffer contained: 5M Tris-HCl, 0.3% w/v SDS, pH 8.45. Anode buffer contained 200mM Tris-HCl, pH 8.9 and cathode buffer contained 100mM Tris, 68mM tricine, 1% w/v SDS, pH 8.2.

The reagents were added together as shown in table [**2.1**] to make the resolving and stacking gels.

Table [2.1] Reagents for SDS-PAGE

Volume (ml)	**Stacking gel 1 %**	**Resolving gel 15 %**
Acrylamide	1	9
Gel buffer	10	10
Glycerol	-	3
Water	8.4	7.7

Gels were polymerised by the addition of 30µl 1% w/v APS and 3µl TEMED.

[2.5.2] Preparation of protein samples for loading

Samples were heated at 95°C for 5 minutes in the ratio 3:1 with sample buffer containing 0.125mM Tris-HCl pH 6.8, 2mM EDTA, 6% SDS, 20% glycerol, 0.025% bromophenol blue and 5% β-mercaptoethanol.

[2.5.3] Electrophoresis

Electrophoresis was carried out at 20mA (current limiting) until the dye front moved into the resolving gel and then 40mA until the dye front had reached the bottom of the gel.

[2.5.4] Coomassie staining

Gels were fixed for 30 minutes in 50% v/v methanol, 10% v/v glacial acetic acid and were stained in a solution containing 0.02% w/v Coomassie-Brilliant Blue in 10% v/v glacial acetic acid for 2 hours. The gels were destained in four successive washes of destaining solution containing 10% glacial acetic acid and 40% v/v methanol over 4 hours.

[2.5.5] Silver staining

The gels were fixed as described above. Gels were subsequently soaked in water for at least 1 hour with 3 changes of water. The silver stain was prepared from 21ml of NaOH (0.36% w/v), 1.4ml of NH_4OH (30%), 4ml of $AgNO_3$ (20%) and 100ml of water. Gels

were soaked in this solution for 15 minutes and then rinsed in water. The proteins were visualised with developing solution containing: citric acid (0.005% w/v) and formaldehyde (0.019% v/v). Gels were placed in acetic acid (1% v/v) to stop further colour development.

[2.6] Western blotting

[2.6.1] Transfer of proteins from a gel onto nitrocellulose

The gels and nitrocellulose membranes were placed between 6 sheets of Whatmann filter paper soaked in transfer buffer containing: 144mM Tris, 117mM glycine, methanol (20% v/v) and SDS (0.1%w/v), pH 9.2. The transfer of proteins from the gel to the nitrocellulose was carried out by a Biorad wet transfer unit at 100V for 1 hour 30 minutes at room temperature.

[2.6.2] Probing the nitrocellulose membranes with antibodies

The nitrocellose membranes were blocked with non-fat dried milk (Marvel, 8% w/v) in phosphate buffered saline (PBS) and Tween 20 (0.1%v/v) for 1 hour at room temperature. Membranes were then washed in PBS, Tween 20 (0.1% v/v) for 15 minutes and twice for 5 minutes at room temperature. The antibodies were diluted in PBS containing non-fat dried milk (3% w/v), Tween 20 (0.1% v/v) to give the following concentrations: Bax- 0.66μg/ml, Bcl-X_L- 0.7μg/ml, cytochrome c- 0.5μg/ml, VDAC-1μg/ml. ANT and Cyp D antibodies were diluted 5000x and 3000x, respectively. The anti-mouse IgG was diluted to give a final concentration of 0.5μg/ml and the anti-rabbit IgG to 0.67μg/ml. The membranes were probed with the primary antibody for 1 hour at

room temperature and were washed for 15 minutes followed by two 5 minute washes before the addition of the secondary antibody for 1 hour at room temperature. After final washing the blots were developed using ECL reagents and X-ray film. As an alternative to X-ray film a Fuji-LAS 100 phosphoimaging system was sometimes used.

[2.6.3] Assay for cytochrome c release

Rat heart mitochondria were isolated as described in section **[2.7.1]** and resuspended in respiratory buffer containing 1mM glutamate and 1mM malate. GST-BaxΔc, in buffer containing 50mM HEPES, 100mM NaCl, 0.5mM EDTA, 5mM DTT, 10μl/ ml protease inhibitor cocktail, 1mM PMSF, pH7.3, was added at 125nM, 250nM, 500nM and 1μM to the mitochondria and incubated at 37°C for 15 minutes. The mitochondria were pelleted and the supernatant was filtered using a 0.2μM Millipore filter. The proteins in the pellets and supernatant were separated by SDS-PAGE and cytochrome c was detected by Western blotting.

[2.6.4] BCA Protein assay

GST-BaxΔc was quantified using the BCA protein assay using known concentrations of BSA standards. Each well of the microtitre plate contained: 25μl of each standard or unknown sample and 200μl of working reagent. The working reagent was prepared by mixing 50 parts of BCA reagent A and 1 part of BCA reagent B. The contents of each well were mixed and the plate was incubated at 37°C for 30 minutes. The absorbance of each well was read at 562nm. A standard curve of absorbance at 562nm against the

protein concentration for the BSA standards was used to calculate the concentration of the GST-BaxΔc.

[2.7] Preparation of rat heart mitochondria and mitochondrial membranes

[2.7.1] Rat heart mitochondria

Mitochondria were isolated from the hearts of male Sprague-Dawley rats (200-300 g body weight) using the following protocol. Rats were sacrificed by cervical dislocation and their hearts removed and placed into an ice-cold solution of 210mM mannitol, 70mM Tris-HCl, 1mM EDTA and 0.5mg/ml BSA (bovine serum albumin) (MSTEB) at pH 7.2. The hearts were chopped into small pieces with a pair of scissors and transferred to a 30 ml centrifuge tube (1 tube for each heart) and homogenised for approximately 10 seconds using a Polytron homogeniser. The polytron probe was pre-cooled to 4°C before use. Samples were centrifuged at 1800 rpm for 5 minutes in a refrigerated superspeed centrifuge, Sorvall RC5B (rotor-SS34) at 4°C. Supernatant fluids were decanted into new 30ml tubes and centrifuged at 7500 rpm for 8 minutes to sediment the mitochondria. The pellets were then washed by resuspending in a small volume of ice-cold 210mM mannitol, 70mM sucrose, 10mM Tris-HCl (MST) pH 7.2 using a glass test-tube filled with crushed ice. The volumes were made up to 30ml with ice-cold MST before further centrifugation at 1800rpm for 5 minutes at 4°C. Pellets were then washed as before; another centrifugation step carried out at 7500rpm for 8 minutes at 4°C before the mitochondrial pellets were finally resuspended in MST at around 10 mg/ml of protein and kept on ice until ready for use.

[2.7.2] Quantification of mitochondrial protein

Protein was estimated by a modified biuret method (Kroger & Klingenberg, 1966). BSA was used as a standard. Each cuvette contained: 0.5ml of sample, 0.5ml of water, 0.2 ml of 4 % sodium cholate, 2 ml of 10% sodium hydroxide and 0.3 ml of 1% copper (II) sulphate. The reactions were mixed and left to stand for 10 minutes, after which the absorbance of the sample was read against the blank at 540 nm.

[2.7.3] Preparation of mitochondrial membranes

Lysosomal membrane contamination was removed from isolated mitochondria using digitonin. This detergent is a naturally occurring steroid glycoside that binds to and extracts cholesterol. At lower concentrations (0.0125mg/mg of mitochondrial protein) it selectively removes the lysosomal membranes that contain more cholesterol than the mitochondrial membranes. When higher concentrations of digitonin are used (above 0.2mg/mg of mitochondrial protein) the outer mitochondrial membrane is selectively lysed whilst leaving the inner mitochondrial membrane intact. Membrane lysis is not only dependent on the concentration of digitonin used but also on the protein concentration. At lower protein concentrations (<20mg/ml) the efficiency of outer membrane removal is substantially reduced (Boyer et al., 1994).

After protein quantification, mitochondrial suspensions were diluted to 2mg/ml in MST and digitonin was added (0.06mg/mg of mitochondrial protein) before the suspensions were incubated on ice for 15 minutes. Mitochondria were centrifuged at 8000 rpm for 10 minutes and were resuspended in buffer containing: 50mM HEPES, 100mM NaCl,

1mM PMSF, 0.5mM DTT, 1mM leupeptin, 1mM antipain, 1mM pepstatin, pH 7.3. Sonication was used to lyse the mitochondria and was carried out intermittently (10secs on /10 secs off) for a total of 6 minutes. The mitochondrial membranes were pelleted in a Beckman 7L ultracentrifuge (70 Ti rotor) at 40 000 rpm for 30 minutes and the pellets stored at –60 °C until use.

[2.7.4] Detergent extraction of membrane proteins from the mitochondrial membranes

Proteins in the mitochondrial membranes were extracted using CHAPS or Nonidet P-40 detergent. A mitochondrial membrane pellet containing approximately 20-30mg of protein was added to 2ml of buffer containing: 50mM HEPES, 100mM NaCl, 1mM ATP, 1mM $MgCl_2$, 1mM PMSF, 6% w/v CHAPS and 5mM final concentration of a broad range protease inhibitor cocktail. The membrane pellet was placed in a hand-held glass homogeniser and homogenised for 5 minutes and then left on ice 45 minutes. The extract was then centrifuged at 10 000rpm for 15 minutes and the pellet discarded. Atractyloside (50μM), bongkrekic acid (50μM) or His-Bcl-X_L/Bax (125ng) was added to 50μl of the solubilised mitochondrial membrane proteins (0.25mg of mitochondrial membrane proteins) before addition to the immobilised fusion protein (section **[2.7.5]**).

[2.7.5] Addition of the mitochondrial membrane extract to GST-Bax, GST-BaxΔc and GST-Cyp D

The fusion proteins were immobilised on the agarose-GSH matrix as described in section **[2.4.3]**. Matrix (50μl), which consisted of agarose-GSH-GST-Bax or truncated

Bax or Cyp D instead of full-length Bax, was placed in Eppendorf tubes with the 50µl of supernatant described above. The matrix was washed with 600µl of wash buffer containing: 50mM NaCl, 10mM HEPES, 25% glycerol, 1mM EGTA, 8µM ADP, 8µM ATP, 8mM DTT and 0.5mM $MgCl_2$ and this was repeated 5 times. Proteins that bound the agarose-GSH were eluted with 50µl of 50mM GSH, 50mM NaCl, pH 7.3 and were analysed by SDS-PAGE and Western blotting.

[2.8] Immunoprecipitation

GFP-Bax was immunoprecipitated from cell extracts using an anti-GFP monoclonal antibody coupled to Sepharose beads. The coupling was carried out by incubating 30µg of antibody with 30mg of CNBr-activated Sepharose 4B in 0.5M NaH_2PO_4 and 1M NaCl, and left overnight in 100mM ethanolamine, pH 7.5 at 4°C. Cell extracts for immunoprecipitation were prepared by scraping the cells from the coverslips into lysis medium containing: 10mM HEPES, 100mM NaCl, 1mM EGTA, 1mM $MgCl_2$, 1mM KH_2PO_4, 6% w/v CHAPS, 1mM PMSF, pH 7.4 and 2µg/ml of each of the protease inhibitors aprotinin, pepstatin, leupeptin and antipain. Extracts were centrifuged at 12000 rpm for 5 minutes and each supernatant was gently shaken with 50µl of anti-GFP-antibody-coupled Sepharose for 2 hours at 4°C. The supernatant from each incubation was retained and the sepharose beads were washed 6 times in lysis buffer. The beads were then extracted with SDS sample loading buffer at 90°C for 3 minutes. The immunoprecipitated proteins were analysed by SDS-PAGE and Western blotting to detect whether VDAC was present. Blots were subsequently stripped and then re-probed to detect if ANT and Cyp D were present in the immunoprecipitated extract.

The nitrocellulose membranes were incubated at 50°C for 30 minutes in stripping buffer containing 100mM 2-mercaptoethanol, 2% w/v SDS, 62.5mM Tris-HCl, pH 6.7and then washed in PBS-Tween twice for 20 minutes. After blocking for 1 hour in non-fat dried milk (Marvel) 5% w/v the membranes were probed with anti-ANT or anti-Cyp D antibody (see section **[2.6.2]**).

[2.9] Fluorescence imaging

Cells on coverslips were incubated in 100mM NaCl, 4mM KCl, 24mM HEPES, 1mM $MgSO_4$, 1mM $CaCl_2$, 1mM KH_2PO_4, pH 7.4. Mitochondria were sometimes visualised with MitoTracker red before the induction of apoptosis with 1mM NaCN. For dual imaging, loading with MitoTracker Red was kept as low as possible i.e. 10ng/ml, 10 minutes at room temperature. Images were obtained with an Olympus 1X-70, fluorescence microscope (Micromax 140IE; Princeton Instruments) fitted with a cooled CCD camera and an excitation filter wheel (Sutter) with band-pass filters for the excitation of GFP (490nm) and the excitation of MitoTracker Red (570nm). Fluorescent light was collected via a poly chromic beamsplitter (51006 bs; Chroma) and a two-band-pass emission filter in the filter cube (530nm, 635nm; Chroma). The appropriate emission band was then selected by band-pass filters in a simple slider in the emission light path. Data was analysed by Metamorph Software (Universal Imaging) which allowed calculation of mean and S.D of the pixel intensities within individual cardiomyocytes.

[2.10] Ru 360 and the mitochondrial calcium uniporter

[2.10.1] Preparation of Ru360 from Ruthenium red

Ru 360 has the formula $[CH_3(NH_3)_4Ru\text{-}O\text{-}Ru(NH_3)_4CH_3]^{3+}$ and was prepared from a commercial preparation of ruthenium red by ion-exchange chromatography using CM-cellulose. Ruthenium red (500mg) was dissolved in 200ml of 100mM ammonium formate, pH 5.5, and applied to a 50ml CM-cellulose column pre-equilibrated with the same buffer. The ruthenium red was fractionated using an ammonium formate gradient (0.1M-1M). Ru360 was detected from its absorption maximum at 360nm (Ying et al., 1991). Following elution, Ru 360 was lyophilised and stored at -20°C. It was diluted in 10mM HEPES, 50mM KCl, pH7.3 before use.

[2.10.2] Ru 360 inhibition of Ca^{2+} influx into mitochondria

Mitochondria were prepared as described in section **[2.6].** Calcium uptake was measured using a Dual-wavelength Perkin–Elmer, model 356 spectrophotometer, operating at 375-385nm according to Goldstone et al (Goldstone et al., 1987). Mitochondria (2-3mg of protein) were added to 3ml of standard reaction mixture containing 120mM KCl, 0.5mM KH_2PO_4, 1mM $MgCl_2$, 10μM $CaCl_2$ and 1μg of rotenone/mg protein with 60μM arsenazo III as a Ca^{2+} indicator. Ru 360 was added as indicated. The mitochondria were energised by the addition of 6mM succinate and 20μM ATP to initiate Ca^{2+} uptake.

[2.10.3] Conjugating SAED and DAPPAC

SAED-Sulfosuccinimidyl 2-(7-azido-4-methylcoumarin-acetamido) ethyl-1,3-dithiopropionate (Pierce, Rockford, Illinois) is a heterobifunctional, amine reactive, water soluble, cleavable, photoreactive crosslinker. It also has the fluorescent molecule (AMCA) incorporated into its structure. This cross-linker has two functional groups: 1) a sulpho-N-hydroxysuccinimide ester which provides an activated carboxyl group for conjugation to the primary amino group of DAPPAC and, 2) a photoactive azido group forming a highly reactive nitrene on illumination. The linker between the two groups contains a cleavable disulphide bond. It has a maximum uv absorbance at 327nm and an extinction coefficient of 18 200$M^{-1}cm^{-1}$. The structure of SAED is shown below in figure [**2.1**]:

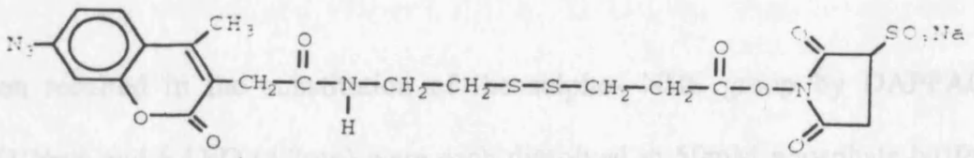

SAED
MW 621.6
Spacer Arm Length 22.5 Å

Figure [2.1] Structure of SAED

DAPPAC is a cobaltammine complex ion that was synthesised by Crompton and Andreeva (Crompton and Andreeva, 1994). SAED and DAPPAC were conjugated together in the dark.

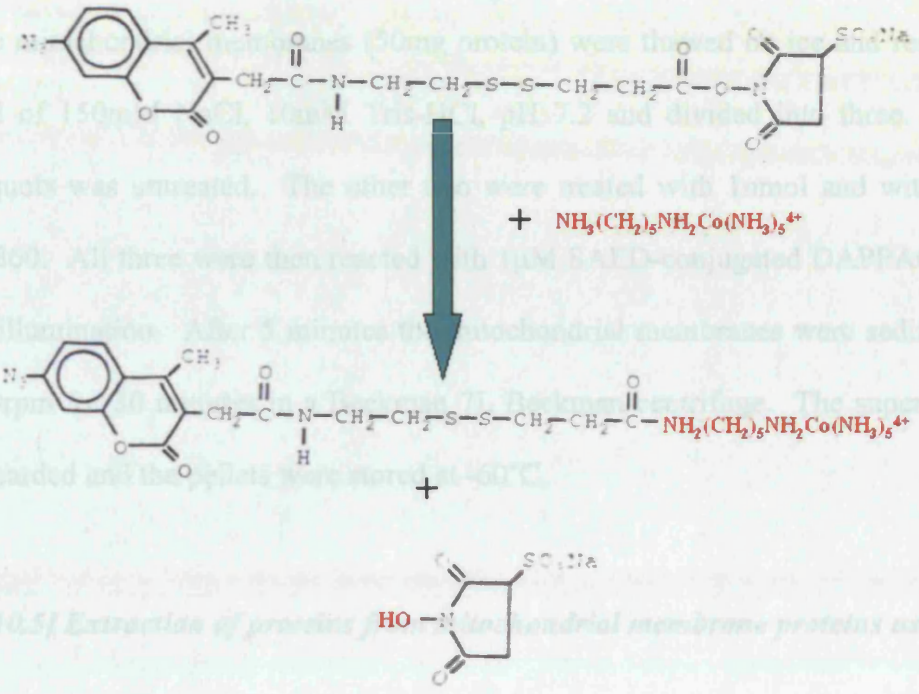

Figure [2.2] Conjugation of SAED and DAPPAC

The reaction resulted in the substitution of the sulpho- NHS group by DAPPAC. DAPPAC (10mg) and SAED (4.2mg) were each dissolved in 50mM phosphate buffer, pH 7.3, mixed, and incubated for 4 hours in the dark, after which conjugation was judged to be largely complete. Excess SAED was removed by addition of 100mM β-alanine and incubated for a further 4 hours. The conjugate was then stored in aliquots at -20°C.

Mitochondrial membranes were prepared as described in section **[2.7].**

[2.10.4] Photolabelling mitochondrial membranes with SAED-conjugated DAPPAC

The mitochondrial membranes (50mg protein) were thawed on ice and resuspended in 5ml of 150mM NaCl, 10mM Tris-HCl, pH 7.2 and divided into three. One of the aliquots was untreated. The other two were treated with 1nmol and with 10nmol of Ru360. All three were then reacted with 1μM SAED-conjugated DAPPAC under long uv illumination. After 5 minutes the mitochondrial membranes were sedimented at 40 000rpm for 30 minutes in a Beckman 7L Beckman centrifuge. The supernatants were discarded and the pellets were stored at -60°C.

[2.10.5] Extraction of proteins from mitochondrial membrane proteins using CHAPS

The mitochondrial membrane pellets were extracted using a hand-held homogeniser in 50mM HEPES, 100mM NaCl, 1mM $MgCl_2$, 1mM PMSF, 5mM final concentration of a broad-range inhibitor cocktail and 6%w/v CHAPS. 2ml of this medium was used to extract 30mg of mitochondrial protein. The homogenate was left on ice for 45 minutes and then the membrane extract was centrifuged in an Eppendorf centrifuge at 10000rpm for 10 minutes.

[2.10.6] Separation of mitochondrial membrane proteins using ion-exchange chromatography

The mitochondrial membrane extracts **[7.5]** were fractionated by FPLC (Pharmacia). The extracts were applied to a Mono Q HR 5/5 anion-exchange column and pre-equilibrated with the 50mM Tris-HCl, 100mM NaCl, pH 8.0. Proteins were eluted

using a NaCl gradient 100mM-500mM. The pass-through from the MonoQ was applied to a Mono S, cation-exchange column. The same buffer was used and a NaCl gradient was used as before. The fluorescence of the collected fractions was measured using a Perkin-Elmer fluorimeter.

Chapter 3: Results

Expression of Bax, C-terminally truncated Bax and Bcl-X_L as Fusion Proteins in *E.coli*

[3.1] Expression of hexahistidine-tagged Bax and hexahistidine-tagged C-terminally truncated Bax tagged proteins

Pure Bax protein was required in order to study its interaction with mitochondria. The simplest way to achieve this was to express Bax with a tag at either the C or N-terminus of the protein to enable purification using an affinity matrix. Bax fusion proteins could be coupled to an agarose affinity matrix to pulldown mitochondrial membrane proteins that interact with Bax after its translocation from the cytosol to the mitochondria during apoptosis (Wolter et al., 1997). Other groups have produced N-terminally-tagged Bax and BaxΔc. Workers in Jean-Claude Martinou's group expressed Bax and BaxΔc with N-terminal hexahistidine-tags (Lewis et al., 1998). Others have produced GST-Bax fusion proteins (Pastorino et al., 1999, von Ahsen et al., 2000). N-terminal tags may have been preferred for two reasons. Firstly, when Bax was expressed with a GST-tag present at the N-terminus of the fusion protein it was shown to reduce Bax toxicity to *E.coli* (Reed et al., 1999). Secondly, the C-terminus contains the hydrophobic membrane anchor that was initially thought to be essential for Bax interaction with mitochondria (Wolter et al., 1997). However, later studies showed that the C-terminus is not required for the cellular localisation of Bax or its ability to mediate cytochrome c release (Priault et al., 1999). *E. coli* strain M15 and BL21 cells, containing the

recombinant plasmids pQE31 and pQE60-containing human bax and baxΔc respectively, were used to produce the Bax proteins. The baxΔc was 3' truncated and the corresponding protein lacked 22 amino acids at the C-terminus. The tag encoded by the vectors consists of six histidine residues fused to the termini of the proteins (the N-terminus for Bax and the C-terminus for BaxΔc). This small 0.7kDa tag was less likely to affect the overall structure and function of the protein than a larger tag. This tag facilitates purification by chelating with the metal ion affinity matrix Ni^{2+}- NTA-agarose (Porath et al., 1975).

[3.1.1] Expression of His_6-Bax

E.coli strain M15 was co-transformed with plasmids pQE-31-bax, pQE-70- bcl-X_L Δc (3' truncated *Bcl-X_L*) and pREP4 containing the *lac* repressor gene. The full-length Bax protein has been shown to be toxic to *E.coli* (Asoh et al., 1998). Therefore the rationale for this system was to keep expression tightly regulated by controlling gene expression with the lac repressor encoded by the pREP4 plasmid and at the protein level by the Bcl-X_LΔc, which dimerises with Bax to reduce its toxicity (Asoh et al., 1998). The expression of Bax and Bcl-X_LΔc was induced by the addition of IPTG, when the cell growth reached mid-log phase. The bacterial cells were lysed after 3 hours. Bcl-X_L expression was detected by Western blotting, however Bax expression was not detected in either the pellet or supernatant fractions of the bacterial cell lysate. Various conditions were tested to induce the expression of Bax. These were: the optical density at which the cells were induced with IPTG (0.4 to 1 OD at 600nm), the length of time the cultures were left to grow after induction (1 hour to 5 hours), transformation of the

plasmids into different strains of *E. coli* DH5α, BL21 and XL-blue, and the pQE-31 plasmid alone (containing bax) was used to transform *E. coli.* . However the Bax protein was not detected. A previous study (Asoh et al., 1998) showed that an amount of full-length His-Bax as low as 0.01% of the total bacterial protein was sufficient to induce death in *E. coli.* His-Bax expression in *E.coli* DH5α was demonstrated by Montessuit and co-workers (Montessuit et al., 1999). The authors used the pBad expression vector. His-bax gene expression was under the control of the ara c promoter and expression was induced by the addition of arabinose and large-scale purification of His-Bax was facilitated by the use of a 50-litre fermenter to obtain large quantities of *E. coli* expressing the His-Bax protein. In this investigation His-Bax expression was carried out on a smaller scale (1 litre) and the His-Bax protein was not detected by Western blotting. The same antibody (6A7 monoclonal antibody) that recognises a N-terminal epitope of the Bax protein was also used to detect the GST-Bax fusion proteins (section **[3.2]**). The choice of expression system may be important to obtain optimum levels of His-Bax expression. Nevertheless it was surprising that His-Bax was not even detectable by Western blotting in the present study.

[3.1.2] Expression and purification of the BaxΔc-His$_6$

The truncated Bax protein, BaxΔc-His$_6$, lacked 22 amino acids at the C-terminus. The absence of this hydrophobic C-terminal domain increased the solubility of the Bax protein (Pastorino et al., 1999). Pastorino and co-workers have used a truncated form of Bax that lacked 19 amino acids at the C-terminus. (Pastorino et al., 1999). This truncated form of the protein was shown to be biologically active in that it could induce

the release of cytochrome c from isolated mitochondria (Pastorino et al., 1999, Appaix et al., 2000).

E. coli (BL21) were transformed with the pQE60 plasmid contained *baxΔc.* In this case the hexahistidine tag was present on the C-terminus of the protein. It was found that the optimum OD_{600nm} to induce *E.coli* cultures with IPTG was 0.8. After induction the cells were grown at 37°C for 3 hours. SDS-PAGE was used to separate the proteins in the bacterial lysates derived from cells that were uninduced and those induced with IPTG. Coomassie staining showed no difference in the proteins produced by the induced and uninduced cells. However, the Western blotting confirmed that BaxΔc-His_6 was present in the induced sample. Since Bax was poorly expressed, a litre of culture was required. The BaxΔc-His_6 in the bacterial cell lysate was purified using a Ni-NTA column followed by a Mono Q anion-exchange column. A protein elution profile from the Ni-NTA column and a Western blot, figures **[3.1]** and **[3.2]** show which fractions contained BaxΔc-His_6. A two-step gradient (50-150mM, 150-1000mM imidazole) was used to elute the proteins that were bound to the column.

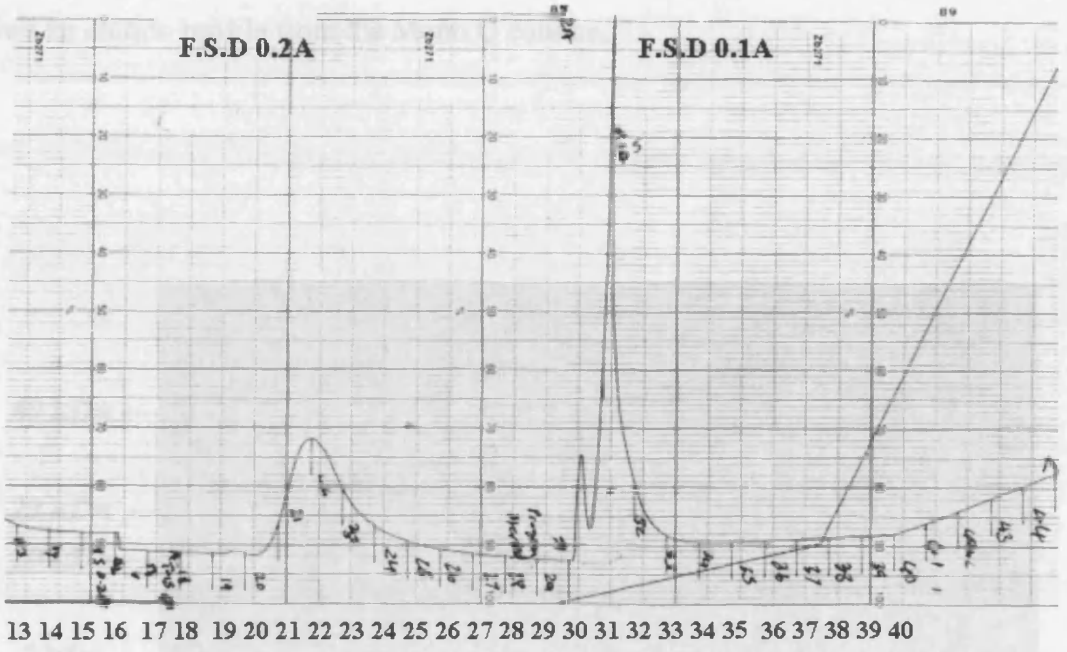

Figure [3.1] Elution profile from the Ni-NTA column. A two-step imidazole gradient was used to elute the bound proteins (50-150mM, 150-1000mM). BaxΔc-His_6 eluted between 60-70mM imidazole in fractions 31 and 32. The volume of each fraction collected was 1ml. A full-scale deflection (F.S.D) of 0.2A was used until fraction 29. After this 0.1A was used.

The fractions containing BaxΔc-His_6 were not pure; therefore a second purification step involving anion-exchange chromatography (Mono Q) was used. The pH at which the anion-exchange chromatography step was performed was varied to find out at which pH BaxΔc-His_6 was retained on the Mono Q column with fewer bacterial proteins. At pH 6.0 BaxΔc-His_6 was retained on the anion-exchange column and co-eluted with fewer

bacterial proteins present. The BaxΔc-His_6 was eluted with 350 mM NaCl. Figure **[3.3]** shows an elution profile from the Mono Q column.

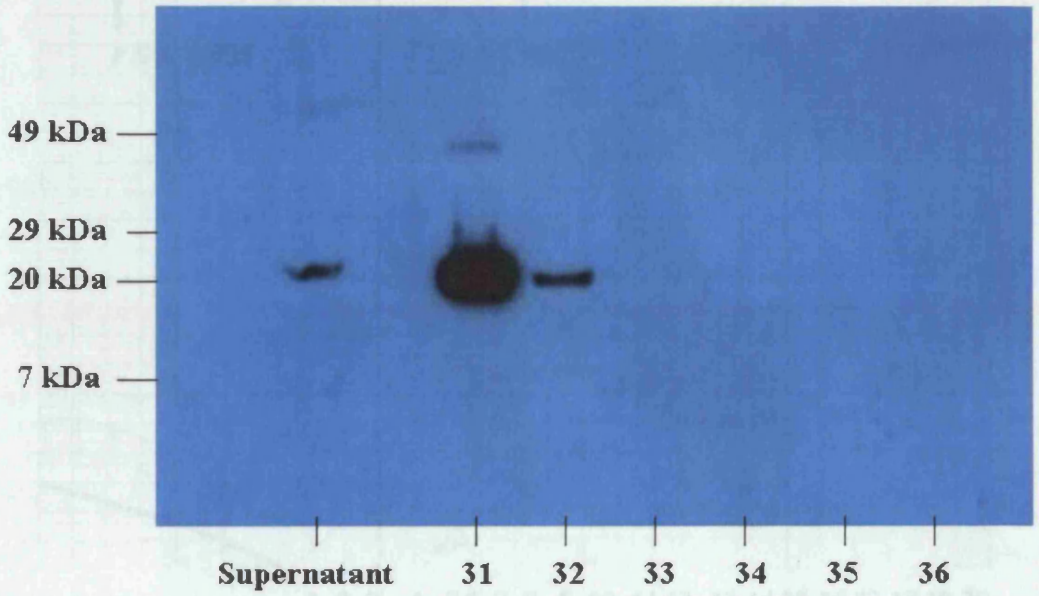

Figure [3.2] The content of BaxΔc-His_6 in fractions eluted from the Ni-NTA column. The proteins present in the fractions eluted from the Ni-NTA column (see **figure [3.1]**) were separated by SDS-PAGE and Western blotting was used to determine which fractions contained BaxΔc-His_6 (20µl aliquot of each 1ml fraction). BaxΔc-His_6 was eluted in fractions 31 and 32.

Western blotting was used to determine which fractions contained BaxΔc-His_6. Figure **[3.4]** shows that BaxΔc-His_6 was eluted in fraction 16. The purity of this fraction was

assessed by SDS-PAGE and silver-staining (Figure **[3.5]**). The fraction containing BaxΔc-His_6 was dialysed against 20mM HEPES, 50mM NaCl, pH 7.3.

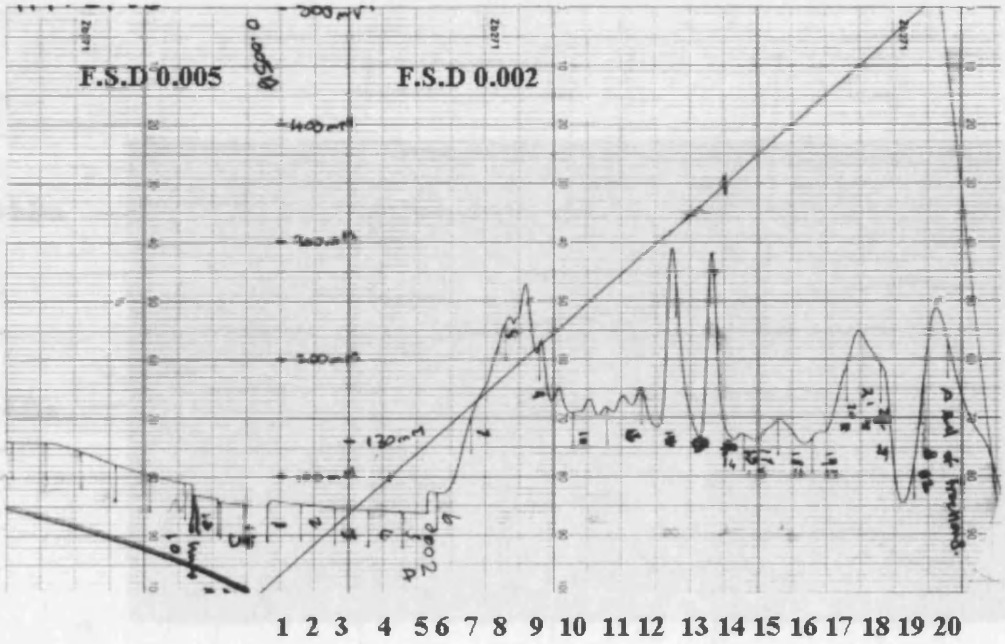

Figure [3.3] Anion-exchange chromatography was used as a second step to purify BaxΔc-His_6 from the bacterial cell lysate. Fractions 31 and 32 eluted from the Ni^{2+}-NTA column were diluted 25x in buffer containing 50mM MES, 50mM NaCl, pH 6.0, applied to the Mono Q column and then eluted in the same buffer with a salt gradient (50-500 mM NaCl). The truncated Bax eluted in fraction 16 with 350mM NaCl. Full-scale deflection (F.S.D) of 0.005A was used up to fraction 5 and then 0.002A was used. The volume of each fraction collected was 1ml.

Although BaxΔc was partially purified, the protein was not stable during dialysis. The proteins were separated by SDS-PAGE and the BaxΔc-His_6 was not detected by

Western blotting, only smaller degradation products. A third purification step was not deemed practical, as the yield would further decrease. In light of this, and the lack of stability during the dialysis step, another approach was used.

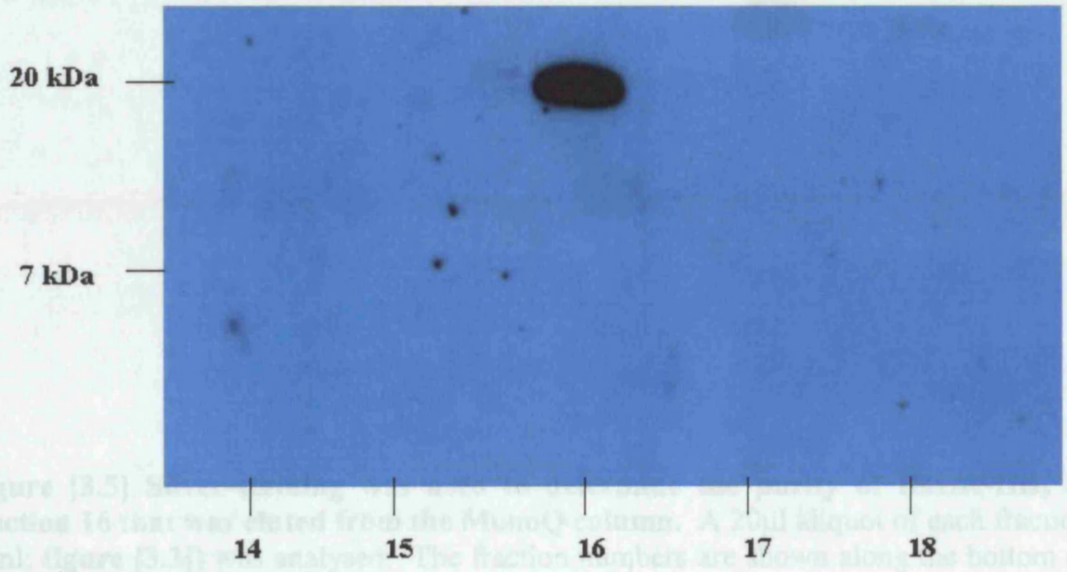

Figure [3.4] Western blotting showed that BaxΔc-His$_6$ was eluted in fraction 16. A 20µl aliquot of each fraction (1ml; **figure [3.3]**) that was eluted from the Mono Q column was analysed (the fraction numbers are shown along the bottom of the blot).

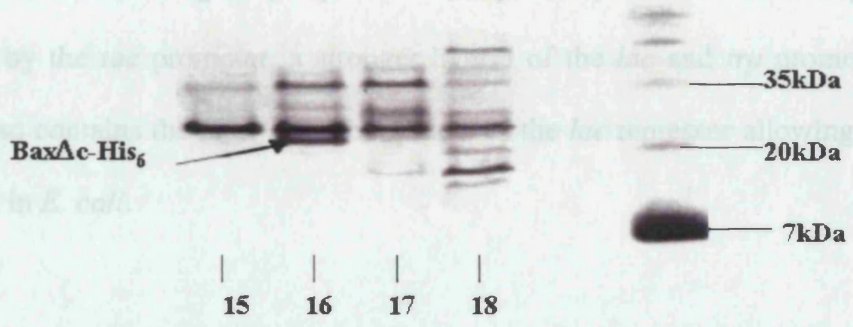

Figure [3.5] Silver-staining was used to determine the purity of BaxΔc-His_6 in fraction 16 that was eluted from the MonoQ column. A 20µl aliquot of each fraction (1ml; **figure [3.3]**) was analysed. The fraction numbers are shown along the bottom of the gel and the arrow indicates the band corresponding to BaxΔc-His_6.

[3.2] GST-Bax and GST-BaxΔc

[3.2.1] Subcloning of Bax and BaxΔc into the pGEX-3X vector

The pGEX plasmid contains the glutathione-s-transferase gene (*gst*) upstream of the cloning site (Smith and Johnson, 1988). Therefore the Bax fusion proteins contained

GST at the N-terminus. The pGEX expression system was chosen because higher levels of expression were obtained than with His-tagged Bax. GST is a bacterial protein and its presence at the N-terminus of the fusion proteins renders Bax less toxic to *E. coli* (Asoh et al., 1998). Figure **[3.6]** shows the pGEX plasmid. Gene expression is controlled by the *tac* promoter, a stronger hybrid of the *lac* and *trp* promoters. This plasmid also contains the $lacI^q$ gene that produces the *lac* repressor allowing controlled expression in *E. coli*.

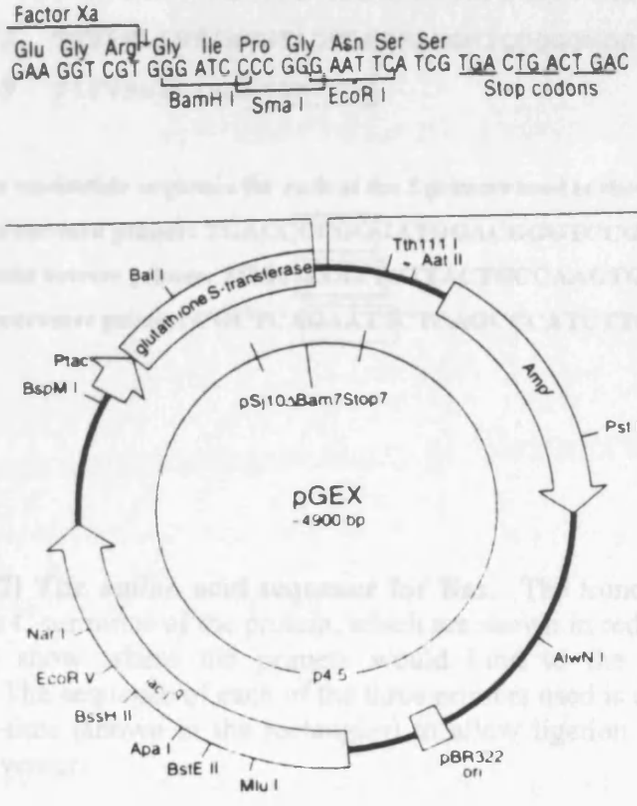

Figure [3.6] The pGEX-3X plasmid was ligated with *bax* and *baxΔc*. The *SmaI/XmaI* and *EcoRI* restriction sites were used.

PCR was used to obtain the bax and baxΔc cDNA and these were ligated in frame with the *gst* gene of the pGEX vector. The presence of the restriction sites in the primer sequences produced strong secondary structure (information obtained with primers from Amersham-Pharmacia) within the primers and therefore a hotstart PCR protocol was used. Figure **[3.7]** shows the amino acid sequence for Bax and BaxΔc, and where the primers would bind to the corresponding nucleotide sequence.

```
1    MDGSGEQPRGGGPTSSEQIMKTGALLLQGFIQDRAGRMGGEAPELAL
48   DPVPQDASTKKLSECLKRIGDELDSNMELQRMIAAVDTDSPREVFFR
95   VAAVDTDSPREVFFRVAADMFSDGNFNWGRVVALFYFASKLVLKALC
142  TKVPELIRTIMGWTLDFLRERLLGWIQDQGGWDGLLSYFGTPTWQTV
189  TIFVAGVLTASLTIWKKMG
```

The nucleotide sequence for each of the 3 primers used is shown below:

Bax forward primer: TGACCCCGGGATGGACGGGTCCGGGGAGCA

BaxΔc reverse primer: TGACGAATTCTTACTGCCAAGTGGGGCGTCCAA

Bax reverse primer: CGCTCAGAATTCTCAGCCCATCTTCTTCCACATG

Figure [3.7] The amino acid sequence for Bax. The truncated form lacks 22 amino acids at the C-terminus of the protein, which are shown in red. The amino acids that are underlined show where the primers would bind to the corresponding nucleotide sequence. The sequence of each of the three primers used is also shown. These include restriction sites (shown in the rectangles) to allow ligation into the same sites in the pGEX-3X vector.

DMSO (5%) was added to the PCR reactions as this prevents the formation of secondary structure within the primers. Figure **[3.8]** shows the effect of DMSO on the amount of bax produced by PCR.

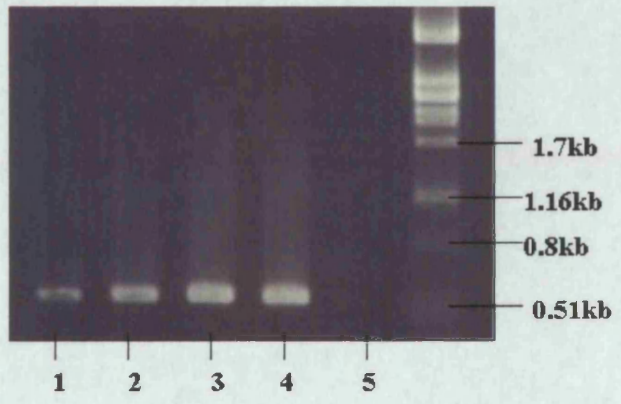

Figure [3.8] Analysis of bax PCR product by agarose gel elctrophoresis. DMSO was varied. Lane 1, no DMSO, lane 2, 2.5% DMSO, lane 3, 5% DMSO, lane 4, 10% DMSO and lane 5, no template control.

After ligation, *E.coli* XL-Blue cells were transformed with the recombinant plasmids. Digestion of the plasmids with the restriction enzymes *XmaI* and *EcoRI* confirmed that the bax inserts were present. In figure **[3.9]** recombinant plasmid DNA cut with *Xma I*

and *Eco RI* was analysed by agarose gel. The same was carried out for recombinant plasmid containing baxΔc (not shown).

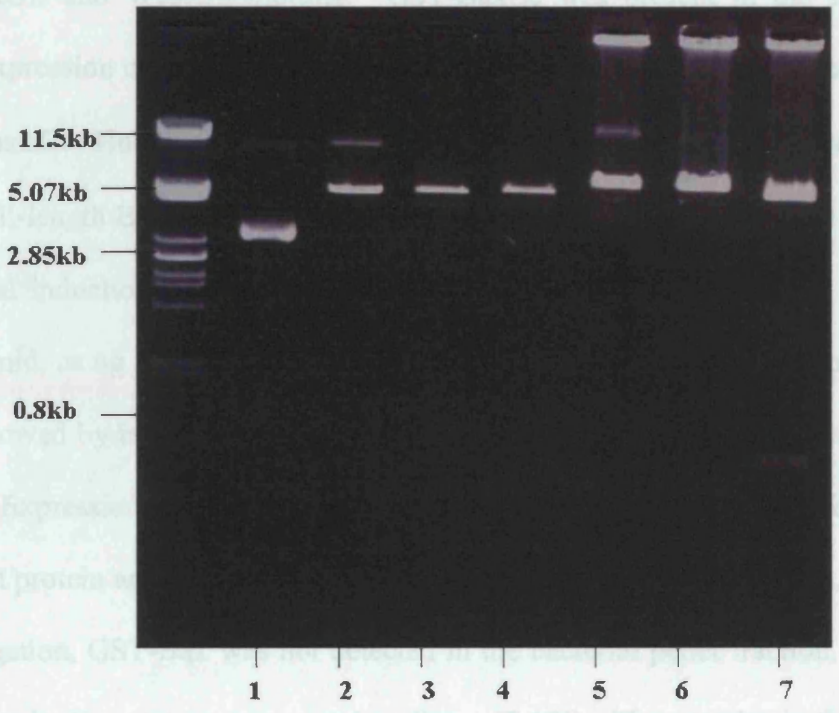

Figure [3.9] Analysis of the recombinant plasmid, digested with *Xma I and EcoRI*, by agarose gel electrophoresis. Lane 1, uncut recombinant plasmid (pGEX+bax). The expected size for the recombinant plasmid is 4.53kb, however, the plasmid is supercoiled and has an apparent size of approximately 3kb. Lane 2, pGEX plasmid digested with *Xma I;* lane 3 pGEX plasmid digested with *EcoRI;* lane 4, pGEX plasmid digested with *Xma I* and *EcoRI.* Lane 5, recombinant plasmid digested with *Xma I;* lane 6, recombinant plasmid digested with *EcoRI.* The plasmids cut with a single restriction are no longer supercoiled and therefore their migration through the gel is not retarded and the plasmids have approximately the expected sizes of 3.98kb for pGEX and 4.53kb for the recombinant plasmid. The pGEX plasmid digested *Xma I* and *Eco RI* (lane 4) has the size as the plasmid cut with only one enzyme because the cleavage sites for both enzymes are located next to each other (see Figure **[3.6]**). Lane 7, recombinant plasmid digested with *XmaI* and *EcoRI.* Two bands are present in lane 7; the bax insert migrates at 0.55kb and pGEX at 3.98kb. The PCR product was sequenced to check for errors.

[3.2.2] Expression of GST-Bax and GST-BaxΔc

Expression of GST-BaxΔc was induced with 0.4 mM IPTG at an OD_{600nm} of 0.8. The proteins in the supernatant and pellet fractions of the bacterial cell lysate were analysed by SDS-PAGE and Western blotting. GST-BaxΔc was present in the supernatant fraction. Expression of GST-Bax was carried out using the same method that was used for GST-BaxΔC. However, expression levels for the full-length fusion protein were low. The full-length Bax protein is toxic to *E.coli*. A protocol was designed to allow a slow gradual induction of expression of GST-Bax from the *tac* promoter within the pGEX plasmid, using a low concentration of IPTG. The cells were grown for 12 hours at 37°C followed by induction with 10μM IPTG and cell growth for a further 24 hours at 22°C. Expression at lower temperatures facilitates the correct-folding of the recombinant protein and therefore prevents inclusion body formation (Schein, 1991). In this investigation, GST-Bax was not detected in the bacterial pellet fraction, indicating that inclusion bodies were not present (see figure **[3.10]**). The proteins in the bacterial cell lysates were analysed and GST-Bax was found to be present in the supernatant fractions from the uninduced cells as well as those induced by IPTG indicating that expression from the *tac* is not tightly regulated possibly due to the insufficient amounts of the *lac* repressor that binds to the promoter and prevents transcription taking place. Two products were detected by the Bax antibody in the induced supernatant fraction (figure **[3.10]**). The larger product corresponded to the GST-Bax (47 kDa) and the smaller product (30 kDa) to a C-terminally truncated form of the fusion protein. The Bax monoclonal antibody (6A7) recognises the epitope PTSSEQI. These amino acids

are present at the N-terminus of Bax (amino acids 13-19). One product was detected in the uninduced supernatant fraction.

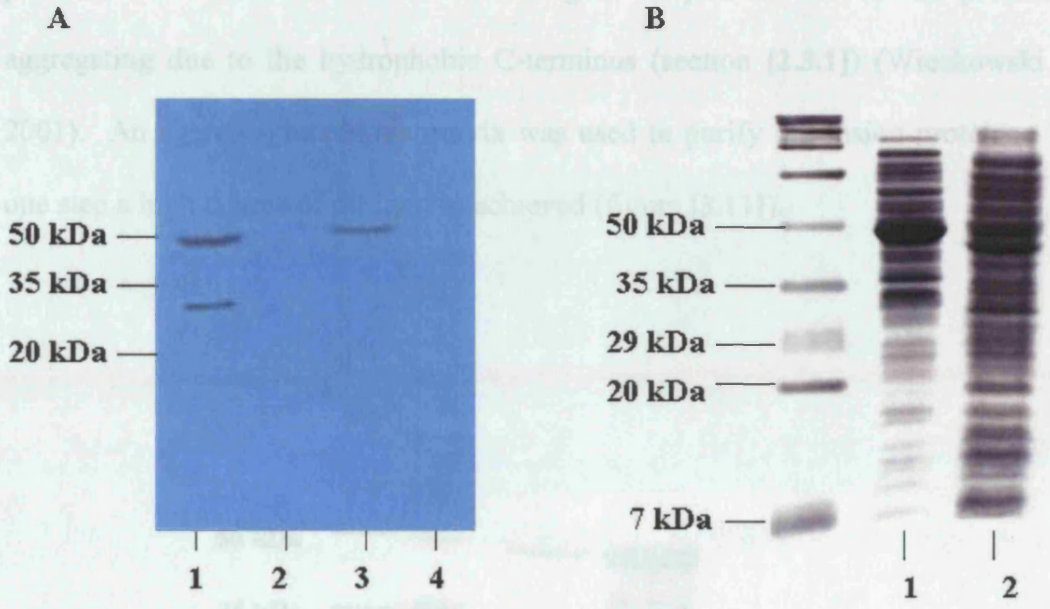

Figure [3.10] Western blot analysis identifies GST-Bax in the supernatant fractions of the bacterial cell extracts. A. GST-Bax was detected with the 6A7 anti-human Bax monoclonal antibody raised against the N-terminal epitope PTSSEQI. Equal amounts of supernatant and pellet fractions were used (20µl of each fraction in each lane). Lane 1, supernatant fraction from *E.coli* (XL-blue) transformed with pGEX-bax and were induced with10µM IPTG. Lane 2, pellet fraction from induced cells. Lane 3, supernatant from uninduced cells. Lane 4, pellet fraction from uninduced cells. **B.** The proteins in the supernatant fractions were separated by SDS-PAGE and visualised by Coomassie-blue stain. Lane 1, supernatant from induced cells. Lane 2, supernatant from uninduced cells.

[3.2.3] Purification of GST-Bax and GST-BaxΔ using an agarose-glutathione affinity matrix

Bacterial extracts containing GST-Bax (full-length) were prepared by sonication in the presence of 1% Nonidet P-40 as detergent to prevent the fusion protein from aggregating due to the hydrophobic C-terminus (section **[2.3.1]**) (Wieckowski et al., 2001). An agarose-glutathione matrix was used to purify the fusion proteins. In this one step a high degree of purity was achieved (figure **[3.11]**).

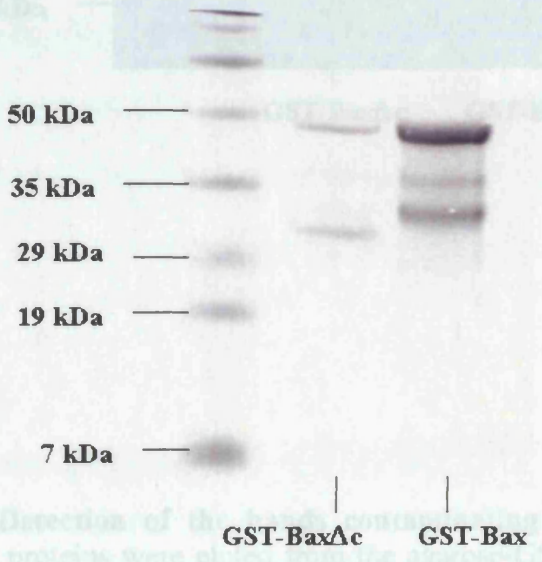

Figure [3.11] Purification from bacterial cell lysates of GST-Bax fusion proteins using agarose-GSH. GST-Bax and GST-BaxΔc were eluted from the GSH-matrix with 50mM GSH, 50mM NaCl. The proteins in the eluate were separated by SDS-PAGE and were visualised by Coomassie-blue staining. The above gel shows two bands present just below the 50 kDa marker which are GST-BaxΔc (44 kDa) and GST-Bax (47 kDa). Other bands are likely to be breakdown products of the fusion protein (see text).

Other bands are visible on the Coomassie-stained gel. As these lower molecular weight bands were also detected by Western blotting (figure **[3.12]**), they are likely to be breakdown products of the fusion protein.

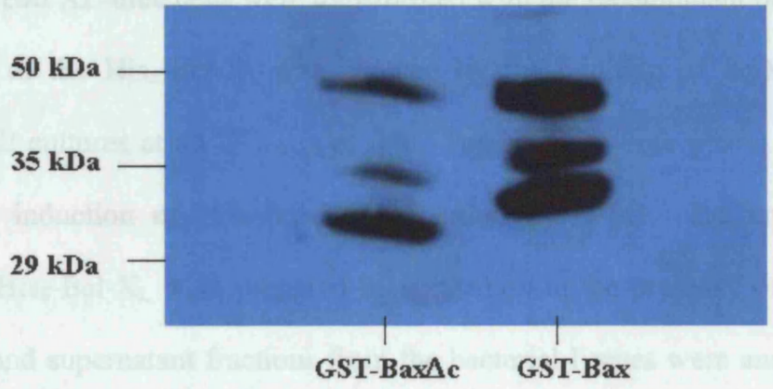

Figure [3.12] Detection of the bands contaminating GST-Bax by the anti-Bax antibody. The proteins were eluted from the agarose-GSH matrix and then separated by SDS-PAGE. GST-Bax fusion proteins and N-terminal breakdown products of the fusion proteins were detected using the 6A7 anti-human Bax monoclonal antibody which recognises amino acids 13-19 of Bax.

[3.3] His_6-Bcl-X_L

[3.3.1] Expression of hexahistidine-tagged Bcl-X_L

The pQE-31 plasmid containing *bcl-X_L* was obtained from Dr. John Ward, Department of Biochemistry and Molecular Biology, UCL. The expression of His_6-Bcl-X_L was more straightforward than for the Bax proteins because His_6-Bcl-X_L is not toxic to bacteria. *E.coli* XL-blue cells were transformed with the recombinant pQE-31 plasmid. Expression of the His_6-Bcl-X_L was induced by the addition of 1mM IPTG to the bacterial cell cultures at an OD_{600nm} of 0.8. The bacteria were grown for up to three hours after induction of His_6-Bcl-X_L expression by IPTG. Bacterial cell lysates containing His_6-Bcl-X_L were prepared by sonication in the presence of Nonidet P-40. The pellet and supernatant fractions from the bacterial lysates were analysed by SDS-PAGE followed by Coomassie-blue staining (figure **[3.13]**). His_6-Bcl-X_L was found in the supernatant fractions and was not found in the pellets indicating that the product was soluble.

[3.3.2] Purification of hexahistidine-tagged Bcl-X_L

The purification of the His_6-Bcl-X_L protein involved a two-step process. The first was an affinity purification step on the Ni^{2+}-NTA column and the second step involved the further separation of the proteins by anion-exchange chromatography on a Mono Q HR 5/5 column attached to a FPLC system. The protein elution profile from the second purification step, the Mono Q anion-exchange column, is shown in figure **[3.14]**.

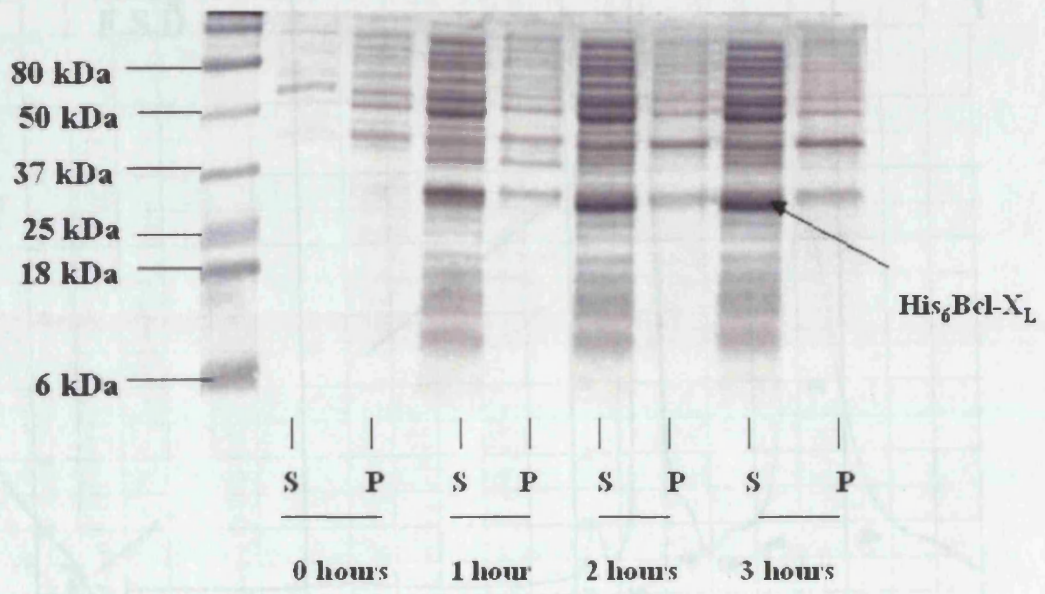

Figure [3.13] Expression of His_6-Bcl-X_L. Four-10ml cultures of *E. coli* transformed with the recombinant the pQE-31 plasmid containing *His_6-Bcl-X_L* were harvested at the times indicated above after induction with 0.4mM IPTG. The cultures were sedimented by centrifugation and then resuspended in sonication buffer containing 50mM HEPES, 50mM NaCl, 0.5mM EDTA, 5mM DTT, 10µl/ml protease inhibitor cocktail, 1mM PMSF, 1% Nonidet P-40, pH 7.3. Proteins in the supernatant (**S**) and pellet (**P**) fractions of the bacterial cell lysate were separated by SDS-PAGE visualised by Coomassie-blue staining. 20µl of the supernatant and pellet were loaded onto the gel (20µl of 1.5ml of **S** and **P** resuspended in loading buffer).

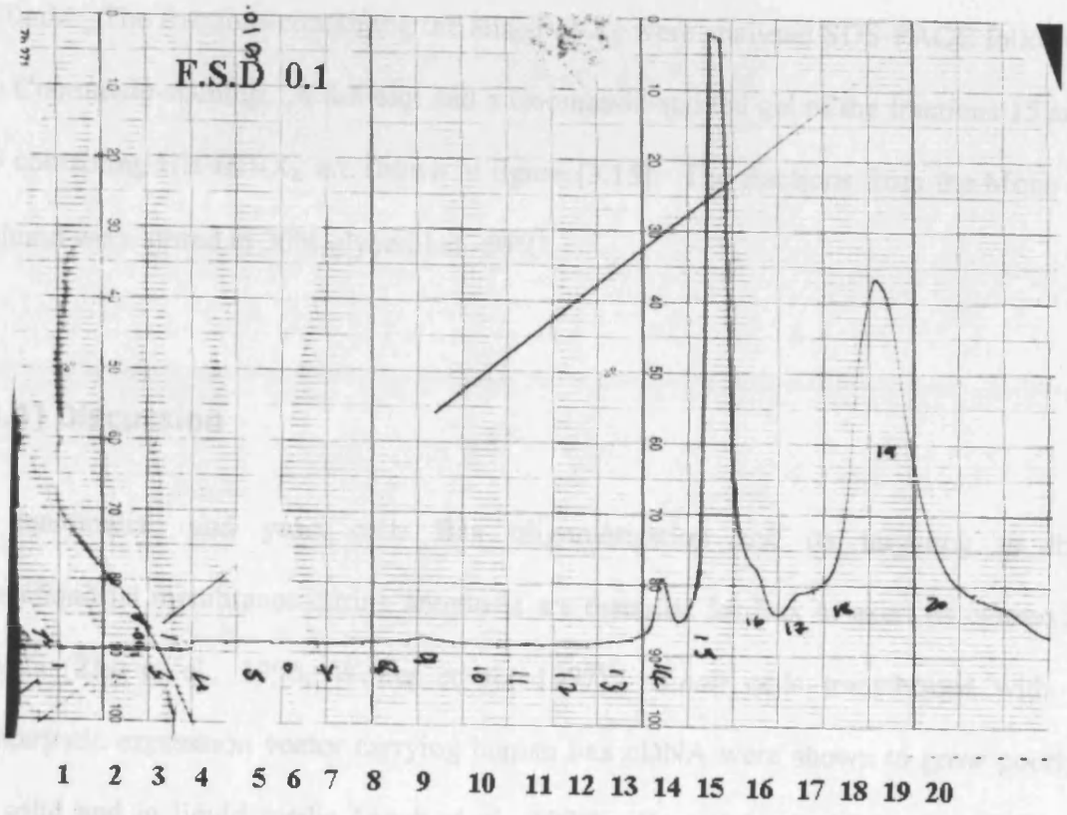

Figure [3.14] Elution profile from the Mono Q anion-exchange column. His_6-Bcl-X_L eluted in fractions 14, 15 and 16. Full-scale deflection (F.S.D) of 0.1A was used. The volume of each fraction collected was 1ml.

The His_6-Bcl-X_L protein was detected in the fractions eluted from the Ni^{2+}-NTA column and the Mono Q anion-exchange by dot blotting. His_6-Bcl-X_L was present in fractions 14, 15 and 16 shown in the protein elution profile in figure **[3.14]**. The His_6-Bcl-X_L eluted from the Mono Q column at a salt concentration of approximately 370mM. The fractions containing the His_6-Bcl-X_L were analysed SDS-PAGE followed by Coomassie-staining. A dot blot and a Coomassie-stained gel of the fractions 15 and 16 containing His-Bcl-X_L are shown in figure **[3.15]**. The fractions from the Mono Q column were stored in 30% glycerol at -60°C.

[3.4] Discussion

In mammalian and yeast cells Bax oligomerisation and its targeting to the mitochondrial membranes during apoptosis are essential for Bax to exert its cytotoxic affects (Zha et al., 1996, Wolter et al., 1997). *E.coli* cells transformed with a prokaryotic expression vector carrying human bax cDNA were shown to grow poorly on solid and in liquid media (Asoh et al., 1998). Bacterial cells lack mitochondria, however, a trace amount of Bax protein (0.01% of the total cellular protein) is sufficient to kill *E. coli*. Bax expression in bacteria is also associated with physiological changes. These include increases in monosaturated fatty acids, O_2 consumption, superoxide production, nicked DNA and the frequency of mutations. Co-expression of Bcl-X_L

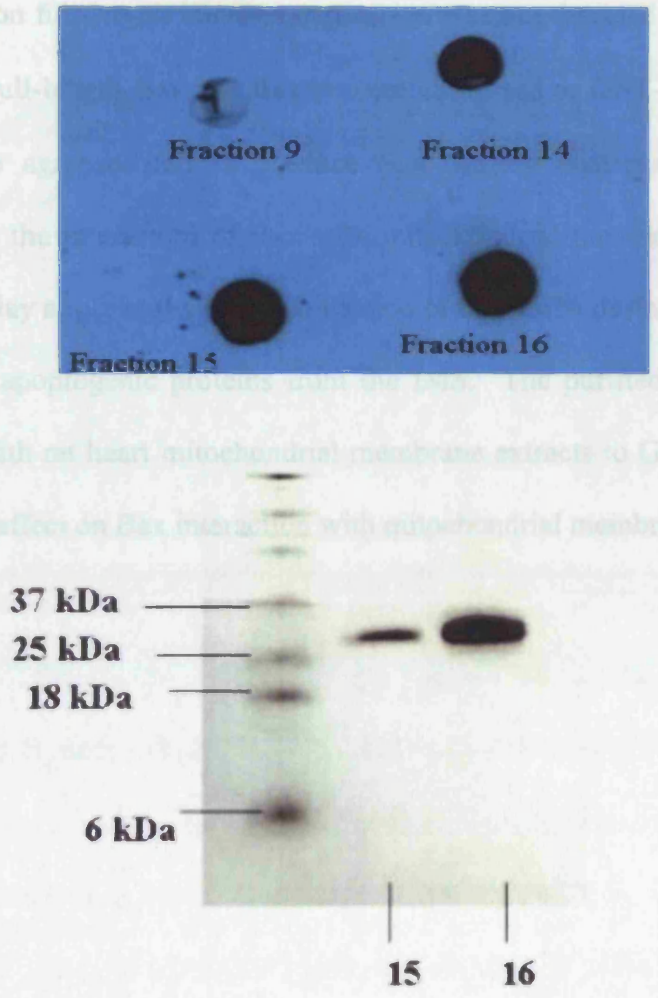

Figure [3.15] His_6-Bcl-X_L was detected in the fractions from the anion-exhange column by dot-blotting and analysed by SDS-PAGE followed by Coomassie-blue staining. 20µl of each 1ml fraction obtained from the Mono Q anion-exchange was loaded onto the blot and the gel.

with Bax was shown to have an inhibitory affect on Bax-induced cytotoxicity. In this investigation full-length His-Bax expression was not detected even when co-expressed Bcl-X_L. Full-length Bax and BaxΔc were expressed as GST-fusion proteins and were coupled to agarose-GSH to produce Bax affinity matrices. These were used to investigate the interaction of Bax with mitochondrial membrane proteins (Chapter 4) that may play a role in the permeabilisation of the OMM during apoptosis and cause the release of apoptogenic proteins from the IMS. The purified His_6-Bcl-X_L was added together with rat heart mitochondrial membrane extracts to GST-Bax to investigate its inhibitory affect on Bax interaction with mitochondrial membrane proteins.

Chapter 4: Results

Interactions of Bax and BaxΔc with a junctional mitochondrial membrane complex

[4.1] Interaction of Bax fusion proteins with VDAC and ANT

Previous studies indicated that the MPT-pore played a central role in apoptosis by facilitating the release of apoptogenic proteins (e.g. cytochrome c) from the IMS. The proposed mechanism involved the opening of the MPT-pore and the subsequent swelling of the matrix leading to the rupture of the OMM. Disruption of the mitochondrial inner membrane potential ($\Delta\psi_m$) was shown to be an early biochemical alteration that occurs in apoptotic cells (Deckwerth & Johnson, 1993, Vayssiere et al., 1994, Zamzami et al., 1995, Petit et al., 1995). The MPT-pore was shown to consist of ANT in the inner mitochondrial membrane and Cyp D in the matrix (Woodfield et al., 1998). Previous studies in our laboratory using GST-Cyp D demonstrated that the MPT-pore consists of CyP D in the matrix, ANT in the inner membrane and VDAC in the outer membrane (Crompton et al., 1998). Pharmacological and functional studies indicated that the reduction in $\Delta\psi_m$ during apoptosis was due to the opening of the MPT-pore rather than non-specific mitochondrial membrane damage (Marchetti et al., 1996). Marchetti and co-workers investigated glucocorticoid-induced apoptosis in thymocytes. The ANT ligand and MPT-pore inhibitor bongkrekic acid was shown to inhibit apoptotic changes including $\Delta\Psi_m$ dissipation, depletion of non-oxidised

glutathione, and generation of reactive oxygen species and exposure of phosphatidylserine on the outer surface of the plasma membrane. In another study, hexokinase-associated protein complexes containing the MPT-pore components ANT, Cyp D and possibly VDAC, in addition to Bax and some unidentified proteins, were purified from rat brain and were incorporated into liposomes. These complexes were shown to have MPT-pore activity in liposomes (Marzo et al., 1998a, Zamzami et al., 1998). The function of the reconstituted MPT-pore complexes was explored using ligands of the components of the pore. The ANT ligands atractyloside, ter-butylhydroperoxide, $Ca^{2+}$and diamide, which all promote MPT-pore opening were found to induce the release of the fluorochrome $DiOC_6$ (622 Da) entrapped in liposomes while bongkrekic acid, which inhibits MPT, prevented $DiOC_6$ release. The Cyp D ligands, cyclosporin A (CSA) and N-methyl-Val-4-cyclosporin (mCSA), the non-immunosupressive Cyp D ligand which does not interact with calcineurin, both of which prevented MPT-pore opening in isolated mitochondria (Zamzami et al., 1996, Zorrati & Szabo, 1995) also prevented $DiOC_6$ release from liposomes. Bax was immunodepleted from the MPT-pore complexes prior to reconstitution into liposomes loaded with $DiOC_6$. Bax-deficient MPT-pore liposomes failed to release $DiOC_6$ upon exposure to the ANT ligand atractyloside (Marzo et al., 1998a). In addition, Bax or atractyloside were shown to induce $\Delta\Psi_m$ dissipation and apoptotic nuclear changes when microinjected into rat fibroblasts (Marzo et al., 1998b). These changes were inhibited by bongkrekic acid and both CSA and mCSA. Bax co-immunoprecipitated with ANT and a physical interaction between human ANT-2 and Bax was demonstrated using a yeast two-hybrid system (Marzo et al., 1998b). Further evidence for the role of the MPT-pore in apoptosis was provided using a cell-free system to study

neuronal apoptosis (Ellerby et al., 1997). Atractyloside and the wasp toxin mastoparan, which also promotes MPT-pore opening (Pfeiffer et al., 1995), were shown to promote neural apoptosis, which was dependent on the presence of mitochondria. The activation of apoptosis was measured by fodrin cleavage. Studies using isolated mitochondria provided further evidence for the role of the MPT-pore in Bax-dependent cytochrome c release. Narita and co-workers (Narita et al., 1998) showed that the addition of recombinant Bax to isolated mitochondria resulted in loss of $\Delta\psi$, mitochondrial swelling and cytochrome c release. These changes were dependent on Ca^{2+} and were prevented by CSA and bongkrekic acid. Other work (Jurgensmeier et al., 1998) also showed that Bax induced cytochrome c release from isolated mitochondria. This study showed that it was Ca^{2+} and not Bax that caused mitochondrial swelling which suggested that Bax did not directly induce MPT. However, other data from this study demonstrated that Bax induced cytochrome c release from isolated mitochondria was inhibited by CSA in the absence of Ca^{2+}. MPT-pore opening, as a mechanism for cytochrome c release was controversial since other groups provided evidence for Bax-induced cytochrome c release that did not require MPT-pore opening. Eskes and co-workers (Eskes et al., 1998) showed that Bax-induced cytochrome c release from isolated mitochondria was independent of the MPT-pore. In contrast to studies by other groups (Pastorino et al., 1999, Narita et al., 1998, Jurgenmeier et al., 1998) Eskes and co-workers found that Bax-induced cytochrome c release from isolated mitochondria was not prevented by bongkrekic acid or CSA. Furthermore Mg^{2+} ions, which inhibit MPT-pore opening, were required for cytochrome c release. Other groups have proposed models of Bax-induced cytochrome c release that involve Bax forming pores in the OMM through which cytochrome c can

pass through to the cytosol. NMR structure analysis showed that Bax and Bcl-X_L were structurally similar to the pore-forming subunit of the diphtheria toxin (Suzuki et al., 2000, Muchmore et al., 1996) and are capable of forming channels in synthetic lipid bilayers following oligomerisation (Reed, 1997). Bax channels were shown to be pH-sensitive, voltage-gated channels which are slightly selective for anions at a physiological pH (Antonsson et al., 1997, Schlesinger et al., 1997, Schendel et al., 1997). In addition more recent studies have shown that oligomerised Bax, not monomeric Bax, was able to release fluorescein entrapped in liposomes (Antonsson et al., 2000) and this did not require the presence of mitochondrial membrane proteins. This suggested that Bax alone was sufficient for cytochrome c release.

The aim of this work was to determine if Bax targeted VDAC-ANT intermembrane junctional complexes (contact sites) and whether it was possible to reconstitute a Bax-VDAC-ANT-Cyp D complex. Only then could the MPT-pore be directly implicated in outer membrane lysis and a mechanism for cytochrome c release.

In order to find out if Bax interacted with VDAC and ANT, GST-Bax and the C-terminally truncated form, GST-BaxΔc, were expressed as described in **[3.2]**. The recombinant GST-Bax proteins were immobilised onto agarose-GSH matrices. Pull-down experiments were performed in which a detergent extract of rat heart mitochondrial membranes, containing VDAC and ANT, was applied to the immobilised GST-Bax.

[4.1.1] Detection of VDAC and ANT in detergent extracts of rat heart mitochondria

Detergent extracts of rat heart mitochondrial membranes were used as a source of VDAC and ANT. This mitochondrial membrane extract was prepared as described previously in **[2.7.4]**. Before examining VDAC and ANT interactions with GST-Bax fusion proteins it was important to confirm that the anti-VDAC and the anti-ANT antibodies used in this investigation were specific for VDAC and ANT respectively. Therefore, proteins in the mitochondrial membrane extract were separated by SDS-PAGE and Western blotting was used to specifically detect VDAC (30 kDa) and ANT (32 kDa) present in the extract (figure **[4.1]**).

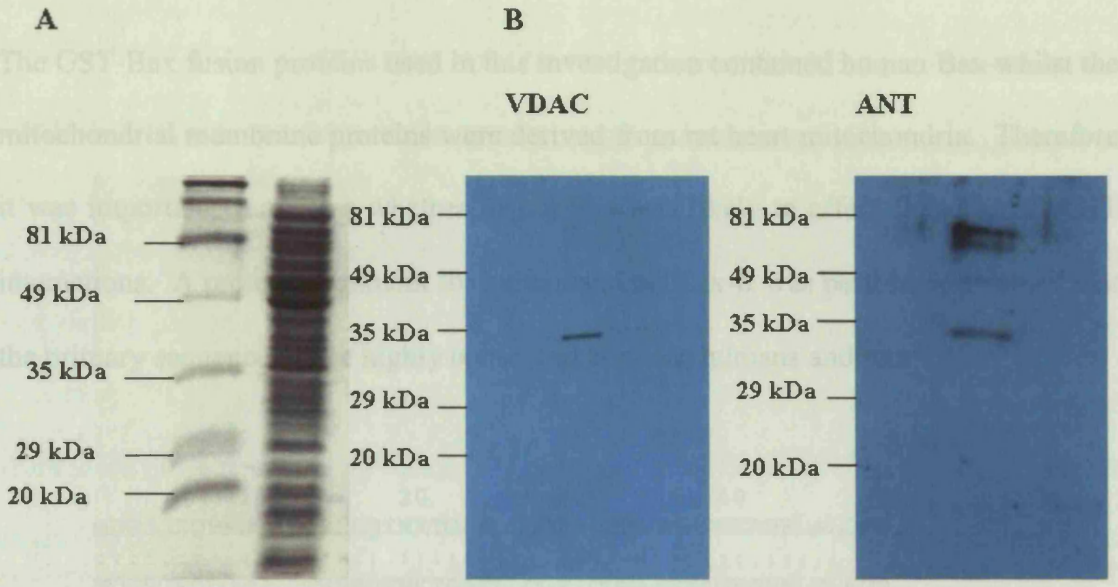

Figure [4.1] Specificity of the anti-VDAC and ANT antibodies used. A Proteins in the mitochondrial membrane extract were separated by SDS-PAGE and visualised by Coomassie-blue stain. **B** Western blotting showed that the anti-ANT and anti-VDAC antibodies specifically detected ANT and VDAC respectively. The ANT antibody used was polyclonal raised against the YDEIKKYV peptide corresponding to the C-terminus of rat ANT-1 (this laboratory). The VDAC antibody used was monoclonal 31HL clone (calbiochem) and is specific for the N-terminal region of VDAC.

[4.1.2] Protein sequence alignments to compare human and rat Bax

The GST-Bax fusion proteins used in this investigation contained human Bax whilst the mitochondrial membrane proteins were derived from rat heart mitochondria. Therefore it was important to address whether or not this was likely to affect Bax-VDAC-ANT interactions. A protein alignment for human and rat Bax-α was performed to show that the primary sequences were highly conserved between humans and rats.

```
          10         20         30         40         50
MDGSGEQPRGGGPTSSEQIMKTGALLLQGFIQDRAGRMGGEAPELALDPV
:::::::  ::::::::::.:::::.:::::::::: ::.::::::.:.
MDGSGEQLGGGGPTSSEQFMKTGAFLLQGFIQDRAERMAGETPELTLEQP
          10         20         30         40         50

          60         70         80         90        100
PQDASTKKLSECLKRIGDELDSNMELQRMIAAVDTDSPREVFFRVAADMF
::::::::::::.:::::::.:::::::: :::::::::::::::::
PQDASTKKLSECLRRIGDELDNNMELQRMIADVDTDSPREVFFRVAADMF
          60         70         80         90        100

         110        120        130        140        150
SDGNFNWGRVVALFYFASKLVLKALCTKVPELIRTIMGWTLDFLRERLLG
.:::::::::::::::::::::::::::::::::::::::::::::::::
ADGNFNWGRVVALFYFASKLVLKALCTKVPELIRTIMGWTLDFLRERLLV
         110        120        130        140        150

         160        170        180        190
WIQDQGGWDGLLSYFGTPTWQTVTIFVAGVLTASLTIWKKMG
::::::::.:::::::::::::::::::::::::::::::::
WIQDQGGWEGLLSYFGTPTWQTVTIFVAGVLTASLTIWKKMG
         160        170        180        190
```

Figure [4.2] Alignment of the amino acid sequences of human and rat Bax-α. The sequence alignment was carried out using the HGMP matcher alignment program. The human sequence is shown at the top. Rat and human Bax are 91% identical (two dots represents sequence identity whereas one dot shows the amino acids are similar).

[4.1.3] GST-BaxΔc induces cytochrome c release from isolated mitochondria

Previously other groups showed that BaxΔc induced cytochrome c release from isolated mitochondria (Pastorino et al., 1998, Narita et al., 1998). At the beginning of this work it was important to establish whether or not the fusion proteins retained Bax activity despite the presence of the large GST-tag (26 kDa) at the N-termini of the proteins. Therefore GST-BaxΔc was assayed to assess its ability to induce cytochrome c release from isolated rat heart mitochondria. GST-BaxΔc rather than GST-Bax was used in this assay because detergent (Nonidet-P40) required for GST-Bax solubilisation would lead to OMM lysis in the absence of GST-Bax. Rat heart mitochondria were isolated and then resuspended in respiratory buffer (section **[2.6.3]**). GST-BaxΔc (0-1μM) was added to the mitochondria. The mitochondria were then pelleted and the supernatant filtered (0.2μm pore size). Proteins in the pellet and supernatant fractions were separated by SDS-PAGE and cytochrome c was detected by Western blotting. The results showed that GST-BaxΔc induced cytochrome c release from the isolated mitochondria (figure **[4.3]**). In the controls, respiratory buffer only (lane 1) and GST (lane 2), no cytochrome c was present in the supernatant implying little or no cytochrome c release from the mitochondria. This result suggests that the mitochondrial outer membranes were intact and GST-BaxΔc specifically induced cytochrome c release. Increasing the concentration of GST-BaxΔc added resulted in more cytochrome c release (up to 500nM of GST-BaxΔc).

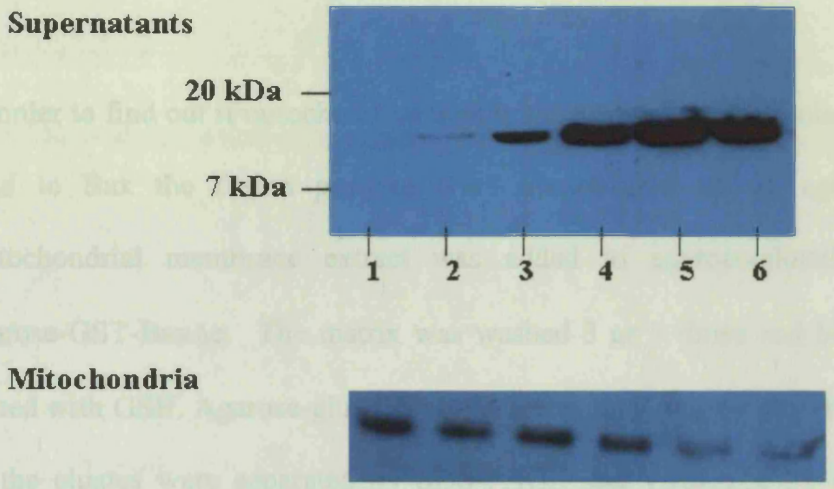

Figure [4.3] GST-BaxΔc induces cytochrome c release from isolated mitochondria. Isolated rat heart mitochondria suspended in respiratory buffer containing 1mM glutamate and 1mM malate were incubated with GST-BaxΔc for 15 minutes at 37°C (section **[2.6.3]**). Proteins in the supernatant and mitochondrial fractions were separated by SDS-PAGE (2μg of protein in each lane) The presence of cytochrome c in the supernatant and mitochondria was detected by Western blotting using a monoclonal anti-cytochrome c antibody. The supernatant blot shows that more cytochrome c was released with increasing concentrations of GST-BaxΔc, up to 500nM GST-BaxΔc. Lane 1, no additions, lane 2, GST alone (500nM) was added. Lanes 3, 4, 5 and 6, 125nM, 250nM, 500nM and 1μM of GST-BaxΔc were added respectively. This result was obtained in three independent experiments.

[4.1.4] GST-BaxΔc and GST-Bax tightly bind to VDAC/ANT

In order to find out if mitochondrial membrane proteins, in particular VDAC and ANT, bind to Bax the fusion proteins were immobilised on an agarose-GSH matrix. Mitochondrial membrane extract was added to agarose-glutathione-GST-Bax or agarose-GST-BaxΔc. The matrix was washed 3 or 5 times and bound proteins were eluted with GSH. Agarose-glutathione-GST was used as a control matrix. The proteins in the eluates were separated by SDS-PAGE and visualised by Coomassie-staining (Figure **[4.4]**).

These data showed two proteins (approximately 34 kDa and 30 kDa) that co-elute with GST-BaxΔc after 3 washes (lane 5) and 5 washes (lane 8) and do not co-elute with GST (lanes 4, 6 and 7). However, the same bands were also detected by the anti-Bax antibody (figure **[3.15]**) and, therefore, are most probably breakdown products of the fusion proteins (GST-Bax, GST-BaxΔc). These bands would obscure any VDAC and ANT (32 kDa and 30 kDa, respectively). The presence or otherwise of VDAC and ANT was therefore detected using the ANT and VDAC specific antibodies (Figure **[4.1]**). Figure **[4.5]** shows that GST-BaxΔc specifically binds VDAC and ANT. Figure **[4.6]** shows that both VDAC and ANT were also present in the eluates from the agarose-GSH-GST-Bax matrix. In both cases there was no detectable binding to GST alone confirming that VDAC-ANT bound to the Bax/BaxΔc moieties of the fusion proteins. With BaxΔc (Figure **[4.5]**), similar amounts of VDAC and ANT were retained

after 3 and 5 washes as shown on the blot (lanes 2 and 5), this confirmed that VDAC and ANT were retained tightly. Similar results were obtained with Bax.

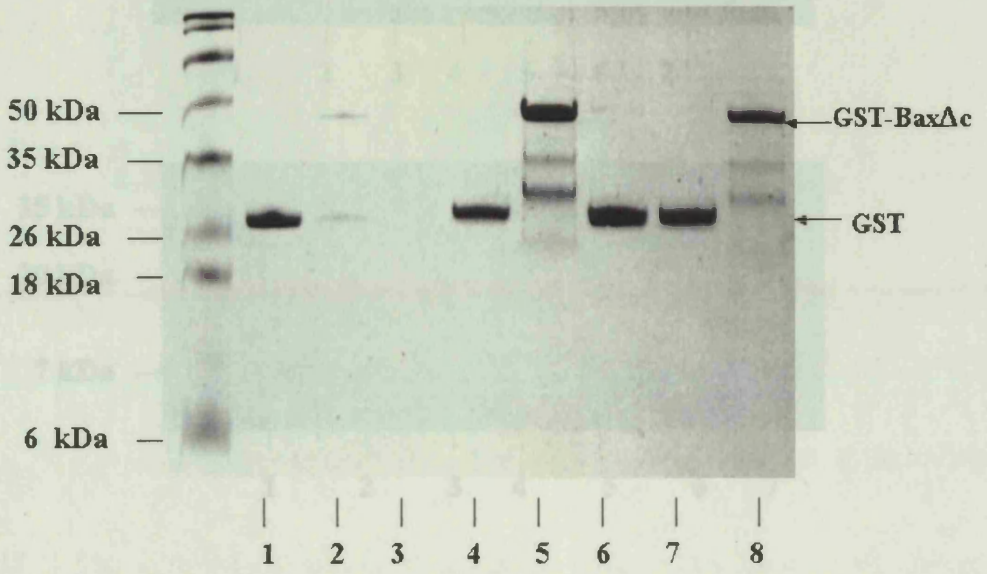

Lane	1	2	3	4	5	6	7	8
Agarose-GSH-GST	+	-	-	+	-	+	+	-
Agarose-GSH-GST-BaxΔc	-	+	-	-	+	-	-	+
Mitochondrial membrane extract	-	-	+	+	+	+	+	+
Agarose-GSH	-	-	+	-	-	+	+	-
Number of washes	5	5	3	3	3	2	5	5

Figure [4.4] Separation of proteins eluted from the GST and GST-BaxΔc matrices by SDS-PAGE. The bound proteins were visualised by Coomassie-staining. A protein extract (300µl, 3mg of protein) derived from mitochondrial membranes was added to the agarose–GSH matrices (50µl of matrix). The extract was removed and the matrices were washed 3 or 5 times with 600µl of buffer containing 50mM NaCl, 10mM HEPES, 25% glycerol, 1mM EGTA, 8µM ADP, 8µM ATP, 8mM DTT and 0.5mM $MgCl_2$. The bound proteins were eluted with 50mM NaCl, 50mM glutathione. (The same result was obtained in three independent experiments)

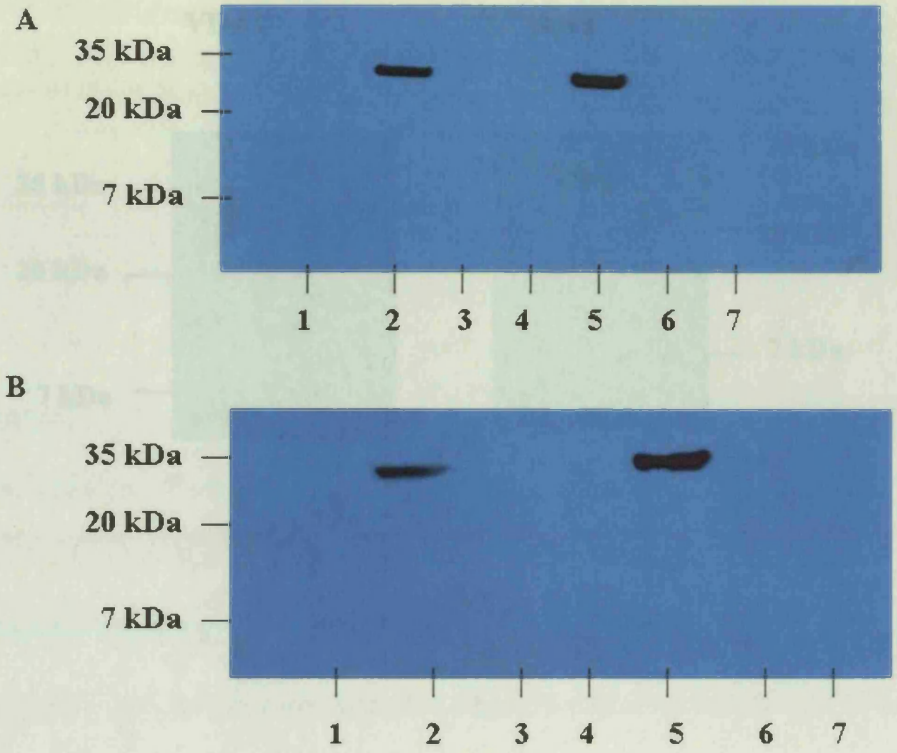

Lane	1	2	3	4	5	6	7
Agarose-GSH-GST	+	-	-	+	-	+	-
Agarose-GSH-GST-BaxΔc	-	+	-	-	+	-	+
Mitochondrial membrane extract	+	+	+	+	+	-	-
Agarose-GSH	-	-	+	-	-	-	-
Number of washes	5	5	3	3	3	5	5

Figure [4.5] VDAC and ANT specifically bind to GST-BaxΔc. **A** and **B** Western blotting was used to detect VDAC and ANT, respectively. Both proteins co-eluted with GST-BaxΔc from the agarose-GSH. (The same result was obtained in three independent experiments)

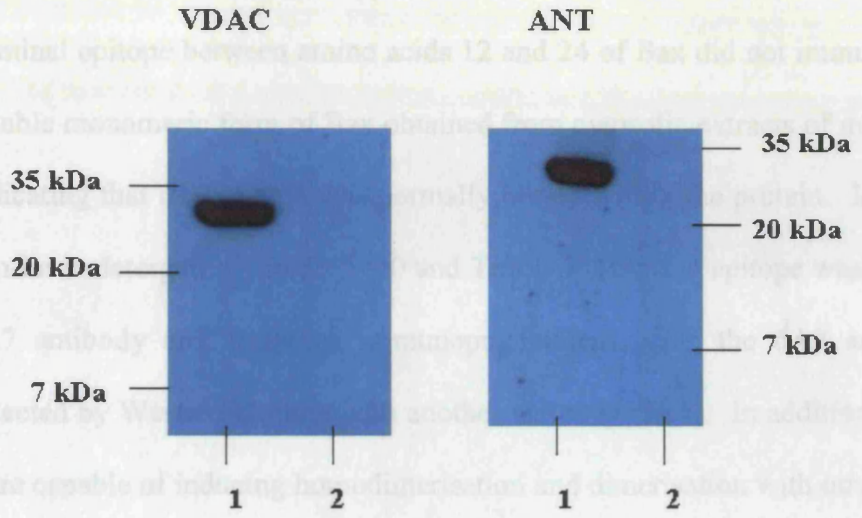

Figure [4.6] The agarose-GSH-GST-Bax matrix binds VDAC and ANT. Western blotting was used to detect VDAC and ANT. Lane 1, eluates from the GST-Bax matrix. Lane 2, eluates from the GST matrix. In each case the agarose-GSH matrices were washed 5 times before the proteins were eluted with 50mM glutathione, 50mM NaCl. (The same result was obtained in three independent experiments)

[4.1.5] The effects of detergents on VDAC/ANT binding to GST-Bax

In experiments shown in this chapter Nonidet-P40 was used during the preparation of GST-Bax and the mitochondrial membrane extract containing VDAC and ANT. However, different detergents were known to influence the conformation of Bax and its oligomeric state. Moreover oligomeric Bax and not monomeric Bax appeared to be the active form of Bax required for cytochrome c release (Antonsson et al., 2000).

Evidence for detergent-induced conformational changes was obtained using anti-Bax antibodies (Hsu & Youle, 1997, Hsu & Youle, 1998). An antibody (6A7) to an N-terminal epitope between amino acids 12 and 24 of Bax did not immunoprecipitate the soluble monomeric form of Bax obtained from cytosolic extracts of murine thymocytes indicating that this epitope was normally buried within the protein. In the presence of non-ionic detergent (Nonidet P-40 and Triton-X 100) the epitope was accessible to the 6A7 antibody and Bax was immunoprecipitated using the 6A7 antibody and was detected by Western blotting with another antibody (5B7). In addition these detergents were capable of inducing homodimerisation and dimerisation with other Bcl-2 proteins, for example Bcl-X_L. Another non-ionic detergent Tween-20 also induced heterodimerisation with Bcl-X_L but not homodimerisation or accessibility to the 6A7 antibody. The zwitterionic detergent CHAPS did not promote Bax dimer formation or 6A7 epitope exposure. The oligomeric forms of recombinant Bax and not the monomeric form were shown to form channels in liposomes and trigger cytochrome c release from isolated mitochondria (Antonsson et al., 2000). With regards to this investigation the detergent-induced conformational changes in Bax may have altered GST-Bax binding to VDAC-ANT. The GST-Bax/GST-BaxΔc was attached to an agarose-GSH matrix therefore it was not clear whether oligomerisation would take place under these conditions. Nevertheless the binding of VDAC-ANT to GST-Bax in the presence of Nonidet P-40, Tween-20 and CHAPS were compared. Figure **[4.7]** shows that the choice of detergent used had no effect on VDAC-ANT binding to GST-Bax. Since binding occurred in the presence of CHAPS this result suggests that no conformational change and exposure of the 6A7 epitope was required for Bax binding to VDAC-ANT.

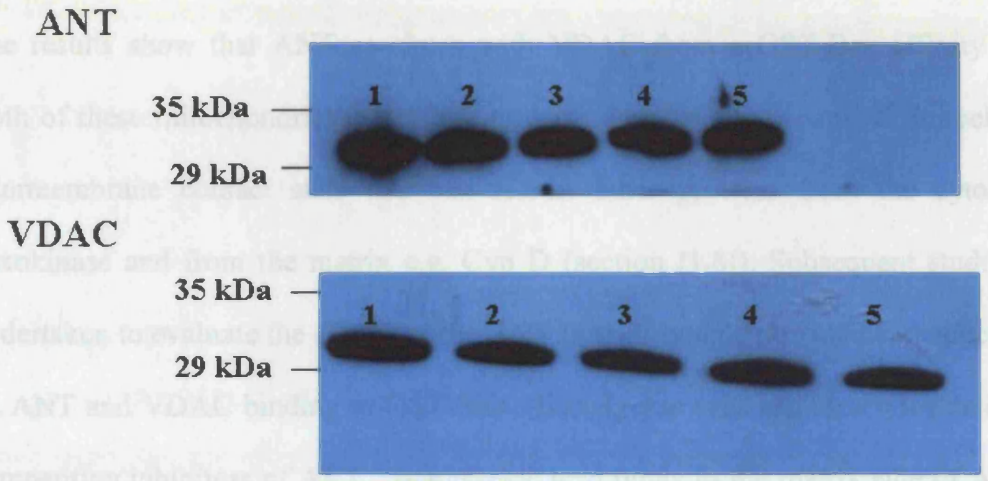

Figure [4.7] The effect of different detergents on binding of VDAC and ANT to GST-Bax. The detergents indicated were present during the purification of the fusion proteins, the solubilisation of the mitochondrial membrane extracts and were present in the buffers during the pulldowns. Lane 1, 0.5% Nonidet-P40 was used during purification of GST-Bax. Lane 2, 0.5 % CHAPS was used and lane 3, 0.5% Tween-20. Lanes 4 and 5, 2% Nonidet P-40 and 2% CHAPS were used respectively. (Similar results were obtained in three independent experiments)

[4.1.6] The effects of Bcl-X_L, atractyloside and bongkrekic acid on VDAC/ANT binding to GST-Bax

The results show that ANT co-elutes with VDAC from a GST-Bax affinity matrix. Both of these mitochondrial membrane proteins are key components of mitochondrial intermembrane contact sites that can recruit other proteins from the cytosol e.g. hexokinase and from the matrix e.g. Cyp D (section **[1.8]**). Subsequent studies were undertaken to evaluate the effects of the ANT ligands bongkrekic acid and atractyloside on ANT and VDAC binding to GST-Bax. Bongkrekic acid and atractyloside are both competitive inhibitors of ANT. Bongkrekic acid binds to the matrix side of ANT and traps it in the m-conformation with the binding site facing the matrix. Atractyloside binds to the cytosolic side of ANT and traps it in the c-conformation. Both of these inhibitors bind to hydrophilic loops in ANT that are exposed to the matrix side of ANT (bongkrekic acid) and the cytosolic side (atractyloside) (Brandolin et al., 1985, Muller et al., 1996, Dianoux et al., 2000). Bongkrekic acid was shown to protect cells from apoptosis (Marchetti et al., 1996 a, b) including apoptosis induced by transient ischaemia in rat neuronal cells (Cao et al., 2001). In isolated mitochondria bongkrekic acid prevents Bax-induced cytochrome c release, Bax-induced dissipation of $\Delta\Psi_m$ and nuclear apoptotic changes in rat fibroblasts (Narita et al., 1998, Marzo et al., 1998b) and the release of pro-caspase-9 (Cao et al., 2001). Atractyloside was shown to have the opposite effect to bongkrekic acid in that it promoted $\Delta\Psi_m$ dissipation, nuclear apoptotic changes (Marzo et al., 1998b) and Bax-ANT channel activity in liposomes (Marzo et al, 1998a, Brenner et al., 2000). In the present study mitochondrial membrane extracts were treated with atractyloside, bongkrekic acid or Bcl-X_L and then

added to GST-Bax immobilised on GSH-agarose. The proteins were eluted from the agarose-GSH-GST-Bax, equal amounts of total protein were separated by SDS-PAGE and VDAC and ANT were detected by Western blotting. The blots were developed and quantified using a Fuji-LAS-100 phosph/fluoro-imaging system (figures **[4.8]** and **[4.9]**). In figure **[4.9]** the results show that bongkrekic acid increased the amount of ANT and VDAC retained by GST-Bax. The presence of atractyloside considerably reduced the amount of ANT retained by GST-Bax and only slightly reduced the amount of VDAC bound to GST-Bax. Figure **[4.9] B** shows that atractyloside increases the amount of VDAC relative to ANT that is bound to GST-Bax by six-fold and bongkrekic acid by two-fold. These results suggest that atractyloside and bongkrekic acid exert their effects by altering the relative amounts of VDAC and ANT bound to Bax. Data from another study has shown that the anti-apoptotic protein Bcl-X_L interacts with VDAC (Shimizu et al., 1999) and that reduction in Bax binding to VDAC was due to competitive inhibition of Bcl-X_L to VDAC. Bcl-X_L can also bind to and form heterodimers with Bax (Oltvai et al., 1993). Minn and co-workers have shown that Bcl-X_L regulates apoptosis by both heterodimerisation dependent and independent mechanisms (Minn et al., 1999). Figure **[4.9]** shows that Bcl-X_L reduces the amount of VDAC and ANT bound to GST-Bax and has little effect on the ratio of VDAC to ANT that interacts with the fusion protein.

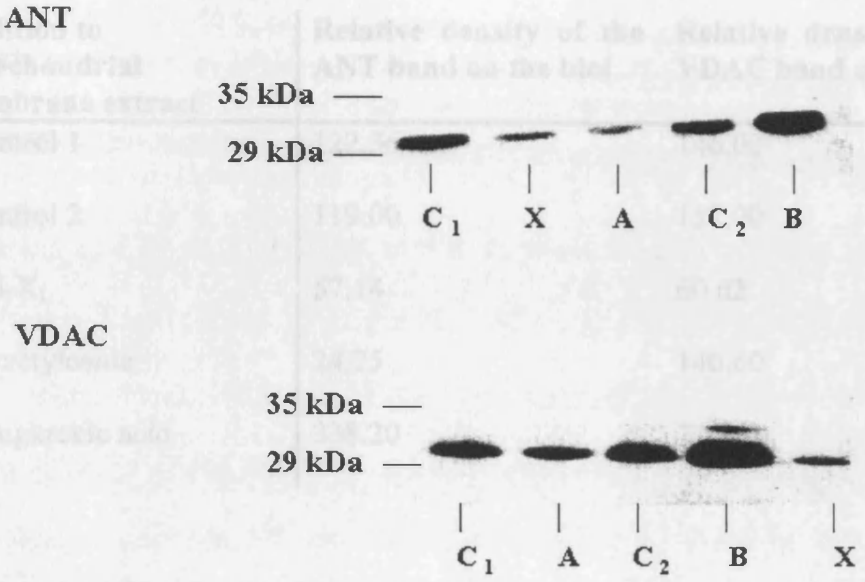

Figure [4.8] The effects of Bcl-X_L, atractyloside and bongkrekic acid on the amount of VDAC and ANT that binds to GST-Bax. 50µl of agarose-GST-Bax slurry was used for each pulldown. C_1 and C_2, controls, mitochondrial membrane extract only, A, mitochondrial extract and atractyloside (50µM), B, mitochondrial membrane extract and bongkrekic acid (50µM) and X, mitochondrial membrane extract and Bcl-X_L (0.125ng). (Similar results were obtained in three independent experiments)

A

Addition to mitochondrial membrane extract	Relative density of the ANT band on the blot	Relative density of the VDAC band on the blot
Control 1	122.36	146.00
Control 2	119.00	157.00
Bcl-X_L	57.14	60.62
Atractyloside	24.25	140.60
Bongkrekic acid	338.20	770.00

B

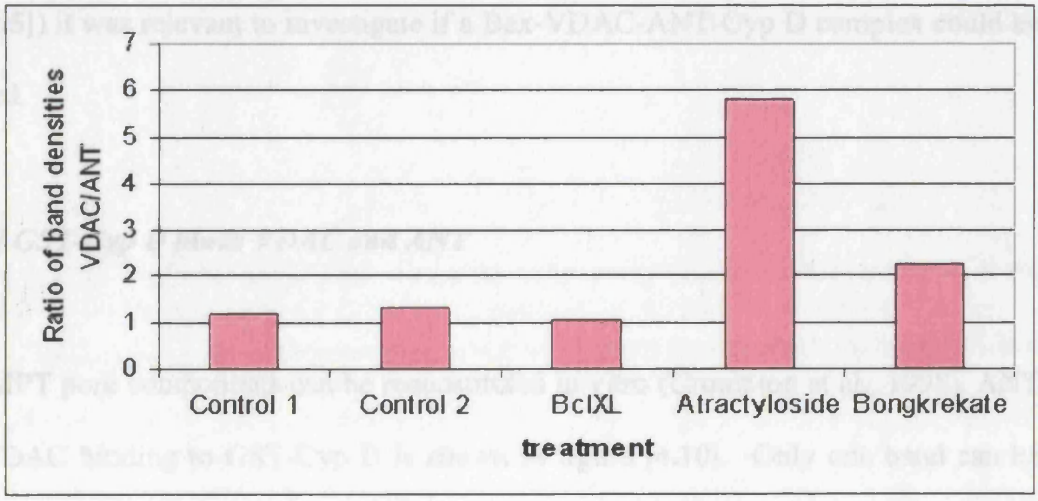

Figure [4.9] Quantifying of the effects of atractyloside, bongkrekic acid and Bcl-X_L on the interactions of VDAC and ANT with GST-Bax. **A** shows the relative band densities of VDAC and ANT on the Western blots shown in figure **[4.8]**. **B** shows the variation in the ratio of VDAC-ANT bound to GST-Bax after the mitochondrial membranes were treated with Bcl-X_L, atractyloside and bongkrekic acid.

[4.2] Bax and the Permeability Transition Pore Complex

Under pathological conditions, for example during ischaemia/reperfusion injury that results in increases in mitochondrial matrix calcium levels, the MPT pore complex can form a large pore in the IMM that results in mitochondrial swelling. MPT-pore opening requires Cyp D since opening is blocked by the Cyp D ligand, Cyclosporin A (CSA) (Crompton et al., 1988). MPT-pore opening may play a role in apoptotic cell death. In particular it was proposed that MPT-pore mediated mitochondrial swelling may provide a mechanism for outer membrane lysis and release of intermembrane space proteins to the cytosol (Loeffler & Kroemer, 2000) although this mechanism is diputed (section **[4.1]**). Since Bax interacts with VDAC and ANT in vitro (figures **[4.4]** and **[4.5]**) it was relevant to investigate if a Bax-VDAC-ANT-Cyp D complex could be isolated.

[4.2.1] GST-Cyp D binds VDAC and ANT

The MPT pore components can be reconstituted in vitro (Crompton et al., 1998). ANT and VDAC binding to GST-Cyp D is shown in figure **[4.10].** Only one band can be seen on the gel at 30 kDa, this is because ANT and VDAC have similar molecular weights of 32k Da and 30 kDa respectively. Western blotting was used to confirm both proteins were present (figure **[4.11]**).

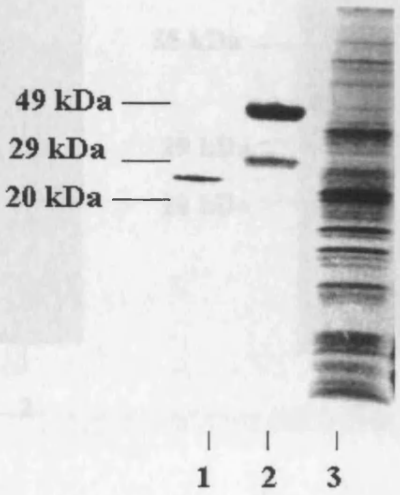

Figure [4.10] Agarose-GST-Cyp D selectively retained a 30kDa protein from mitochondrial membrane extract. Mitochondrial membrane extract was added to 50µl of agarose-GSH-GST and agarose-GSH-GST-Cyp D. The matrices were washed with 600µl of buffer containing 50mM NaCl, 10mM HEPES, 25% glycerol, 1mM EGTA, 8µM ADP, 8µM ATP, 8mM DTT and 0.5mM $MgCl_2$ and the bound proteins were eluted with 50mM NaCl, 50 mM glutathione. The eluted proteins were separated by SDS-PAGE and visualised by Coomassie-blue stain. Lane 1, agarose-GST, lane 2, GST-Cyp D, lane 3, mitochondrial membrane extract.

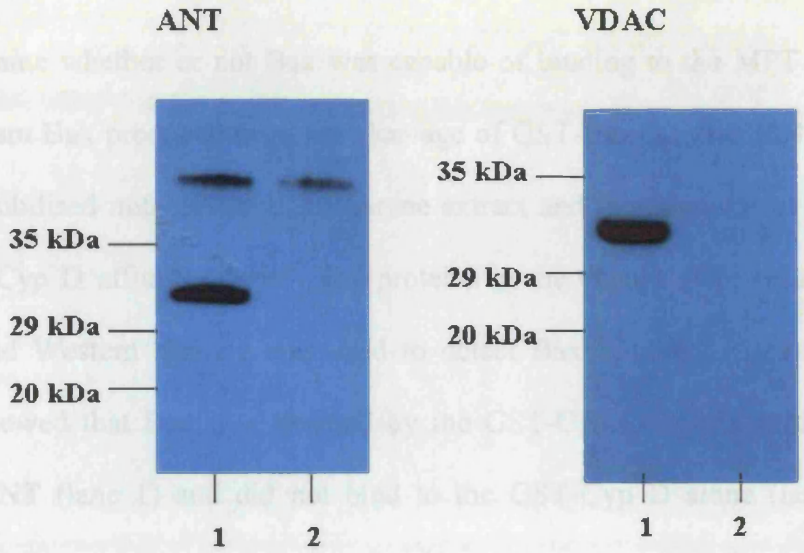

Figure [4.11] VDAC and ANT bind to GST-Cyp D and not GST alone. Western blotting was used to confirm that VDAC and ANT were present in the elutes from the GST-Cyp D matrix. Lane 1, VDAC and ANT co-eluted with GST-Cyp D. Lane 2, VDAC and ANT did not co-elute with GST.

[4.2.2] Bax and Bcl-X_L interact with VDAC-ANT-GST-Cyp D

To determine whether or not Bax was capable of binding to the MPT-pore complex, recombinant Bax produced from the cleavage of GST-Bax (section **[2.4.5]**) was added to the solubilised mitochondrial membrane extract and then the extract was applied to the GST-Cyp D affinity matrix. The proteins in the eluates were separated by SDS-PAGE and Western blotting was used to detect Bax binding (figure **[4.12]**). The results showed that Bax was retained by the GST-Cyp D matrix in the presence of VDAC-ANT (lane 1) and did not bind to the GST-Cyp D alone (lane 2) or when VDAC-ANT and Bax were added to the GST matrix (lane 4) indicating that the Bax-VDAC-ANT-Cyp D interaction was specific. Lane 5 contains recombinant Bax (21 kDa). Other bands can also be seen which are probably breakdown products of Bax generated when GST-Bax was cleaved with factor Xa. None of the breakdown products bound to GST-Cyp D-ANT-VDAC. Figure **[4.13]** shows that VDAC and ANT were present in the eluates from the GST-Cyp D matrix (lanes 1 and 3 in figure **[4.12]**) confirming that they co-elute with Bax (lane 1 figure **[4.12]**). Purified Bcl-X_L (section **[3.3]**) was added to the solubilised mitochondrial membrane extract and the extract was applied to the GST-Cyp D matrix to find out if Bcl-X_L interacts with components of the MPT-pore. Western blotting was used to detect Bcl-X_L in the eluates from the agarose-GSH-GST-Cyp D. Figure **[4.14]** (lane 1) shows that Bcl-X_L was specifically retained by GST-Cyp D in the presence of the mitochondrial extract and VDAC and ANT were also detected in the eluate (not shown). Bcl-X_L was not retained by GST-Cyp D alone (lane 2) or by GST in the presence of the mitochondrial membrane extract (lane 3).

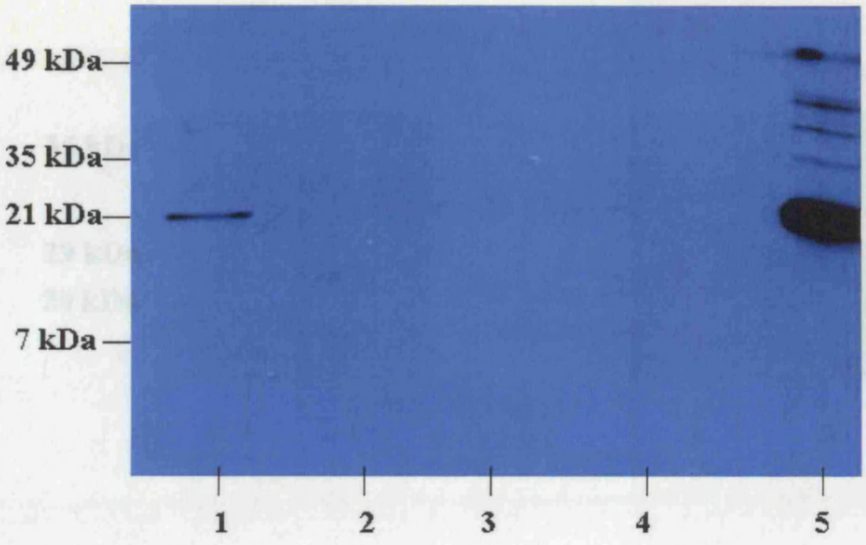

Lane	1	2	3	4	5
Agarose-GSH-GST	-	-	-	+	-
Agarose-GSH-GST-Cyp D	+	+	+	-	-
Mitochondrial membrane extract	+	-	+	+	-
Bax	+	+	-	+	+

Figure [4.12] Bax co-elutes with VDAC and ANT from the GST-Cyp D matrix. Mitochondrial membrane extract (0.25mg protein in 50µl) together with purified Bax (125ng) were added to the agarose-GSH-GST and agarose-GSH-GST-Cyp D matrices. The extract was removed and the matrices were washed 5 times before the bound proteins were eluted with 50mM NaCl, 50mM glutathione. The proteins in the eluates from the GST-Cyp D and GST matrices were separated by SDS-PAGE and the presence of Bax was detected by Western blotting with the 6A7 anti-Bax monoclonal antibody. (The same result was obtained in three independent experiments)

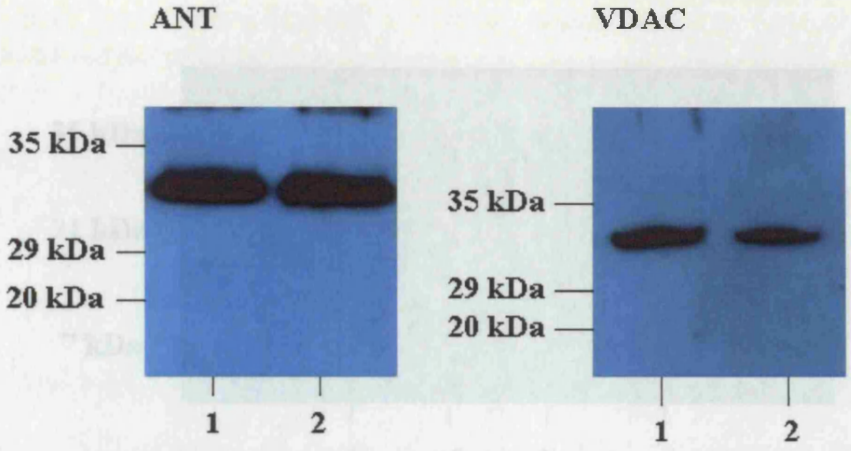

Figure [4.13] VDAC and ANT were present in the eluate from the GST-Cyp D matrix. The presence of VDAC and ANT in the eluates from the GST-Cyp D matrix was detected by Western blotting using the monoclonal anti-VDAC antibody and the polyclonal anti-ANT antibody. Lane 1, eluate from the GST-Cyp D matrix with no Bax added. Lane 2, eluate from GST-Cyp D the matrix with Bax present. (The same result was obtained in three independent experiments)

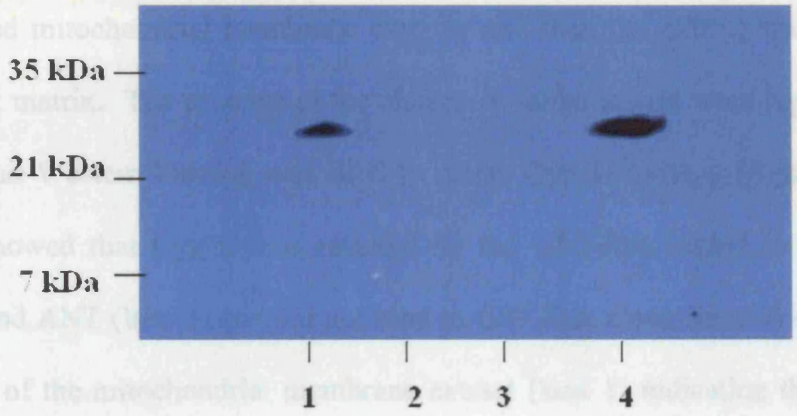

Lane	1	2	3	4
Agarose-GSH-GST	-	-	+	-
Agarose-GSH-GST-Cyp D	+	+	-	-
Mitochondrial membrane extract	+	-	+	-
His-Bcl-X_L	+	+	+	+

Figure [4.14] His_6-Bcl-X_L co-elutes with VDAC and ANT from the GST-Cyp D matrix. Mitochondrial membrane extract (0.25mg of protein in 50µl) together with His-Bcl-X_L (125ng) were added to agarose-GSH-GST or the agarose-GSH-GST-Cyp D. The extract was removed and the agarose matrices were washed 5 times before the bound proteins were eluted with 50mM NaCl, 50mM glutathione. The proteins in the eluates from the GST-Cyp D and GST matrices were separated by SDS-PAGE and the presence of Bcl-X_L was detected by Western blotting with the anti-Bcl-X_L monoclonal antibody. (The same result was obtained in three independent experiments)

[4.2.3] Cyp D interacts with ANT-VDAC-GST-Bax

To confirm the results obtained in section **[4.2.2],** purified Cyp D was added to solubilised mitochondrial membrane extracts and then the extract was applied to the GST-Bax matrix. The proteins in the eluates from the matrix were separated by SDS-PAGE and Western blotting was used to detect Cyp D binding (figure **[4.15]**). The results showed that Cyp D was retained by the GST-Bax matrix in the presence of VDAC and ANT (lane 3) and did not bind to GST-Bax alone (lane 2) or to GST in the presence of the mitochondrial membrane extract (lane 1) indicating the VDAC-ANT-Cyp D complex binds specifically to the Bax moietie (lane 1).

[4.3] Discussion

The results in this chapter show that both GST-Bax and the C-terminally truncated GST-BaxΔc interact with VDAC (OMM) and ANT (IMM) present in rat mitochondrial membranes in the absence of Cyp D which was not present in the mitochondrial membrane preparations (determined by Western blotting data not shown). The GST-Bax proteins used in this investigation retained Bax activity which was determined by adding GST-BaxΔc to isolated rat heart mitochondria and detecting cytochrome c release by Western blotting as described in previous studies using recombinant BaxΔc (Eskes et al., 1998, Jurgenmeier et al., 1998, Pastorino et al., 1999). The results presented in this chapter show increasing the concentration of GST-BaxΔc (lacks 22 amino acids at the C-terminus) resulted in more cytochrome c release up to 500nM of

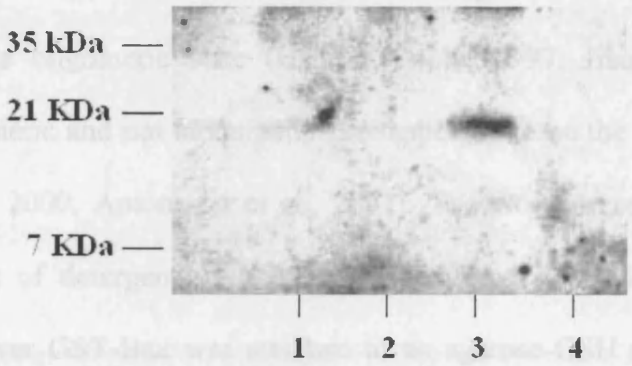

Lane	1	2	3	4
Agarose-GSH-GST	+	-	-	-
Agarose-GSH-GST-Bax	-	+	+	+
Mitochondrial membrane extract	+	-	+	+
Cyp D	+	+	+	-

Figure [4.15] CyP D is specifically retained by GST-Bax in the presence of VDAC and ANT. Mitochondrial membrane extract (0.25mg of protein) together with Cyp D (50ng) were added to agarose-GSH-GST or agarose-GSH-GST-Bax. The extract was removed and agarose matrices were washed 5 times before the bound proteins were eluted with 50mM NaCl, 50mM glutathione. The proteins in the eluates were separated by SDS-PAGE and the presence of Cyp D was detected with an anti-Cyp D raised against the peptide CSDGGARGANSSSQNP, corresponding to the amino acids 1-16 after cleavage of the mitochondrial targeting sequence of Cyp D. (The results are same result was obtained in two independent experiments)

GST-BaxΔc. These results are similar to previously published data using C-terminally truncated Bax (lacks 19 amino acids at the C-terminus) in which Bax induced cytochrome c release in a concentration dependent manner up to 1μM (Pastorino et al., 1999). Other studies have shown that detergents can influence the conformation of Bax and its oligomeric state (Hsu & Youle, 1997, Hsu & Youle, 1998). Moreover oligomeric and not monomeric Bax appeared to be the active form of Bax (Antonsson et al., 2000, Antonsson et al., 2001). The work presented in this chapter shows the choice of detergent used had no effect on VDAC and ANT binding to GST-Bax. However GST-Bax was attached to an agarose-GSH matrix and therefore it was not clear whether conformational changes and oligomerisation would take place under these conditions. Atractyloside and bongkrekic acid are ANT ligands. Other studies have shown that bongkrekic acid protects cells from apoptosis (Marchetti et al., 1996 a, b, Cao et al., 2001). The current study demonstrates that bongkrekic acid increased the amount of both VDAC and ANT retained by GST-Bax whilst atractyloside, which promotes apoptosis by potentiating Bax action on mitochondria (Pastorino et al., 1999), decreased the amount of ANT retained by GST-Bax and slightly reduced the amount of VDAC retained. These results suggest that the stoichiometry of the VDAC and ANT intermembrane complexes may be important in the promotion of apoptosis by atractyloside and the protection by bongkrekic acid. To further investigate the significance of VDAC-ANT stoichiometry in the atractyloside promotion and bongkrekic acid inhibition of the release of apoptogenic proteins from the IMS, isolated mitochondria incubated with Bax in the presence of atractyloside or bongkrekic acid could be treated with reagents to cross-link Bax and VDAC-ANT in the intermembrane

contact sites. Western blotting could be used to examine the relative amounts of VDAC and ANT present. Although bongkrekic acid inhibits apoptosis, its primary action is to inhibit the export of ATP from the mitochondria to the cytosol and therefore would be of little therapeutic value especially in the heart, which is dependent on oxidative phosphorylation and the export of ATP from the mitochondria to the cytosol to drive contractions.

In order to investigate whether or not Bax was capable of interacting with components of the MPT-pore GST-Bax was cleaved with factor Xa and this was added to GST-Cyp D together with the mitochondrial membrane extract containing VDAC and ANT. The results show that Bax was retained by GST-Cyp D in the presence of VDAC and ANT. Cyp D co-eluted with VDAC and ANT from the GST-Bax matrix. These results demonstrate that Bax is capable of direct interaction with the components of the MPT-pore supporting the hypothesis put forward by Kroemer's group that Bax interacts with the MPT-pore to mediate the release of apoptogenic proteins from IMS. The results in this chapter also show that His_6-Bcl-X_L interacts with the MPT-pore and its antagonistic effect against Bax may involve the inhibition of Bax binding to the MPT-pore. Recently De Giorgi and co-workers (De Giorgi et al., 2002) investigated whether MPT-pore opening in live cells was sufficient to activate apoptosis. MPT was induced in live cells using tetramethyl-rhodamine methyl ester (TMRM) whose positive charge causes it to be accumulated within the mitochondria. Using a cell line stably transfected with GFP-cytochrome c they showed that cytochrome c release from the IMS occurred 4 hours after MPT-pore opening and dissipation of $\Delta\psi_m$. Triple wavelength imaging was performed to visualise the mitochondrial matrix compartment, the distribution of Bax

and cytochrome c. Their results showed that after MPT-pore opening but before any visible sign of Bax redistribution from the cytosol to the mitochondria no cytochrome c release was detected. Cytochrome c was still present in the IMS after Bax localisation to mitochondria and was only released after large (100nm) Bax clusters were formed on the outer OMM. They therefore concluded MPT-pore opening and $\Delta\psi_m$ dissipation signals Bax translocation to mitochondria and it is the subsequent clustering/multimerisation and Bax channel formation that results in cytochrome c release. The involvement of the MPT-pore in the release of apoptogenic proteins from the IMS still remains controversial. The dissipation of $\Delta\psi_m$ is not detected in all cell types during apoptosis indicating that this is not a universal mechanism for cytochrome c release. For example, during fenretinide-induced apoptosis in neuroblastoma cell lines cytochrome c release was detected with no significant $\Delta\Psi_m$ dissipation (Lovat et al., 2000). Other studies show that $\Delta\Psi_m$ dissipation does occur however this was not a result of MPT-pore opening. When apoptosis was induced in human leukaemia cell lines with the immunosuppressive, anti-tumour, anti-viral drug didemnin B, $\Delta\Psi_m$ dissipation occurred but was not inhibited by either CSA or bongkrekic acid and was inhibited by the broad-range caspase inhibitor z-VAD-fmk (Grubb et al., 2001). Another study showed that the addition of Bax to isolated rat heart mitochondria resulted in the opening of large pores in the OMM, the inhibition of the respiratory chain and the uncoupling of the IMM by increasing proton leakage without the opening of the MPT-pore as indicated by a lack of sensitivity to CSA (Appaix et al., 2002).

This current study demonstrates that GST-Bax is capable of interacting with VDAC and ANT without the presence of Cyp D. Other work has shown that contact sites between the inner and outer mitochondrial membranes formed the interaction of VDAC and ANT may be responsible for cytochrome c release. Doran and Halestrap (Doran & Halestrap, 2000) showed that Bax dimers were present in Percoll-purified isolated rat liver mitochondria and cytochrome c was released independently of adenylate kinase implying outer mitochondrial membrane rupture did not take place. They showed that cytochrome c release was not inhibited by CSA indicating that the MPT-pore was not involved. Other proteins bind to VDAC-ANT contact sites e.g. hexokinase and this was shown to inhibit Bax-induced cytochrome c release and apoptosis (Pastorino et al., 2002), by competing with Bax for binding at the mitochondrial surface. The cell-free GST pulldown system described in this chapter could be used to investigate which other proteins associate with the contact sites, e.g. creatine kinase and the benzodiazepine receptor, can interact simultaneously with VDAC, ANT and Bax. The experiments could also be performed using other Bcl-2 proteins to determine if they compete with Bax for binding to VDAC and ANT.

Chapter 5: Results

Anoxia-induced translocation of GFP-Bax from the cytosol to mitochondria in rat cardiomyocytes

[5.1] Bax translocation to mitochondria

Apoptosis in cardiomyocytes has been reported in a variety of cardiovascular pathologies including ischaemia/reperfusion injury (MacLellan & Schneider, 1997, Haunstetter & Izumo, 1998). Apoptotic and necrotic cell death both occur during ischaemic injury in the myocardium (Kajstura et al., 1996, Fliss & Gattinger, 1996, Veinot et al., 1997). However, apoptosis was shown to be the earliest form of cell death in ischaemic myocardium in both animal models and humans. Although apoptosis and necrosis are the two accepted and clearly defined forms of cell death, there are increasing reports of cell death which share features of both apoptosis and necrosis (Leist & Jaattela, 2001), raising the question whether they are discrete forms of cell death or if there is a range of responses utlising the same machinery. Whether apoptosis or necrosis is initiated in ischaemic cardiomyocytes is thought to be dependent on the presence or absence of ATP. If ATP is present then cells die by apoptosis since energy is required for the execution of apoptosis (Tatsumi et al., 2003, Shiraishi et al., 2001, Nicotera et al., 1998). However, glucose uptake and glycolysis reduced hypoxia induced apoptosis in neonatal rat cardiomyocytes (Malhotra & Brosius, 1999). Whether hypoxia/anoxia alone is sufficient to induce apoptosis or if it requires a combination of hypoxia and reperfusion leading to acidosis is disputed.

Webster and co-workers (Webster et al., 1999) have demonstrated that in an *in vivo* model, acidosis and reperfusion but not hypoxia alone induced apoptosis. In another study chronic hypoxia was shown to induce apoptosis in rat hearts and in isolated rat cardiomyocytes (Jung et al., 2001). More recently the molecular mechanisms of hypoxia-induced apoptosis in tumour cells were investigated and these results showed cell-death occurred via the intrinsic apoptotic (mitochondrial) pathway (Weinmann et al., 2004). There are two pathways that lead to cell death. The extrinsic pathway requires the triggering of the cell surface death receptors by specific ligands and allows the cell to respond to the immediate environment. Cells can also die via the intrinsic pathway, which is driven by organelles such as the ER and the mitochondria, in response to changes in the internal environment. Both of these pathways have been implicated in apoptosis occurring in myocardial diseases with the mitochondrial pathway playing a role in the acute and chronic phases of myocardial disease and death receptors may play a more significant in the longer term (Clerk et al., 2003).

During hypoxia-induced apoptosis in cardiomyocytes the level of Bax expression was significantly increased in hypoxic rat hearts compared with normoxic hearts (Jung et al., 2001) implying that Bax plays an important role in the hypoxia-induced apoptotic pathway. In many cell types, including cardiomyocytes, Bax is located predominantly in the cytosol but translocates to mitochondria at an early stage in apoptosis (Wolter et al., 1997, Zhang et al., 1998, Capano & Crompton, 2002). Bax present in the cytosol of non-apoptotic cells has the N-terminal domain buried within the protein (Hsu & Youle, 1997) and this prevents its targeting to mitochondria (Cartron et al., 2003). However, previously it was shown that regulated targeting of Bax to mitochondria and its

insertion into the mitochondrial membranes involved the C-terminal hydrophobic domain and was accompanied by conformational changes that expose the N-terminal region and the BH3 domain (Wolter et al., 1997, Goping et al., 1998, Desagher et al., 1999). These changes were shown to be responsible for dimerisation mediated by the exposed BH3 domain (Wang et al., 1999, Antonsson et al., 1991). In contrast other groups have shown that deletion of the C-terminus of Bax did not abolish mitochondrial targeting and therefore proposed that the C-terminus is not a mitochondrial targeting signal (Tremblais et al., 1999). More recently Bax-induced cytochrome c release from mitochondria was shown to be dependent on α-helices –5 and –6 (Heimlich et al., 2004). These α-helices share structural similarities to the pore-forming domains of certain bacterial toxins (Chou et al., 1999, Mc Donnell et al., 1999, Sattler et al., 1997). This study showed that Bax lacking a functional BH3 domain was capable of inducing cytochrome c release, however, deletion of helices -5 and -6 prevented insertion of Bax into mitochondrial membranes and greatly decreased the cytochrome c releasing activity. The ability of Bax to induce the release of apoptogenic proteins from the IMS is thought to be dependent on its oligomeric state. In particular, Bax complexes (4-mers and 12-mers) were isolated from apoptotic cells (Antonsson et al., 2001, Gross et al., 1998). Larger Bax aggregates containing thousands of Bax molecules have been detected close to mitochondria during apoptosis (Nuchushtan et al., 2001). However the role of these Bax aggregates in the permeabilisation of the OMM or other apoptotic functions is not known. Previous studies in our laboratory have shown that endogenous Bax was present throughout the cytosol in primary rat cardiomyocytes (Capano & Crompton, 2002). Induction of apoptosis by staurosporine lead to a punctate distribution of Bax. Further experiments with cardiomyocytes transfected with GFP-

Bax and using MitoTracker red, which accumulates electrophoretically into mitochondria in response to high inner membrane potential, revealed that the GFP-Bax co-localised with the MitoTracker red. Therefore it was concluded that the punctate distribution of Bax during apoptosis was due to its localisation to mitochondria.

In this investigation primary rat cardiomyocytes were transfected with GFP-Bax (green fluorescent protein present at the N-terminal of Bax, section **[2.2]**). GFP-Bax constructs have been used in a number of studies to examine Bax translocation from the cytosol to the mitochondria during apoptosis (Wolter et al., 1997, Neschushtan et al., 2001, Capano & Crompton, 2002). GFP-Bax has the same cellular distribution as endogenous Bax, i.e. in the cytosol of healthy cells, despite the presence of the large GFP-tag (30 kDa) at the N-terminus. The cells were treated with sodium cyanide (1mM) to block mitochondrial electron transport and no glucose was present in the medium in order to impose simulated ischaemia. The aim of this work was to find out if Bax translocation from the cytosol to mitochondria occurred under ischaemic conditions in cardiomyocytes. Another aim was to determine if Bax was capable of interacting with the VDAC-ANT junctional intermembrane contact sites and if Cyp D was present which would provide strong support for the role of the MPT-pore in Bax induced permeabilisation of the OMM.

[5.1.1] GFP-Bax translocation to mitochondria after incubation with cyanide

In this investigation anoxia-induced apoptosis in rat cardiomyocytes was initiated by the addition of sodium cyanide (1mM). Cardiomyocytes transfected with GFP-Bax (section **[2.2]**) were observed by fluorescent microscopy before the addition of cyanide and at half hour intervals after the addition of cyanide. Figure **[5.1]** shows images obtained over a 4 hour time-period of a single cardiomyocyte transfected with GFP-Bax following the addition of sodium cyanide. In figure **[5.1] A,** time-zero before treatment with cyanide, GFP-Bax had a diffuse distribution throughout the cytoplasm and the nucleus with a few denser regions of GFP-Bax present in the cytoplasm. Over a 4 hour time-period the distribution of GFP-Bax became less diffuse and the denser regions of GFP-Bax in the cytoplasm became more apparent. This punctate distribution of GFP-Bax is observed after 2.5 hours after treatment with sodium cyanide (figure **[5.1] C**). Figure **[5.2] A** shows an enlarged region of the cell at time zero and figure **[5.2] B** after 4 hours incubation with cyanide. It clearly shows the punctate GFP-Bax distribution in the cytoplasm. After 4-6 hours the mitochondria began to break up and disappear (results not shown).

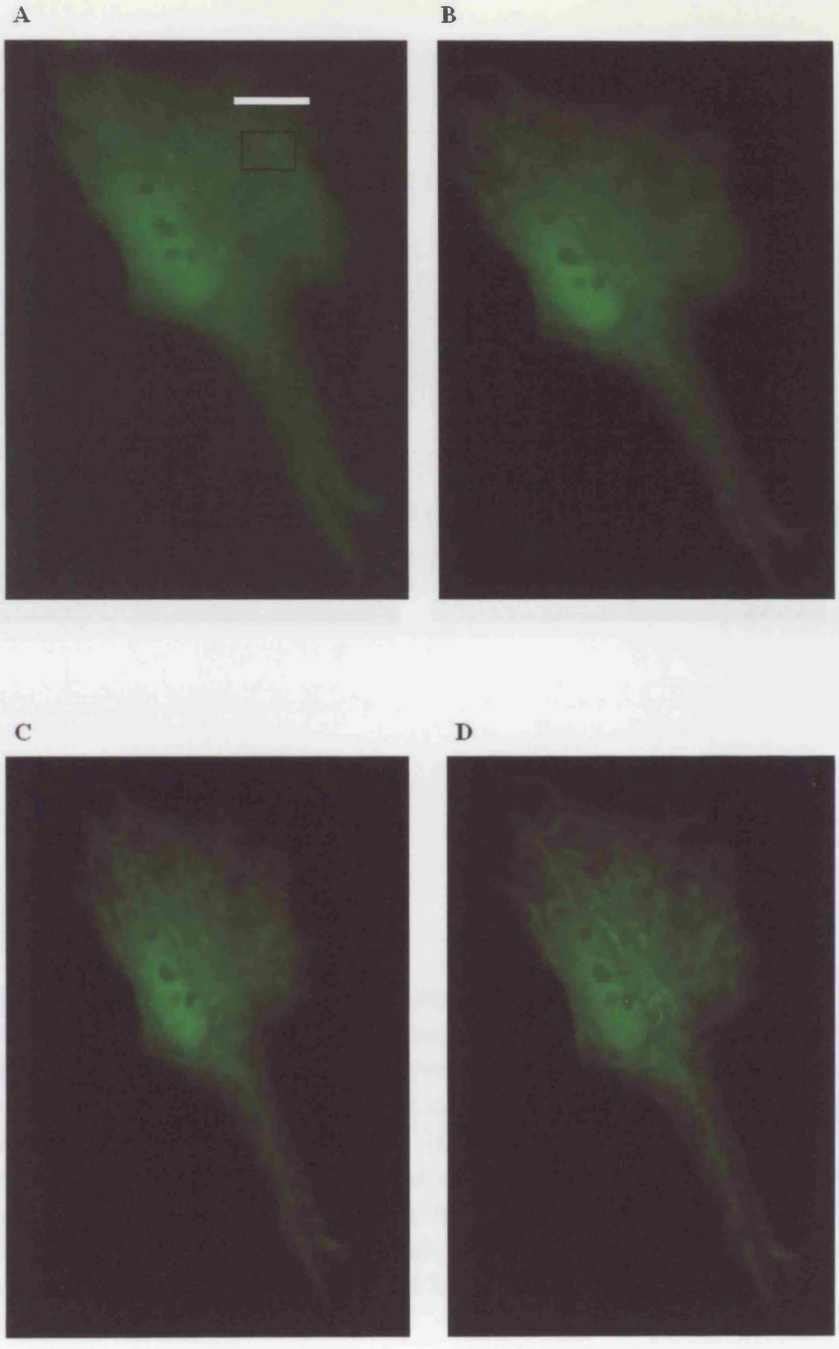
A
B
C
D

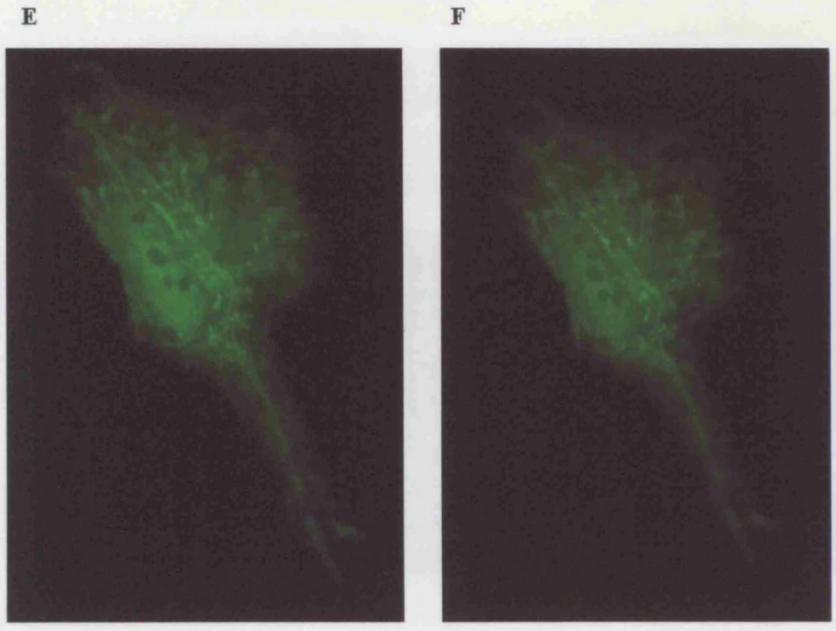

Figure [5.1] Cyanide-induced translocation of GFP-Bax. A cardiomyocyte transfected with GFP-Bax was imaged at the indicated times after the addition of sodium cyanide. Cells were removed from the incubator (37°C) and the cell culture medium was removed and replaced with 1ml of buffer containing 24mM HEPES, 4mM KCl, 100mM NaCl, 1mM $MgSO_4$, 1mM $CaCl_2$, 1mM KH_2PO_4, pH 7.4 (for each cover slip). The imaging of the cells was carried out at room temperature. Sodium cyanide was added to the incubation medium. **A** At time-zero, before the addition of sodium cyanide. Scale bar represents 10μm. **B** After 1.5 hours. **C** After 2.5 hours. **D** After 3 hours. **E** After 3.5 hours. **F** After 4 hours.

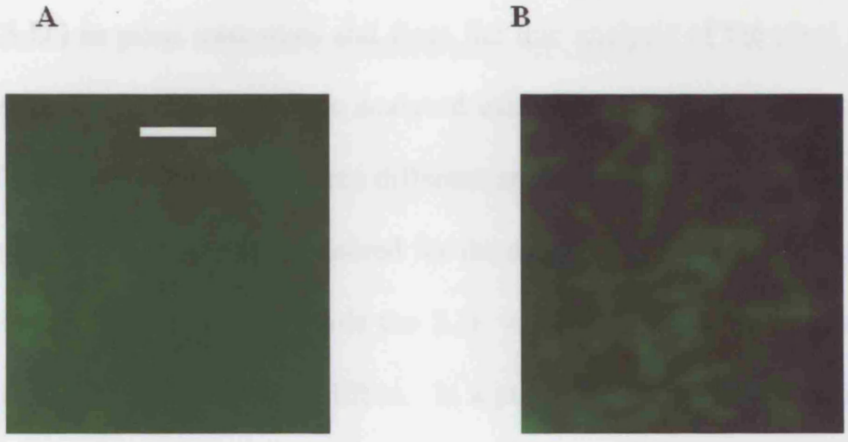

Figure [5.2] Enlargement of an area of a cardiomyocyte transfected with GFP-Bax before and four hours after the addition of sodium cyanide. **A** An enlargement of the area shown in the rectangle of **[5.1] A** showing a cardiomyocyte at time-zero before the addition of sodium cyanide. **B** The same area was selected in **[5.1] F** that shows the same cardiomyocyte 4 hours after the addition of sodium cyanide. Scale bar represents 2.5μm

[5.1.2] Analysis of GFP-Bax translocation

Changes in GFP-Bax distribution were quantified in two ways; from the standard deviation (S.D.) in pixel intensities and from the line analysis of the pixel intensities. The images shown in **[5.1] A-F** were analysed using Metamorph Software to calculate the S.D. of the pixel intensities. Three different areas of the cell were selected and the S.D. of the pixel intensities was measured for the same areas within each image (figure **[5.3]**). Before the addition of cyanide the S.D. values were low but increased as the GFP-Bax distribution became less diffuse. In a previous study GFP-Bax translocation was followed after cardiomyocytes were incubated with staurosporine. Three distinct phases of GFP-Bax sequestration were observed (Capano & Crompton, 2002). The two phases observed in figure **[5.3]** were also seen i.e. the initial diffuse distribution of GFP-Bax followed by its localisation to mitochondria. The third phase characterised was associated with the formation of large Bax aggregates on mitochondria. The Bax aggregates were first observed by Nechushstan and co-workers in HeLa cells undergoing apoptosis after treatment with staurosporine (Nechushstan et al., 2001). When the cardiomyocytes were incubated with cyanide the third phase with GFP-Bax aggregates present on mitochondria was rarely seen. At later time points there was a loss of mitochondrial integrity and GFP-Bax could not be seen.

In figure **[5.4]** the pixel intensities were analysed along a line drawn through the cytoplasm after different times after treatment with sodium cyanide. The analysis shows that at time-zero, before the addition of cyanide, the intensity of the adjacent pixels along the line had a similar intensity that was consistent with the observed diffuse distribution of GFP-Bax in the cytoplasm (figure **[5.4] A, C**). After 4 hours

incubation with sodium cyanide the pixel intensity of adjacent pixels varied which is consistent the observed punctate GFP-Bax distribution (figure **[5.4] B, D**).

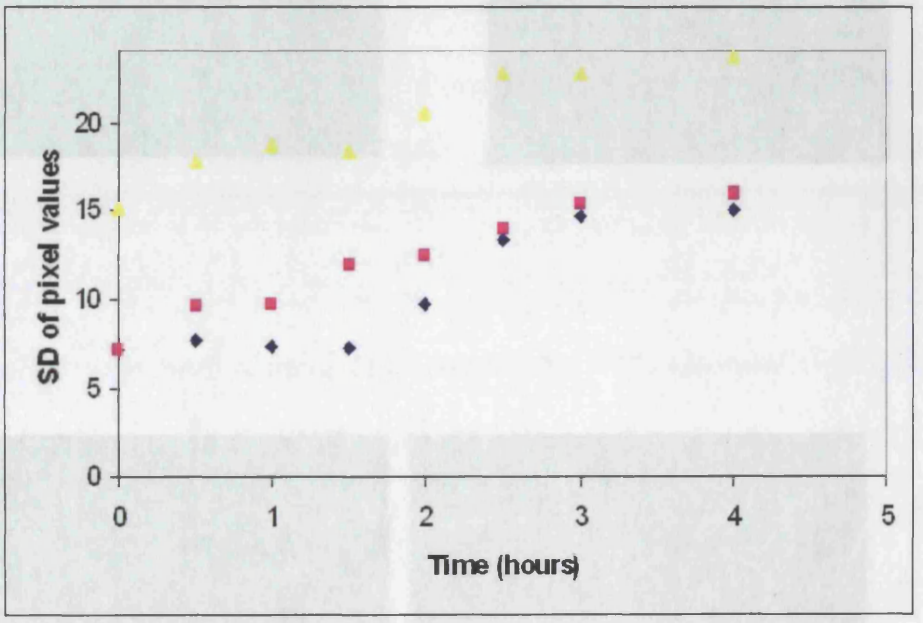

Figure [5.3] Analysis of S.D. of pixel intensities for each time-point. Three different areas with the same dimensions were selected for each of the images (A) to (F) shown in figure **[5.1]** and the Metamorph software was used to determine the S.D. for each of the selected regions as to obtain a quantitative measure of the changes in the intracellular distribution of GFP-Bax from time-zero before the addition of sodium cyanide up to 4 hours after treatment with cyanide.

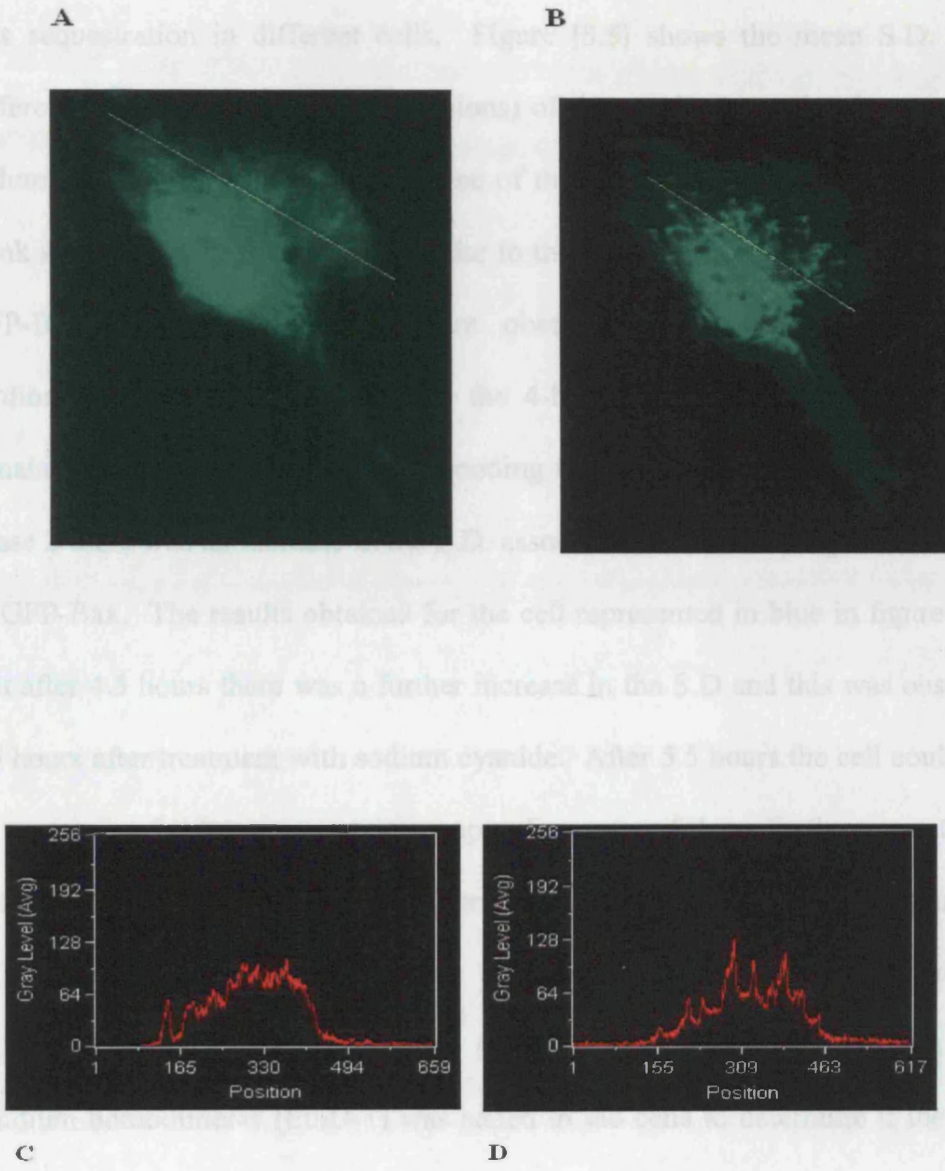

Figure [5.4] Line analysis of pixel intensities. **A** Cardiomyocyte at time-zero before the addition of sodium cyanide. **B** After 4 hours incubation with sodium cyanide. The pixel intensities along the same line shown are given in **C** (time-zero) and **D** (after 4 hours).

The analysis of the S.D. of pixel intensities was also performed to compare the GFP-Bax sequestration in different cells. Figure **[5.5]** shows the mean S.D. from three different areas (with the same dimensions) of three different cells after treatment with sodium cyanide for up to 6 hours. One of the cells shown is the same as figure **[5.1]** (pink squares). These results are similar to those shown in figure **[5.3]**. The same two GFP-Bax sequestration phases were observed when the areas of the single cardiomyocytes were examined over the 4-hour time-course. In phase 1, the S.D. remains low up until 2 hours corresponding to a diffuse GFP-Bax distribution and in phase 2 there was an increase in the S.D. associated with the more punctate distribution of GFP-Bax. The results obtained for the cell represented in blue in figure **[5.5]** show that after 4.5 hours there was a further increase in the S.D and this was observed up to 5.5 hours after treatment with sodium cyanide. After 5.5 hours the cell could no longer be seen using the fluorescent microscope. For most of the cells the punctate GFP-Bax distribution was observed up to 4 hours after the addition of cyanide after which the cells began to break up and disappear. Figure **[5.6]** shows the images obtained for the cell represented in blue in figure **[5.5]**. After 5 hours, following the addition of cyanide, ethidium homodimer-1 (EthD-1) was added to the cells to determine if they were still viable. EthD is excluded by the intact plasma membrane of live cells but enters cells with damaged membranes and undergoes a 40-fold enhancement of fluorescence upon binding nucleic acids, thereby producing a bright red fluorescence in dead cells.

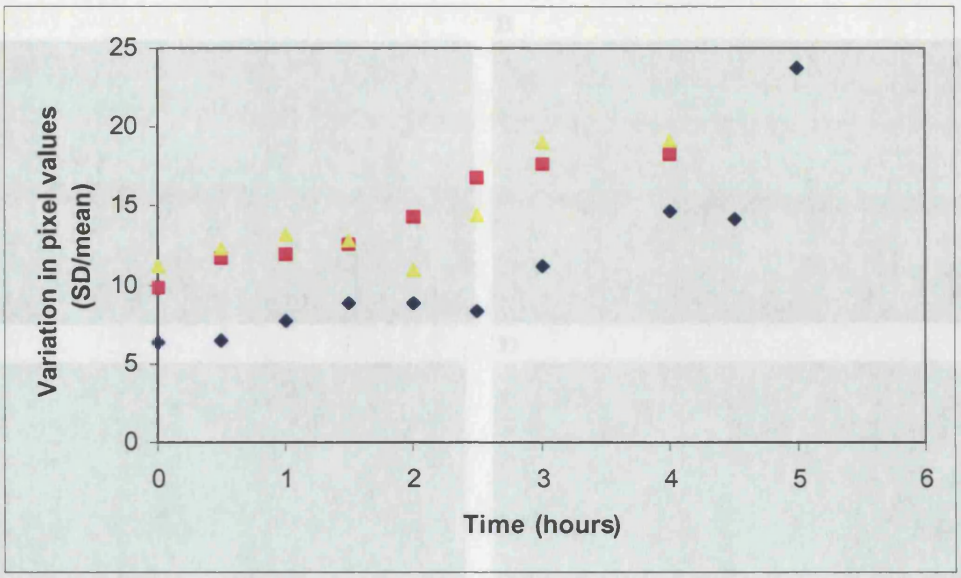

Figure [5.5] Analysis of mean S.D. of pixel intensities for each time-point for three different cells. Each colour (yellow, blue and pink) represents a different cell. The pink line shows the mean data for the cell shown in figure **[5.1]**. Three areas (with the same dimensions) of each cell were analysed for each time-point after the addition of sodium cyanide and the mean value for the S.D. was calculated.

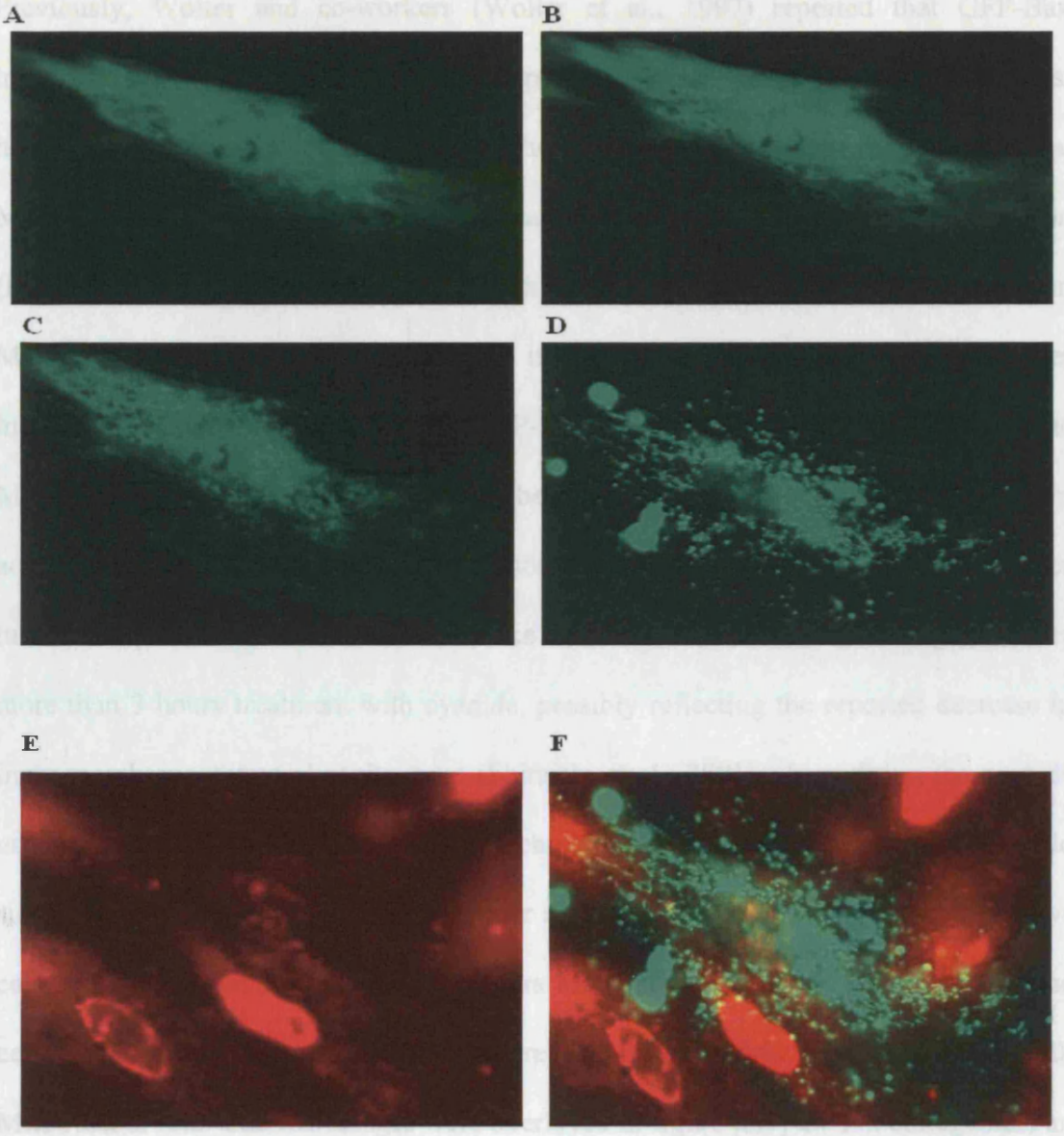

Figure [5.6] Cell viability after treatment with sodium cyanide. A cardiomyocyte transfected with GFP-Bax was imaged at the indicated times after addition of cyanide. **A** At time-zero. **B** After 2 hours. **C** After 3 hours. **D** After 5 hours. **E** After 5 hours the cells were stained with EthD-1. The nuclei of dead cells stain bright red. **F** Overlay of the images of GFP-Bax and EthD-1.

Previously, Wolter and co-workers (Wolter et al., 1997) reported that GFP-Bax translocated to mitochondria in staurosporine-induced apoptosis in Cos-7 cells; however, GFP-Bax also accumulated at other sites that did not stain for mitochondria. More recently it was shown that Bax also targets the ER where it affects Ca^{2+} retention (Pan et al., 2001, Oakes et al., 2003). In this investigation the mitochondrial stain MitoTracker red was used to determine if the punctate GFP-Bax distribution after incubation with cyanide was due to GFP-Bax localisation with mitochondria. The MitoTracker red was added immediately before the induction of apoptosis. This stain accumulates electrophoretically into mitochondria in response to the high inner membrane potential. Mitochondrial uptake of the MitoTracker became impaired after more than 3 hours treatment with cyanide, possibly reflecting the reported decrease in inner membrane potential at this time (Shiraishi et al., 2001). In addition the cyanide used in this investigation inhibits the mitochondrial electron transport chain that would subsequently lead to a decrease in the inner membrane potential. Figure **[5.7] A** shows cells transfected with GFP-Bax three hours after the addition of cyanide. The same cells are shown in figure **[5.7] B** where the mitochondria were visualised with MitoTracker red. The two images were overlayed in figure **[5.7] C**. An enlargement an area of the cell shown in figure **[5.7]** is shown in figure **[5.8]**. The overlayed images show that the punctate distribution of GFP-Bax is due to its localisation to mitochondria. However, ER tracker would be required to determine whether or not GFP-Bax translocates to the ER.

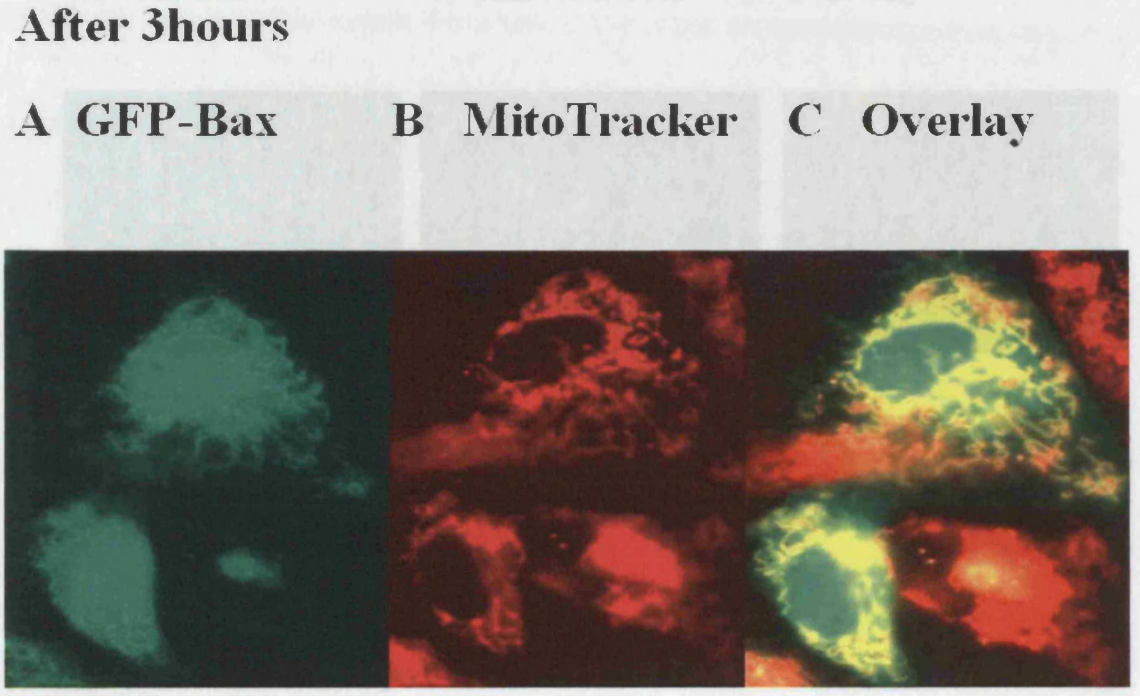

Figure [5.7] Localisation of GFP-Bax to mitochondria. **A** Cardiomyocytes transfected with GFP-Bax. **B** Cardiomyocytes stained with MitoTracker red. **C** Overlay of images **A** and **C**.

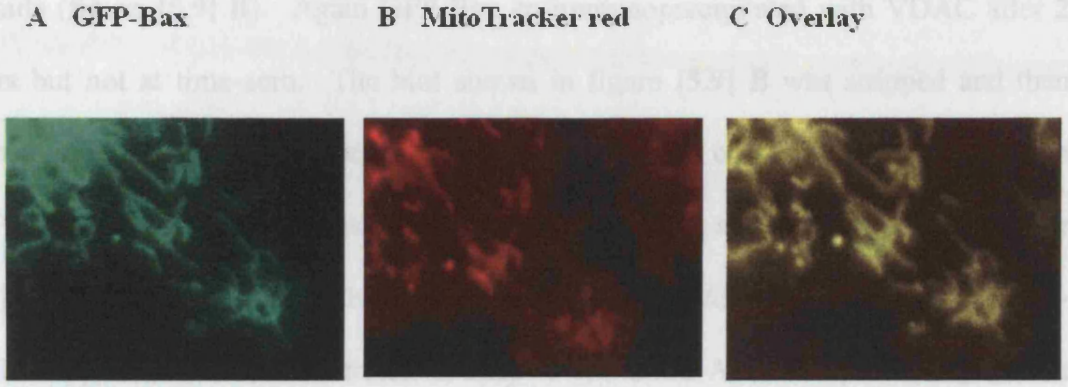

Figure [5.8] Enlargement of an area of the cardiomyocyte shown in figure [5.7] 3 hours after treatment with sodium cyanide

[5.2] GFP-Bax co-immunoprecipitates with VDAC and ANT

Immunoprecipitations were performed to find out if Bax targets VDAC-ANT intermembrane contact sites in rat cardiomyocytes. Cell extracts were prepared from GFP-Bax and GFP transfected cardiomyocytes (section **[2.8]**). These extracts were incubated with anti-GFP monoclonal antibody coupled to sepharose beads. The immunoprecipitated proteins were extracted in SDS-PAGE sample buffer and analysed by Western blotting. Figure **[5.9] A** shows that VDAC co-immunoprecipitates with GFP-Bax 1.5 hours and 3 hours after cells were treated with cyanide. In addition only a very small amount of VDAC co-immunoprecipitated with GFP-Bax at time-zero, before the addition of cyanide. VDAC did not co-immunoprecipate with GFP 3 hours after the

cells were treated with cyanide. In two separate experiments, with different cells, immunoprecipitations were carried out at time-zero and 2 hours after incubation with cyanide (figure **[5.9] B**). Again GFP-Bax co-immunoprecipitated with VDAC after 2 hours but not at time-zero. The blot shown in figure **[5.9] B** was stripped and then probed with an anti-ANT polyclonal antibody. ANT also co-immunoprecipitates with GFP-Bax 2 hours after the cells were treated with cyanide and not at time-zero (figure **[5.9] C**). These data indicate that Bax not only interacts with VDAC, but also VDAC-ANT complexes. As demonstrated in chapter 4, VDAC-ANT complexes can recruit Cyp D from the mitochondrial matrix to produce a complex that forms the PT pore under pathological conditions (Crompton et al., 1998). Therefore Western blotting was used to detect Cyp D in the immunoprecipitates, however, none was detected.

[5.3] Discussion

In this investigation rat cardiomyocytes transfected with GFP-Bax were treated with cyanide to induce apoptosis and GFP-Bax translocation was examined in single rat cardiomyocytes. Initially the GFP-Bax displayed a diffuse distribution throughout the cytosol and 1.5 hours after treatment with cyanide a more punctate GFP-Bax distribution was observed. The mitochondrial stain MitoTracker red was used to show that GFP-Bax localised to mitochondria. In Chapter 4 the results showed that GST-Bax interacted with VDAC and ANT in mitochondrial membrane extracts derived from rat hearts. When purified Cyp D was added, together with the mitochondrial membrane extract, it was also retained by the GST-Bax matrix indicating that Bax interacted with

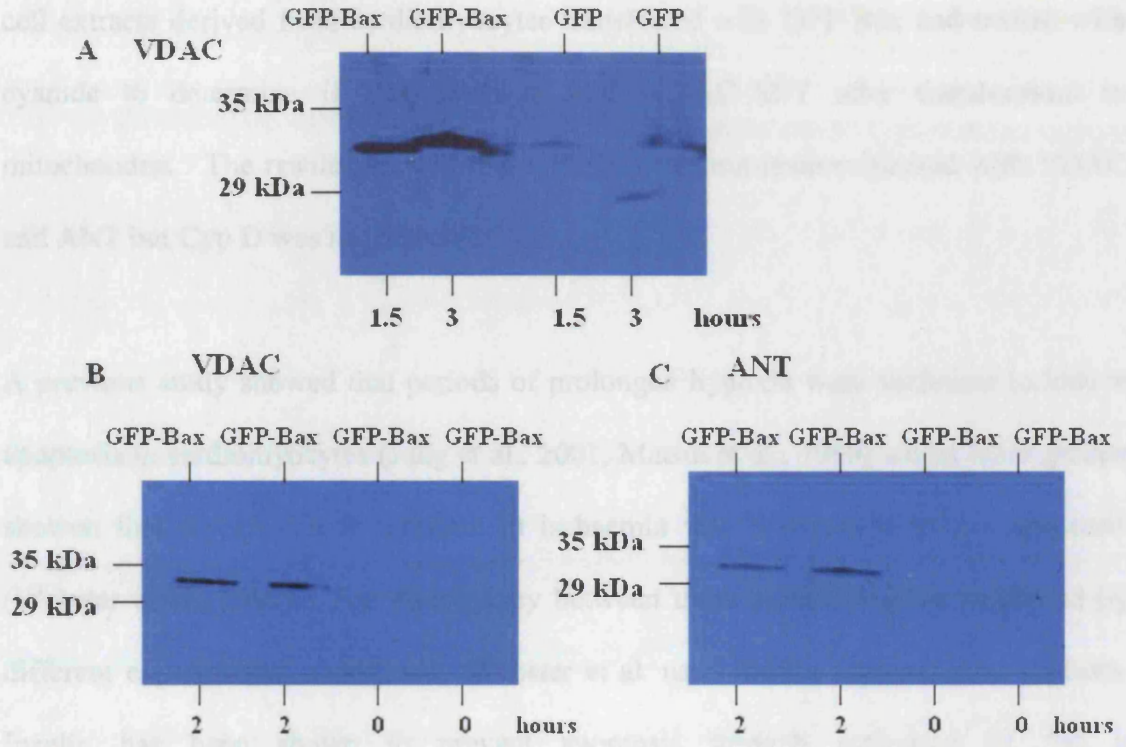

Figure [5.9] GFP-Bax co-immunoprecipitates with VDAC and ANT after translocation to mitochondria. A GFP-Bax transfected cells were treated with 1mM sodium cyanide for the time indicated. Anti-GFP antibody coupled to sepharose beads was used to immunoprecipitate GFP-Bax or GFP from extracts of the transfected cells (as indicated above each lane; whether cells were tranfected with either GFP alone or with GFP-Bax). Western blotting was used to determine if VDAC was present in the immunoprecipitate (IP). **B** In two other experiments, using different cells, Western blotting was used to detect VDAC in the IPs before treatment with cyanide and two hours after treatment with cyanide. **C** The blot shown in **B** was stripped and Western blotting was used to determine if ANT was present in the GFP-Bax IPs.

components of the MPT-pore. Therefore immunoprecipitations were performed using cell extracts derived from cardiomyocytes transfected with GFP-Bax and treated with cyanide to determine if Bax interacts with VDAC-ANT after translocation to mitochondria. The results showed that GFP-Bax co-immunoprecipitated with VDAC and ANT but Cyp D was not detected.

A previous study showed that periods of prolonged hypoxia were sufficient to induce apoptosis in cardiomyocytes (Jung et al., 2001, Matsui et al., 1999) whilst other groups showed that reperfusion in addition to ischaemia was required to induce apoptosis (Webster et al., 1999). The discrepancy between these studies may be explained by different experimental conditions. Webster et al. used insulin-supplemented medium. Insulin has been shown to prevent apoptosis through activation of Akt a serine/threonine kinase, which is a downstream effector of growth factor mediated cell survival (Hermann et al., 2000). In the work presented in this chapter cardiomyocytes were subjected to simulated ischaemia. Treatment of the cells with cyanide inhibited the electron-transport chain to induce anoxia and no glucose was present in the medium to simulate ischaemia. Jung and co-workers compared the levels of Bax expression in hypoxic and normoxic rat hearts and in cultured cardiomyocytes. Their data showed that Bax expression levels were increased in hypoxic rat hearts but not in cultured hypoxic cardiomyocytes. Jung and co-workers suggest this difference may be due to a daily 10-minute period of re-oxygenation in room air while the rats were fed and the cages were changed. Whether or not hypoxia increases Bax expression may not be critical since Bax is present in the cytosol of non-apoptotic cardiomyocytes and transient transfection with GFP-Bax does not result in apoptosis. Bax action is

dependent on apoptotic stimuli that results in conformational changes that expose the N-terminal region of Bax, the oligomeric state of Bax (Antonsson et al., 2001) and translocation to mitochondrial membranes (Wolter et al., 1997, Capano & Crompton, 2002). Evidence for the central role of mitochondria in hypoxia-induced apoptosis was provided in a recent study by Weinmann and co-workers (Weinmann et al., 2004). Their results showed that a lack of caspase-8 or FADD, that are important mediators of the extrinsic pathway which is activated by ligation of receptors on the plasma membrane and in which mitochondria do not play a central role, had no affect on the time-course or rate of hypoxia induced apoptosis in Jurkat T-lymphoma cells. In contrast, overexpression of Bcl-2 or expression of a dominant negative caspase-9 mutant, both known to interfere with mitochondrial apoptotic signalling, significantly inhibited hypoxia-induced apoptosis. Therefore it was concluded that hypoxia-induced apoptosis occurs via the intrinsic apoptotic pathway.

In this study EthD-1 was used to determine cell viability after treatment with cyanide, however, this did not show whether the cells were apoptotic or necrotic. The relative levels of apoptotic and necrotic cell death could be measured in a number of ways. Phoshatidylserine is exposed on the surface of apoptotic cells. Annexin V binds to phosphatidylserine with high affinity and this can be conjugated with fluorescein in order to detect apoptotic cells using flow cytometry (van Engeland et al., 1998). In addition the cationic dye PI could be used together with fluorescein-annexin since PI is excluded by intact plasma membranes. Therefore it would be possible to determine if the cells were unaffected, non-apoptotic cells (annexin V negative/PI negative), early apoptotic cells (annexin V positive/PI negative), and late apoptotic or necrotic cells (PI

positive). Other ways in which apoptotic cells can be identified is by detecting DNA strand breaks, for example using terminal deoxynucleotide transferase-mediated dUTP-biotin nick-end labeling (TUNEL) (Gavrieli et al., 1992). The incorporation of biotinylated bases into damaged DNA allows their subsequent detection by anti-biotin antibodies.

The mechanism of Bax-induced permeabilisation of the OMM remains unresolved. Tsujimoto's group has proposed that VDAC forms a pore through which apoptogenic proteins are released from the IMS into the cytosol (Shimizu et al., 1999, Shimizu et al., 2000). The VDAC pore was opened by Bax and closed by Bcl-X_L. However, other studies have demonstrated Bax-only mechanisms of outer membrane permeabilisation. These include the assembly of Bax oligomers in the mitochondrial outer membrane to form pores (Antonsson et al., 2001, Pavlov et al., 2001, Saito et al., 2000, Korsmeyer et al., 2000) and Bax-induced destabilisation of the phospholipid bilayer, leading to transient breaks in the outer membrane (Bansnez et al., 1999, Kuwana et al., 2002). Another study in our laboratory demonstrated that during staurosporine-induced apoptosis Bax translocates from the cytosol to the mitochondria. Immunoprecipitations performed after staurosporine-induced apoptosis in cardiomyocytes also showed that VDAC and ANT co-immunoprecipitate with GFP-Bax (Capano & Crompton, 2002). In the same study GFP-Bax translocation to mitochondria and interaction with VDAC and ANT was shown to occur in the same time frame as the release of red-fluorescent protein-tagged cytochrome c (RFP-cytochrome c). Previously it was shown that apoptosis and necrosis are initiated in the same way during liver damage and both involve the MPT-pore but have different outcomes (Lemasters, 1999). The results in

this chapter show that in neonatal cardiomyocytes transfected with GFP-Bax treated with cyanide, to simulate ischaemia, VDAC and ANT co-immunoprecipitate with GFP-Bax but not Cyp D suggesting Bax does not interact with the MPT-pore under these conditions. However, other work suggests the MPT-pore does play a role in cytochrome c release from mitochondria in cardiomyocytes undergoing apoptosis induced by ischaemia (Borutaite et al., 2003). Rat hearts were perfused using a Langendorff-perfusion system and stop-flow ischaemia was induced for 30-60 minutes. Their results showed that ischaemia alone was sufficient to induce apoptosis and mitochondrial dysfunction. MPT was implicated in cytochrome c release because pre-perfusion of hearts with cyclosporin A prevented the release of cytochrome c from mitochondria during ischaemia. In this investigation GFP-Bax co-immunoprecipitated with ANT in the IMM as well as VDAC. From these findings it is not possible to tell whether the co-immunoprecipitation of ANT with VDAC merely reflects the ability of VDAC to bind to ANT (Brdiczka, 1991) or whether it points to the formation of a stable Bax-VDAC-ANT complex which interacts with Bax. The latter is favoured by other lines of research that implicate ANT in apoptosis. The overexpression of ANT-1 leads to apoptosis in a number of cell types (Bauer et al., 1999). Bax has also been shown to interact with ANT which results in the modulation of ANT antiporter activity, reducing ADP/ATP exchange (Belzacq et al., 2003). These findings point to Bax targeting a VDAC-ANT mitochondrial intermembrane complex. The role of this complex in the permeabilisation of the OMM is not clear. Bax may form a pore with VDAC (Shimizu et al., 2000) or the VDAC-ANT complex may function as a receptor for Bax localisation to mitochondria and permeabilisation of the OMM may occur via a Bax-

only model involving destabilisation of the phospholipid structure of the OMM (Kuwana et al., 2002).

In order to determine whether or not the MPT pore is involved in the mechanism of cyanide-induced apoptosis in cardiomyocytes MPT could be measured. In other studies MPT was measured as a loss of mitochondrial membrane potential ($\Delta\Psi_m$) (Bialik et al., 1999, Lovat et al., 2000). However, this method would be unsuitable for this current study as sodium cyanide inhibits the mitochondrial electron-transport chain leading to a loss of $\Delta\Psi_m$. Previously the fluorochrome calcein (622Da) was used to measure MPT-pore opening in intact cells (Nieminen et al., 1997). Another approach would be to treat the cardiomyocytes with ligands of Cyp D that are known to inhibit MPT-pore opening, for example CSA or Sanglifehrin A (SfA) (Clarke et al., 2002) before the induction of apoptosis with cyanide to determine whether the inhibition of MPT would prevent translocation of Bax to mitochondria and apoptosis from occurring. However Bax has also been shown to localise to the ER and reduces its ability to retain calcium (Pan et al., 2001). Further experimental work could be carried out to determine whether or not Bax localises to the ER during cyanide-induced apoptosis. Other Bcl-2 proteins (Nuchushtan et al., 2001) e.g. Bak translocate to mitochondria and permeabilise the OMM leading to the loss of apoptogenic proteins from the IMS. Interfering RNA (RNAi) technology could be used to inhibit Bax expression in cardiomyocytes to determine whether Bax is essential in the cyanide-induced apoptotic mechanism or whether Bak or other pro-apoptotic Bcl-2 proteins are capable of mediating apoptosis in the absence of Bax.

Chapter 6: Results

Attempts to identify the mitochondrial calcium uniporter

[6.1] Calcium and apoptosis

Mitochondria are key players in apoptotic signalling (Hengartner, 2000) but other organelles, including the ER, have also been implicated (Ferri & Kroemer, 2001). The ER can initiate apoptosis when unfolded proteins accumulate within the ER or when ER-Golgi transport inhibition results in the so-called ER stress response (Oyadomari et al., 2002). It also regulates apoptosis through its role in intracellular Ca^{2+} signalling. The ER is the main intracellular Ca^{2+} store and is physically and physiologically interconnected with mitochondria. This spatial and functional organisation impacts on the regulation of mitochondrial function and complex cellular processes (Hajnoczky et al., 2003, Hajnoczky et al., 1995, Rizzuto et al., 1998). Mitochondria have been shown to modulate and synchronise Ca^{2+} signalling (Berridge et al., 2000). In addition, stimuli that produce inositol 1,4,5-triphosphate (IP3) cause the release of Ca^{2+} from the ER that is rapidly taken up by juxtaposed mitochondria (Rizzuto et al., 1993). Ca^{2+} is also an important modulator of the MPT-pore (section **[1.8.4]**). This non-selective pore in the IMM allows the permeabilisation of the IMM to solutes up to 1500 Da (Bernardi, 1999, Crompton, 1999) and opens under pathological conditions involving increases in intracellular Ca^{2+} and P*i* e.g. during ischaemia/reperfusion injury in the heart (reviewed in Halestrap et al., 2004).

The MPT-pore has been implicated in both apoptotic and necrotic cell death (Zamzami et al., 1996, Scorrano et al., 1999). During apoptosis Bcl-2, Bax and Bak localise to the ER as well as mitochondria (Pinton et al., 2001, Wei et al., 2001, Scorrano et al., 2003). Bcl-2 has been shown to modulate Ca^{2+} fluxes during the course of cell death. Several groups have shown that overexpression of Bcl-2 leads to a reduction in the resting ER Ca^{2+} concentration and a reduction in the extent of Ca^{2+} entry into the ER (Pinton et al., 2000, Foyouzi-Youssefi et al., 2000). Bax and Bak double knockouts were shown to be resistant to death induced by thapsigargin (Wei et al., 2001), an irreversible inhibitor of the sarco-endoplasmic Ca^{2+} ATPase (SERCA) responsible for the re-uptake of Ca^{2+} from the cytosol into the ER lumen (Distelhorst et al., 1996). Inhibition of the SERCA pump by thapsigargin caused the passive release of the ER Ca^{2+} and a rise in cytosolic Ca^{2+}. In the absence of extracellular Ca^{2+}, the increase in cytosolic Ca^{2+} was proportional to the ER Ca^{2+} content. Bax and Bak deficient cells displayed a lower cytosolic Ca^{2+} peak compared to wildtype cells due to the diminished steady Ca^{2+} levels assessed by calcium-sensitive organelle specific fluorescent probes (Scorrano et al., 2003). Scorrano and co-workers (Scorrano et al., 2003) assessed the relative impact of reduced ER Ca^{2+} levels observed in Bax and Bak deficient cells on the regulation of apoptosis. The defects in the double knockouts were corrected by targeting Bax exclusively to the mitochondria and by overexpressing SERCA. The expression of mitochondrially targeted Bax in the knockouts did not correct levels of ER Ca^{2+}. Double knockout cells were used to determine whether the outcome of different apoptotic stimuli was primarily controlled by ER Ca^{2+} or mitochondrial-based Bax or

Bak. Apoptosis induced by the BH3-only domain protein tBid (Wei et al., 2000) was restored in the knockouts by mitochondrially targeted Bax but not by the overexpression of SERCA. However, apoptosis induced by ceramide, arachidonic acid or oxidative stress (Pinton et al., 2001, Scorrano et al., 2001, Scorrano et al., 2003) was restored by the overexpression of SERCA in the Bax and Bak deficient cells and not by mitochondrially targeted Bax. To achieve the same level of apoptotic cell death in Bax and Bak deficient cells as the wildtype in response to proapoptotic stimuli such as etoposide or staurosporine; both mitochondrially targeted Bax and the overexpression of SERCA were required.

[6.1.1] Mitochondrial calcium cycling

Mitochondrial Ca^{2+} uptake was first described in 1961 by De Luca and Engstrom (De Luca & Engstrom, 1961). The mitochondrial calcium uniporter located in the IMM passes Ca^{2+} down the electrochemical gradient maintained across this membrane without direct coupling to ATP hydrolysis or the transport of other ions (Gunter & Gunter, 1994). Calcium exits mitochondria by exchange with sodium on the Na^{+}/Ca^{2+} carrier (Crompton et al., 1976). This is shown in Figure **[6.1]**. Continuous Ca^{2+} cycling across the inner membrane occurs and is established by the kinetic properties of the uniporter and efflux system(s). Calcium influx via the uniporter is driven by the electrochemical gradient, and the rate of this process increases with increasing membrane potential but only up to -110mV (isolated liver mitochondria) (Goldstone et al., 1987). Above this value, uniporter activity reaches a plateau. As a result, decreases

in inner membrane potential to 110mV do not produce losses of mitochondrial Ca^{2+}, at least not in isolated mitochondria. This transport cycle enables changes in cytosolic $[Ca^{2+}]$ to be relayed into changes in matrix $[Ca^{2+}]$. Changes within the limits 0.1-10 μM are appropriate to regulate the activity of the dehydrogenases involved in controlling the rate of intramitochondrial oxidative metabolism (McCormack & Denton, 1990). These key enzymes are: pyruvate dehydrogenase, oxoglutarate dehydrogenase and NAD-linked isocitrate dehydrogenase. These three enzymes catalyse oxidative decarboxylations at control points in mitochondrial oxidative metabolism. By extending the messenger role of Ca^{2+} to the mitochondria, the Ca^{2+} transport cycle allows oxidative metabolism to respond to Ca^{2+}-dependent events in the cytosol (Hansford, 1991). An obvious example is in the case of cardiac muscle contraction. When heart muscle contractions increase, the height and frequency of the cytosolic transients also increase leading to an increase in mitochondrial $[Ca^{2+}]$ and consequent activation of the TCA cycle and oxidative phosphorylation (Denton and McCormack; 1984).

[6.1.2] Mitochondrial Calcium Uniporter

Previously it was unclear as to whether the mitochondrial calcium uniporter was a carrier or a channel (Gunter & Pfieffer, 1990). Carriers are characterised by turnover numbers that are about 1000-fold lower than ion channels. However, a recent study involving the patch-clamping of single mitoplasts (mitochondria with the outer membrane removed) isolated from COS-7 cells showed that the uniporter is a Ca^{2+}

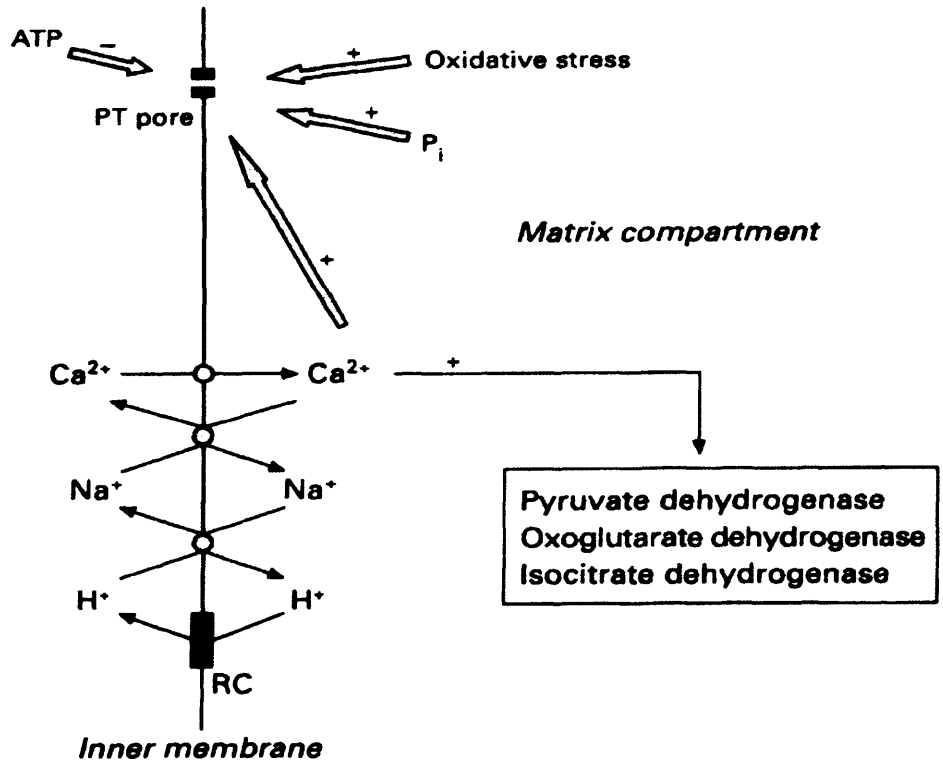

Figure [6.1] Mitochondrial calcium cycle. Calcium enters mitochondria through the uniporter and exits through the Na^+/Ca^{2+} antiporter. This process is driven by the proton pumps of the respiratory chain. Mitochondrial calcium controls key regulatory dehydrogenases in the mitochondrial matrix. Under pathological conditions associated with ATP depletion and oxidative stress, mitochondrial Ca^{2+} triggers PT pore opening. (taken from Crompton, 1999)

selective ion channel (Kirichok et al., 2004). Their results showed that a voltage from –160mV (potential across the IMM of energised mitochondria) to +80 mV elicited a current that gradually increased as the free Ca^{2+} concentration at the cytosolic surface of the IMM was varied from 20μM to 100μM. These concentrations are comparable with the Ca^{2+} concentration in microdomains near the ER/SR or plasma membrane channels, sensed by neighbouring mitochondria (Rizzuto et al., 2000, Montero et al., 2000, Rizzuto et al., 1993, Neher et al., 1998). The uniporter is activated by ADP, aminoglucoside antibiotics and triethylenetetramine (Gunter et al., 1991, and references therein) and is inhibited by the lanthanides and Ruthenium Red (Moore, 1971, Vasington et al., 1972; Reed and Bygrave, 1974) Ruthenium Red has the formula: $[(NH_3)_5Ru^{III}\text{-}O\text{-}(NH_3)_4Ru^{IV}\text{-}O\text{-}Ru^{III}(NH_3)_5]^{6+}$. However, another ruthenium complex ion, known as Ru 360 is a more potent uniporter inhibitor and is present as an impurity in commercial preparations of Ruthenium Red (Ying et al., 1991) and has the formula $[CH_3(NH_3)_4Ru\text{-}O\text{-}Ru(NH_3)_4CH_3]^{3+}$. As little as 50pmoles Ru 360/mg mitochondrial protein is sufficient for 50% inhibition of uniporter activity. Among other ammine complexes, Crompton and Andreeva (Crompton & Andreeva, 1994) synthesised several cobaltammines. Of these diaminopentanepentamminecobalt (DAPPAC) was the most potent inhibitor (Ki 0.14μM; corresponding to 0.14 nmoles/ mg mitochondrial protein).

[6.1.3] Ca^{2+} Uniporter and Ra M

Gunter and co-workers have postulated the existence of a further Ca^{2+} uptake system. This is known as Ra M. Calcium uptake in nmoles/mg mitochondrial protein was plotted against pulse width in seconds. The rates indicated by the slopes of the lines were consistent with the rate of uptake by the uniporter. However, when extrapolated the line of fit always intersected the ordinate above zero uptake (Sparagna et al., 1994 and Sparagna et al., 1995). Gunter and co-workers suggested that this indicates that uptake of Ca^{2+} occurs very rapidly at the beginning of each pulse. Calcium uptake via Ra M was shown to be inhibited by uncouplers that dissipate the membrane potential suggesting that the thermodynamic driving force for the uptake is the Ca^{2+} electrochemical gradient. This group initially reported Ra M in liver mitochondria but they have also identified it in heart. However, Ra M in heart mitochondria was observed to be smaller than in liver mitochondria. Ra M has also been shown to be sensitive to inhibition by Ruthenium Red, although higher amounts are required to inhibit Ra M than the uniporter. This system is unaffected by millimolar mounts of AMP and ADP but is activated by 1 μM spermine and millimolar amounts of ATP. In addition, spermine and ATP can act in a synergistic manner to further increase Ca^{2+} uptake by Ra M. Calcium uptake by Ra M is so rapid that it cannot be measured directly. Predictions are that Ra M acts at least 300 times more rapidly than the uniporter. Others have published data in support of the other uptake system (Gallitelli et al., 1999). However, since the mechanism of uptake of both systems has not been elucidated it remains to be seen whether Ra M is a separate entity or an alternative conformation of the uniporter complex. The uniporter may have two conformations; one for rapid Ca^{2+} uptake and the other the uniporter.

[6.1.4] Purification of the Ca^{2+} uniporter

So far, the calcium uniporter has not been unambiguously purified. This reflects difficulties inherent in the purification of a low-abundance hydrophobic protein. Mironova and co-workers reported the purification of a low-molecular weight peptide (20kDa) from rat liver mitochondria that formed selective channels in lipid bilayers. These channels were strongly inhibited by 1-4μM Ruthenium Red (Mironova et al., 1994). In another study, Zazueta and co-workers (Zazueta et al., 1998) used two methods to purify the uniporter. Proteins derived from rat kidney submitochondrial particles were separated by isoelectric focussing. Two assays were then carried out to identify the uniporter. One assay involved the reconstitution of the liquid-phase isoelectrofocussed proteins into cytochrome oxidase vesicles (COVs). Transport activity was measured as the ability of COVs to support uptake of radiolabelled $^{45}Ca^{2+}$ in the presence of cytochrome c and the electron donor pair ascorbate-TMPD. In addition Western blotting was carried out using antibodies raised against mitochondrial membrane fractions with maximal Ca^{2+} transport activity and which had previously been shown to inhibit calcium uptake by mitoplasts (Zazueta et al., 1994). The other method involved the addition of radiolabelled Ru 360 to submitochondrial particles and separation of the labelled proteins by CM-cellulose chromatography. An 18-kDa protein was found which bound Ru 360 and when reconstituted into vesicles could transport calcium. A 70 kDa protein was also co-purified with the 18-kDa proteins but whether this was part of the uniporter complex or an artefact of the purification was

uncertain. Recent studies from the same group have shown that cardiolipin regulates the activity of the 18 kDa protein in liposomes by modifying the structure of the lipid bilayer (Zazueta et al., 2003).

[6.2] Novel Approach to identify the Calcium Uniporter in rat liver mitochondria

Ru 360 and DAPPAC are both potent inhibitors of the uniporter. In this study attempts were made to combine their inhibitory potential in a novel approach for uniporter identification. DAPPAC was converted to a fluorescent photoactive derivative (DAPPAC-SAED) for sensitive detection of photolabelled proteins. The photolabelling of the mitochondrial membranes by DAPPAC-SAED was carried out in the presence and absence of Ru 360. The rationale for this approach was to identify a protein whose labelling by DAPPAC was blocked by Ru 360. Figure **[6.2]** outlines the strategy used in an attempt to isolate the Ca^{2+} uniporter from rat liver mitochondria. DAPPAC and Ru 360 both inhibit the Ca^{2+} uniporter, Ru 360 rather more strongly than DAPPAC (section **[6.1.2]**). They are both ammine complexes (of Co and Ru, respectively) and would both be expected to occupy the same site on the uniporter and to compete with each other for binding. The rationale was that Ru 360 would decrease photolabelling of the uniporter by SAED-DAPPAC, enabling uniporter-containing fractions to be identified as those in which fluorescent covalent labelling was inhibited by Ru 360.

[6.3] Isolating the inhibitor Ru 360 from a commercial preparation of Ruthenium Red

The inhibitor was purified from a commercial preparation of Ruthenium Red using CM-cellulose chromatography (Ying et al., 1991). The Ru 360 eluted as a pale yellow fraction with 0.4 M ammonium formate. The Ruthenium Red was eluted as a bright pink fraction with 0.8 M ammonium formate. Most of the Ru 360 eluted in fractions 1-20 and Ruthenium Red eluted in fractions 78-85 (figure **[6.3]**). The concentration of Ru 360 present in fractions 1-20 was calculated using Beer-Lamberts Law using a molar extinction coefficient of 2.6×10^4 M^{-1} cm^{-1} at 360nm (Ying et al., 1991). Using this value, 78 nmoles of Ru 360 was recovered from 1.16 mmoles of Ruthenium Red. Figure **[6.4]** shows that fractions 1-20 have the correct absorption maximum (360nm) for Ru 360.

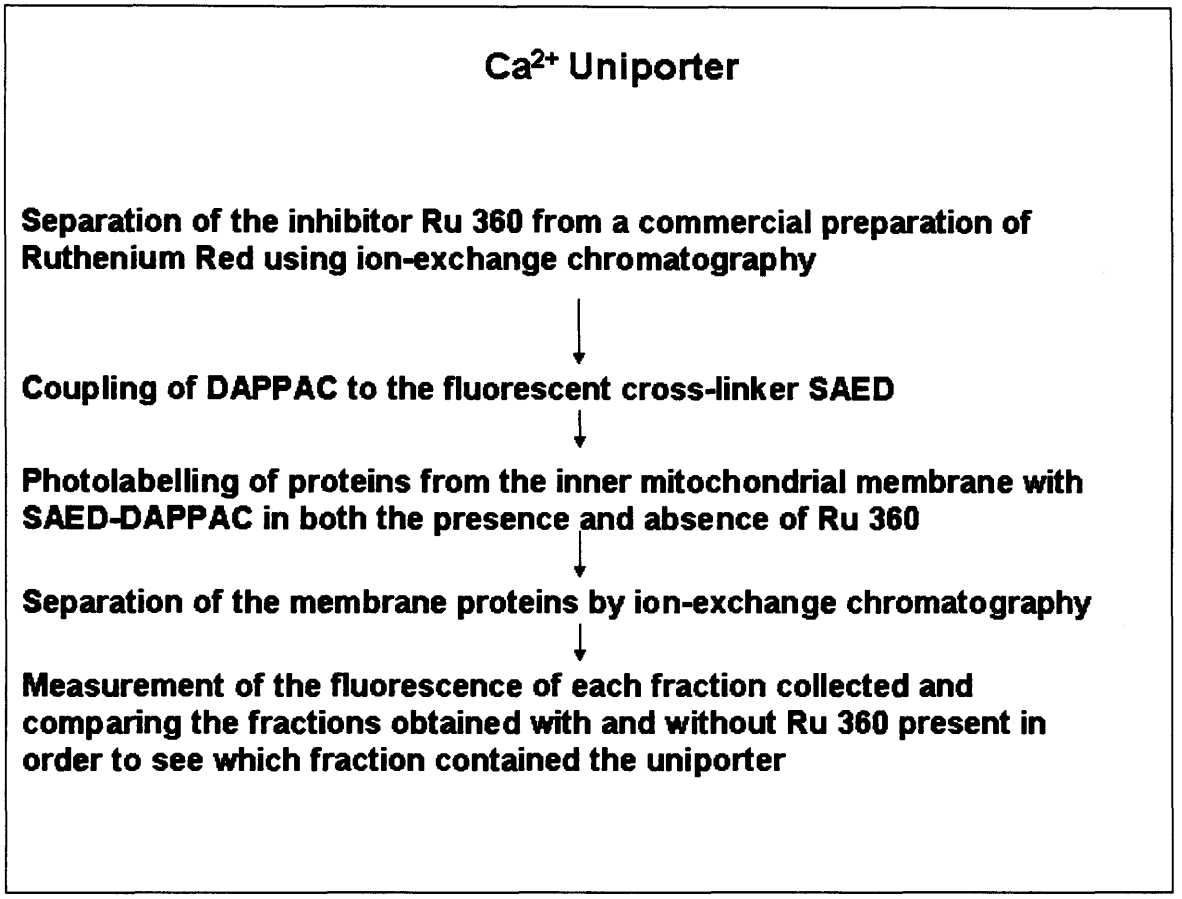

Figure [6.2] Outline of the different steps used to try to identify the calcium uniporter protein in a mitochondrial membrane extract from rat liver.

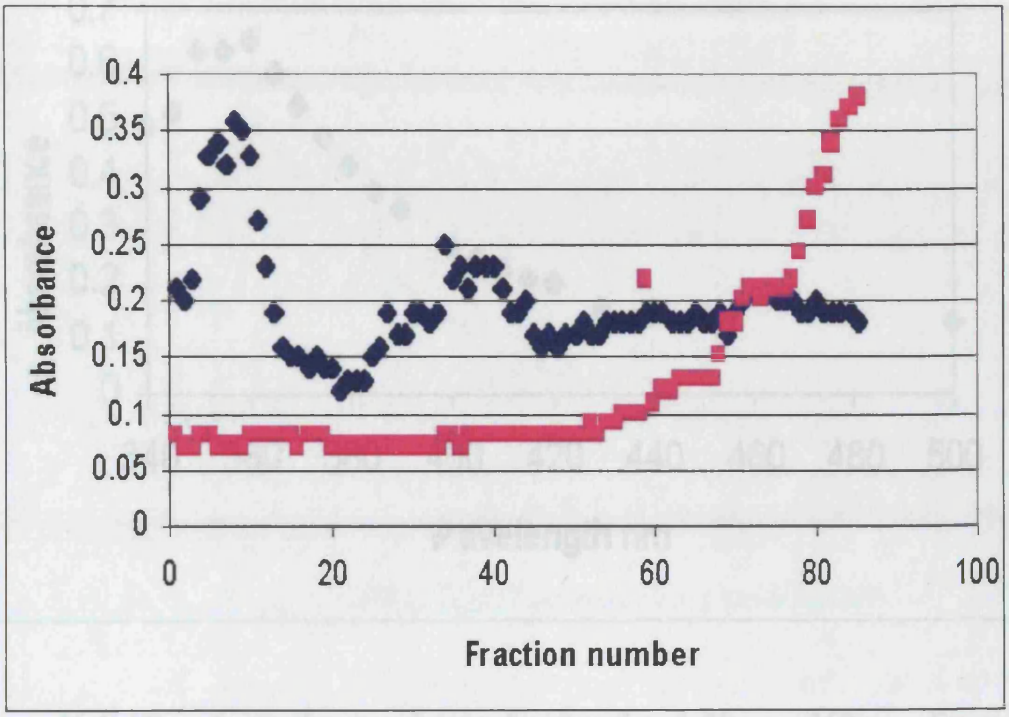

Figure [6.3] Fractionation of Ruthenium Red by ion-exchange chromatography. The absorbance of each fraction eluted from the CM-cellulose column was measured at 360 nm (blue line) and at 532 nm (pink line). 360 nm and 532 nm are the wavelengths at which the maximum absorption occurs for Ru360 and Ruthenium Red respectively (Ying et al., 1991). A linear ammonium formate gradient (0.1M-1M) was applied between fractions 0 and 100. The volume of each fraction was 1ml.

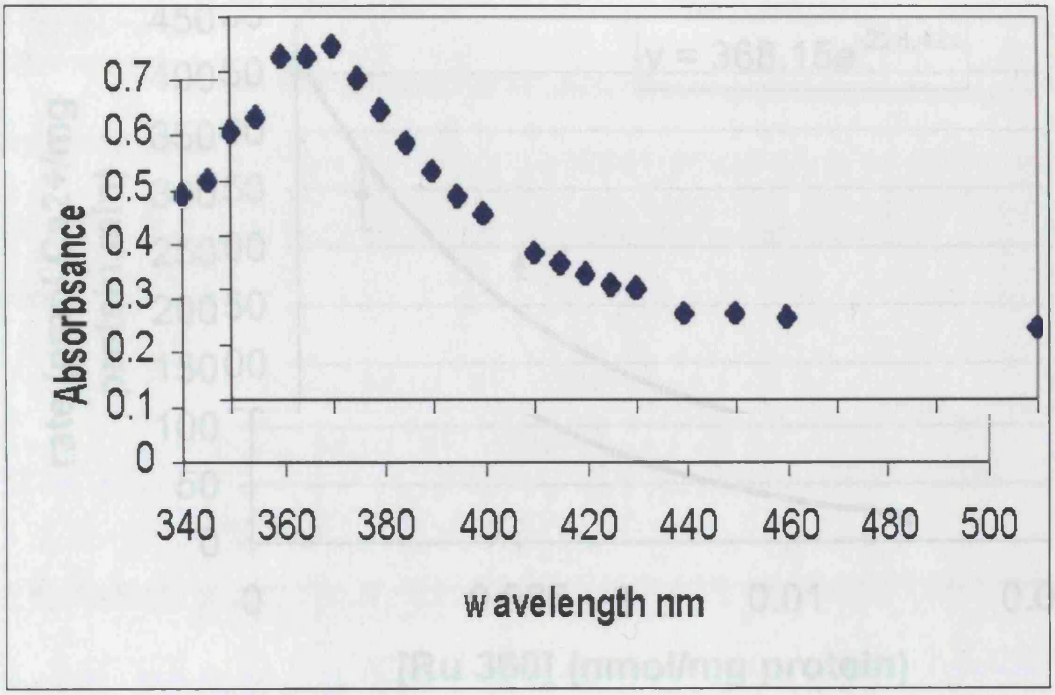

Figure [6.4] The absorption maximum for fraction 1-20 was 360nm. Fractions 1-20, which were thought to contain Ru 360, were pooled and the absorption was measured at wavelengths of 340-500nm.

[6.4] Inhibition of Ca^{2+} uptake into rat liver mitochondria by Ru 360

Ca^{2+} uptake by mitochondria was measured with the Ca^{2+} indicator arsenazo III in the presence of various concentrations of Ru 360 (0-0.012 nmol/mg of mitochondrial protein). The results (figure **[6.5]**) show that 4.2 pmoles Ru 360/mg protein yielded 50% inhibition of the uniporter.

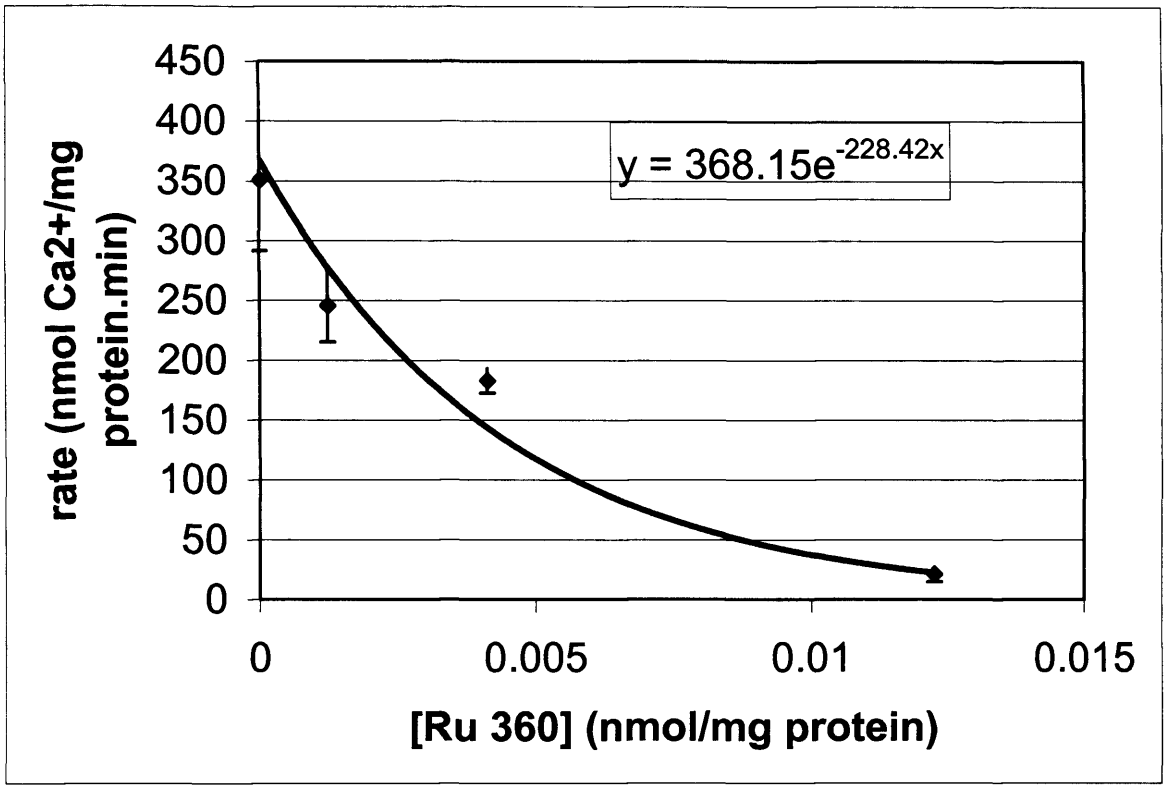

Figure [6.5] Ca^{2+} uptake by liver mitochondria was measured with the Ca^{2+} indicator arsenazo III in the presence of various concentrations of Ru 360 (0-0.012 nmol/mg of mitochondrial protein). The assay was carried out as described in section [6.13]. All measurements relate to 1mg mitochondrial protein, 0.25 mg of mitochondrial protein was used for each assay. The error bars show standard deviation

The equation obtained from the graph was re-arranged to find x-the inhibitor concentration that gives half the amount of uptake of calcium into the mitochondria ie. the 50 % inhibition level.

$$y = 368.15e^{-228.42\,x}$$

therefore: $$x = \text{In } 368.15^{\,y} / -228.42$$

When no Ru 360 inhibitor was added 350.59 nmol/mg/min of calcium was taken up by the mitochondria.

Therefore, half of this was 175.30 nmol/mg/min and using the above equation the amount of Ru 360 that was required to produce this can be calculated:

$$x = \text{In } 368.15^{175.30} / -228.42$$

$$x = 5.908^{175.30} / -228.42$$

$$x = 1.01 / -228.42$$

$$x = 0.0042$$

Therefore, the 50 % inhibition level was found to be 0.0042 nmol/mg protein. This was similar to that published by Ying and co-workers which was 0.0035 nmol/mg protein (Ying et al., 1991). It was concluded from the absorption spectrum (figure **[6.4]**) and its inhibitory potency that Ru 360 had been successfully purified.

[6.5] Photolabelling mitochondrial membrane proteins with SAED-conjugated DAPPAC

The photo-reactive cross-linker molecule SEAD was linked to DAPPAC, as described in section **[2.10.3]**. This conjugation reaction would be expected to produce a molecule capable of binding with some specificity to the uniporter. A number of cobaltammines

including hexamine cobalt ($Co(NH_3)_6$, inhibit the uniporter (Crompton & Andreeva, 1994) with high affinity eg. the Ki for $Co(NH_3)_6$ is 1.7μM. Thus the inhibition by DAPPAC resides in the cobaltammine portion of the molecule such that addition of SAED at the free amino group of DAPPAC, separated from the cobaltammine group by a 5-carbon spacer, would be unlikely to abolish its inhibitory capacity. The fluorescence from the cross-linking azido group could be detected and therefore it would be possible to identify the uniporter in fractions eluted from the ion-exchange columns.

Photolabelling of the membrane proteins with SAED-DAPPAC was carried out as described in section **[2.10.4].** The proteins in the labelled mitochondrial membrane extracts were separated on a Mono Q anion-exchange column equilibrated with Tris buffer (pH 8.0). The bound proteins were eluted with a NaCl gradient (100-500 mM NaCl). The pass through was dialysed against HEPES buffer (pH 7.2) for 14 hours and applied to a Mono S cation-exchange column pre-equilibrated with the same buffer. The bound proteins were then eluted with a NaCl gradient (100-500mM NaCl).

The fluorescence of SAED-DAPPAC present in each of the fractions collected was measured (excitation 340 nm, emission 435 nm). The protein elution profiles from the Mono Q and the Mono S columns for each of the mitochondrial membrane pellets ie. 1 nmol Ru 360, 0.1 nmol Ru 360 and no Ru 360, were compared. In addition, the fluorescence value obtained for each fraction was analysed to see if the calcium uniporter protein could be identified. The protein elution profiles from the Mono Q column together with the fluorescence values for each fraction are shown in figure **[6.6].** Figure **[6.7]** shows the results obtained from the Mono S column.

A

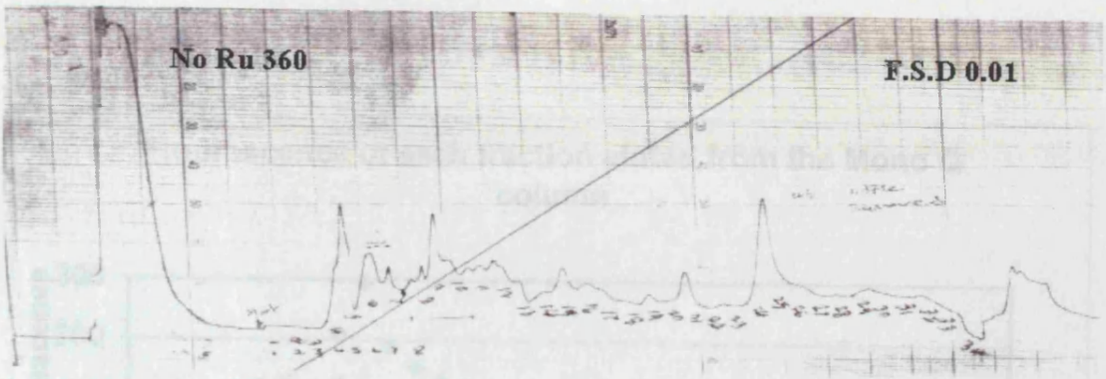

Fraction number 1 2 3 4 5 6 7 8 9

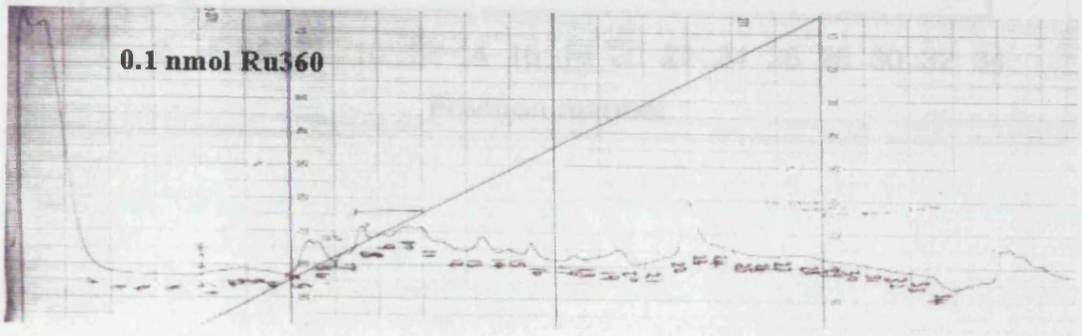

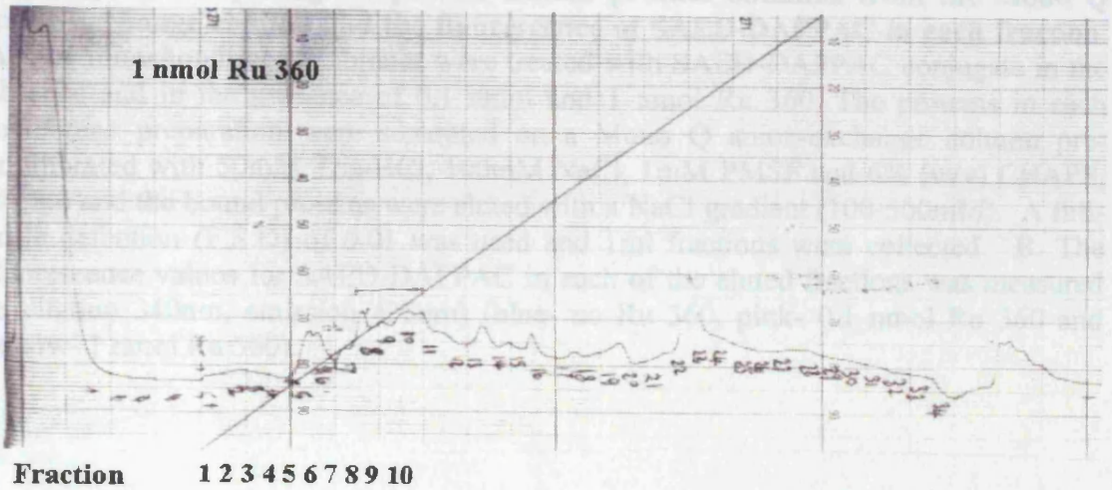

Fraction number 1 2 3 4 5 6 7 8 9 10

B

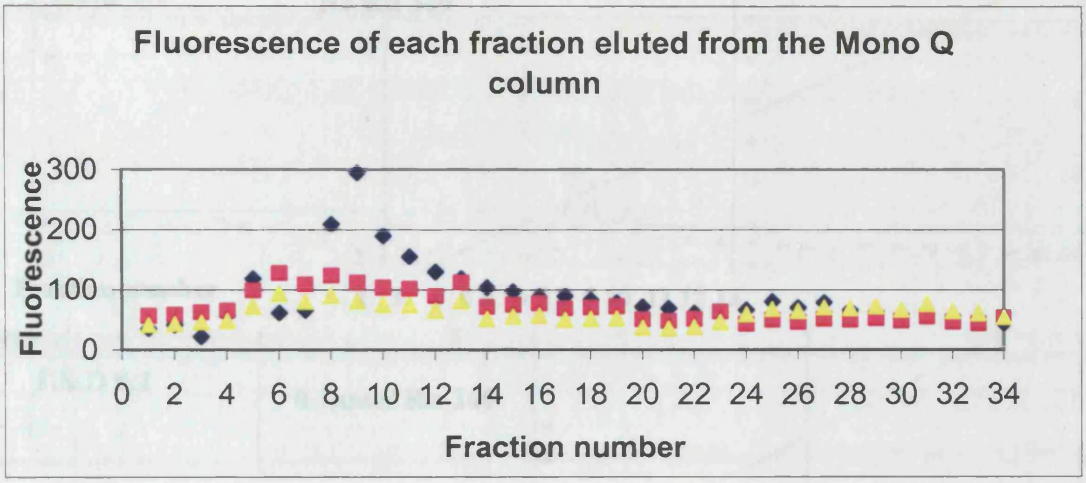

Figure [6.6] Comparing the protein elution profiles obtained from the Mono Q anion-exchange column and the fluorescence of SAED-DAPPAC in each fraction. **A**. The mitochondrial membranes were treated with SAED-DAPPAC conjugate in the absence and in the presence of 0.1 nmol and 1 nmol Ru 360. The proteins in each membrane preparation were separated on a Mono Q anion-exchange column pre-equilibrated with 50mM Tris-HCl, 100mM NaCl, 1mM PMSF and 6% (w/v) CHAPS, pH 8.0 and the bound proteins were eluted with a NaCl gradient (100-500mM). A full-scale defection (F.S.D) of 0.01 was used and 1ml fractions were collected. **B**. The fluorescence values for SAED-DAPPAC in each of the eluted fractions was measured (excitation 340nm, emission 435nm) (blue- no Ru 360, pink- 0.1 nmol Ru 360 and yellow- 1 nmol Ru 360).

A

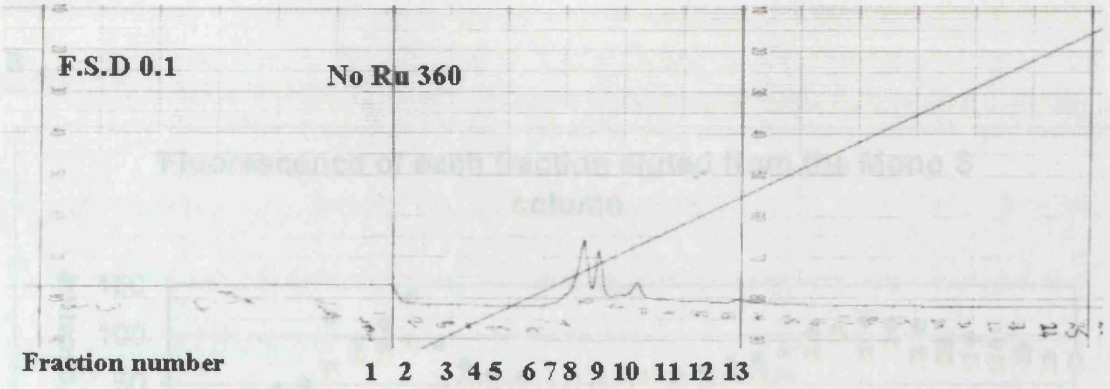
F.S.D 0.1
No Ru 360
Fraction number
1 2 3 4 5 6 7 8 9 10 11 12 13

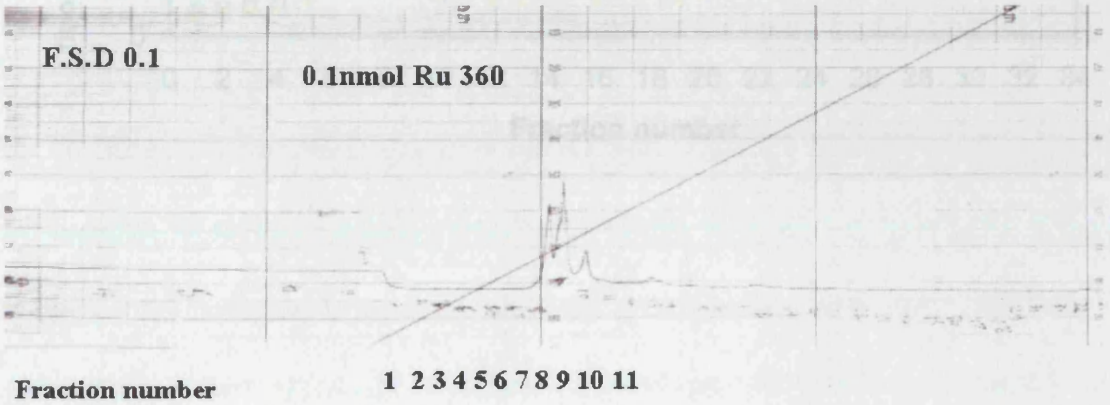
F.S.D 0.1
0.1nmol Ru 360
Fraction number
1 2 3 4 5 6 7 8 9 10 11

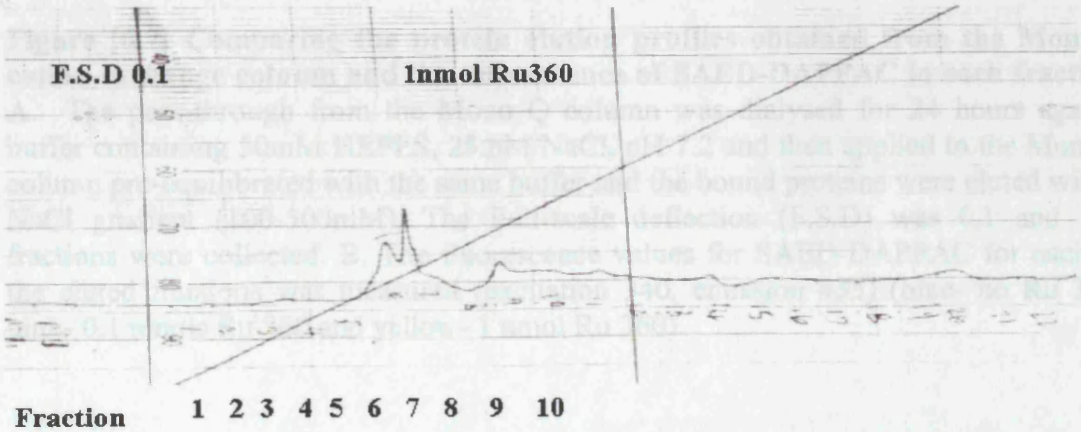
F.S.D 0.1
1nmol Ru360
Fraction number
1 2 3 4 5 6 7 8 9 10

B

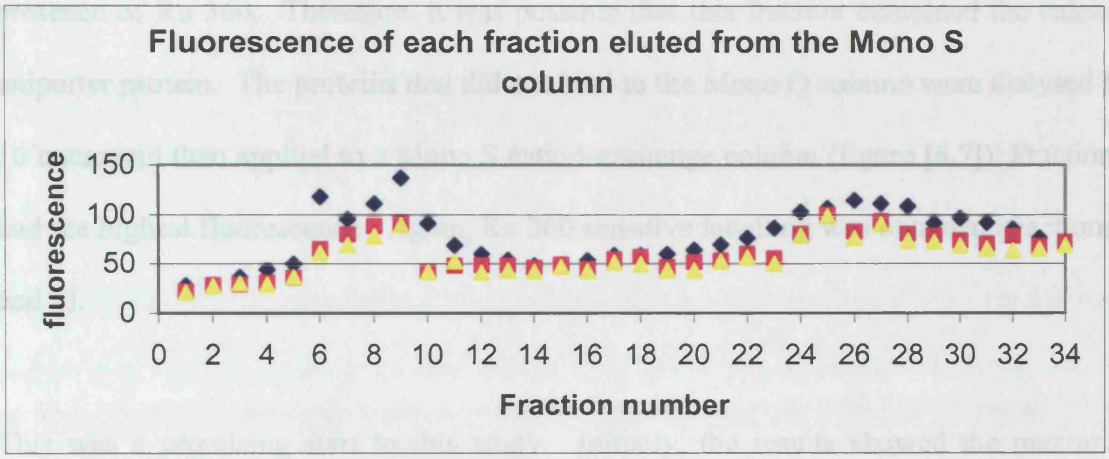

Figure [6.7] Comparing the protein elution profiles obtained from the Mono S cation-exchange column and the fluorescence of SAED-DAPPAC in each fraction. A. The pass-through from the Mono Q column was dialysed for 24 hours against buffer containing 50mM HEPES, 25mM NaCl, pH 7.2 and then applied to the Mono S column pre-equilibrated with the same buffer and the bound proteins were eluted with a NaCl gradient (100-500mM). The Full-scale deflection (F.S.D) was 0.1 and 1ml fractions were collected. B. The fluorescence values for SAED-DAPPAC for each of the eluted fractions was measured (excitation 340, emission 435) (blue- no Ru 360, pink- 0.1 nmols Ru 360 and yellow- 1 nmol Ru 360)

Figure **[6.6]** shows the results obtained from the Mono Q anion-exchange column. Fractions 8- 12 have the highest fluorescence with a peak in fraction 9. The results show the fluorescence from SAED-DAPPAC was reduced almost 3-fold for fraction 9 in the presence of Ru 360. Therefore, it was possible that this fraction contained the calcium uniporter protein. The proteins that did not bind to the Mono Q column were dialysed for 16 hours and then applied to a Mono S cation-exchange column (figure **[6.7]**). Fraction 9 had the highest fluorescence. Again, Ru 360 sensitive labelling was obtained (fractions 6 and 9).

This was a promising start to this study. Initially, the results showed the maximum fluorescence was detected in the 9^{th} fraction eluted from the Mono Q anion-exchange column. The fluorescence was reduced in the in the presence of Ru 360. However, this result could not be reproduced. Ru 360 did not always decrease this fluorescence peak and the fraction in which the maximum fluorescence was observed also changed. These results suggest that SAED-DAPPAC was not specifically interacting with the uniporter protein. Ru 360 and DAPPAC are both positively charged and may therefore bind to other membrane proteins with a negative charge.

[6.6] Discussion

Calcium is an activator of the MPT-pore that has been implicated in necrotic and apoptotic cell death (Crompton, 2000). The opening of the MPT-pore occurs when increases in intracellular Ca^{2+} are relayed to the mitochondrial matrix by the Ca^{2+}uniporter located in the IMM. Therefore the calcium uniporter is a potential therapeutic target in the prevention of Ca^{2+} induced MPT-pore opening e.g in ishaemic/reperfusion injury. The mechanism by which the Ca^{2+} uniporter mediates

mitochondrial Ca^{2+} uptake has now been established (Kirichok et al., 2004). However, the mitochondrial uniporter protein has not been unambiguously identified and the nucleotide and amino acid sequences for the uniporter are not known. This is probably a result of the difficulties associated with the purification a low abundance membrane protein and, with the reconstitution of protein activity in liposomes since membrane protein function may require protein-phospholipid interaction. Recently cardiolipin, which is present in the IMM, was shown to inhibit reconstituted mitochondrial calcium uniporter activity (Zazueta et al., 2003). However it was not clear as to whether the composition of the liposomes reflected the lipid environment of the Ca^{2+} uniporter *in vivo* and therefore whether cardiolipin regulates Ca^{2+} entry into mitochondria. In addition a molecular biology approach could be used to identify the nucleotide sequence for the uniporter. A PCR based method could be designed using degenerate primers that bind to sequences containing Ca^{2+} binding motifs e.g E-F hand motif.

Chapter 7: Discussion

[7.1] Bax interacts with the VDAC-ANT mitochondrial intermembrane contact sites: implications for a mechanism for the Bax-induced release of apoptogenic proteins from the IMS

During apoptosis, Bax translocates from the cytosol to the mitochondria and induces the release of apoptogenic proteins from the IMS (Chapter 1). Bax recruitment to mitochondria involves a conformational change at the N-terminus of the protein which leads to its translocation from the cytosol to mitochondria (Cartron et al., 2003). The mechanisms by which Bax induces the release of proteins from the IMS are not well understood. Several hypotheses have been put forward. These include the involvement of the MPT-pore (Loeffler & Kroemer, 2000) (see **[4.1]**), the formation of Bax-VDAC pores in the OMM (Shimizu et al., 2000) and Bax-only models for example involving Bax-mediated disruption of the phospholipid bilayer structure leading to the in introduction of transient holes in the OMM (Kuwana et al., 2002). The identification of mitochondrial membrane proteins that interact with Bax would enhance our understanding of how Bax participates in the permeabilisation of the OMM. This investigation has shown that GST-Bax interacts with VDAC (OMM) and ANT (IMM) present in mitochondrial membranes derived from rat heart. In addition VDAC and ANT co-immunoprecipitate with GFP-Bax in cell extracts derived from cardiomyocytes undergoing apoptosis after cyanide treatment in order to simulate ischaemia (Chapter 5). These data provide evidence for the role of VDAC-ANT contact sites as mitochondrial receptors for Bax. GST-Bax and the C-terminally

truncated GST-BaxΔc both interact with VDAC and ANT. Previously the C-terminal region of Bax was shown to be involved in Bax translocation to mitochondria and insertion into the OMM (Wolter et al., 1997, Goping et al., 1998). However other studies have demonstrated that the deletion of the C-terminus of Bax did not abolish mitochondrial targeting of Bax (Temblais et al., 1999). Although the substitution of the C-terminus of Bax with that of Bcl-X_L did not affect its subcellular localisation it was shown to abolish its pro-apoptotic function and increased cell survival in a number of cell types (Oliver et al., 2000). Other studies have shown that both full-length and BaxΔc are capable of inducing cytochrome c release (Jurgensmeier et al., 1998, Eskes et al., 1998, Goldstein et al., 2000). The differences in the effect of both forms of Bax was found to be quantitative, 5μM BaxΔc released about 8% of the total mitochondrial cytochrome c from isolated mitochondria, whereas 5μM of full-length Bax released 75% (Appaix et al., 2002).

The rat mitochondrial membrane preparations used in Chapter 4 did not contain either Bax or Cyp D (as assessed by Western blotting, data not shown). Therefore GST-Bax and GST-Cyp D pulldowns were performed in the presence of exogenous Cyp D or Bax to determine if a Bax-VDAC-ANT-Cyp D complex could be isolated. This would indicate that Bax interacts directly with components of the MPT-pore complex. The GST-Bax pulldowns contained VDAC, ANT, Cyp D and GST-Cyp D retained VDAC, ANT and Bax. This indicates that Bax is capable of direct interaction with the MPT-pore complex. Kroemer and co-workers hypothesised that the dissipation of $\Delta\Psi m$ observed during apoptosis was due to opening of the MPT-pores in the IMM leading to

mitochondrial swelling, rupture of the OMM and the release of apoptogenic proteins from the IMS (see section **[4.1]**). They showed that isolated hexokinase-associated mitochondrial membrane complexes containing ANT, Cyp D and Bax as well as other unidentified proteins had MPT-pore activity when reconstituted into liposomes (Marzo et al., 1998a). The role of the MPT-pore is disputed and dissipation of $\Delta\Psi m$ is not observed in all cells undergoing apoptosis (Lovat et al., 2000) or may occur many hours before the permeabilisation of the OMM (De Giorgi et al., 2002). Dissipation of $\Delta\Psi$ might also be caused by the effects of Bax on components of the respiratory chain. Bax was also shown to increase MgATPase activity by the partial uncoupling of the IMM and to inhibit some component(s) of the respiratory chain (Appaix et al., 2002). These other effects of Bax might also explain why Bax is toxic to bacteria even though they lack mitochondria (Chapter 3). In Chapter 5, immunoprecipitation using sepharose-coupled anti-GFP antibodies on cell extracts of apoptotic cardiomyocytes transfected with GFP-Bax showed that VDAC and ANT co-immunoprecipitated with GFP-Bax but not Cyp D indicating that the MPT-pore complex was not targeted by Bax following translocation to the mitochondria. VDAC and ANT mitochondrial intermembrane contact sites interact with other proteins including hexokinase, creatine kinase and the peripheral benzodiazepine receptor (Reichert & Neupert, 2002, Fritz et al.,2001 Joseph-Liauzun et al., 1998). It is not known whether all components reside within the same contact site. Bax and Cyp D might be able to bind to VDAC-ANT contact sites simultaneously but during apoptosis the contact sites might not recruit Cyp D. Hexokinase II binding to contact sites inhibits Bax-induced cytochrome c release and apoptosis (Pastorino et al., 2002). Tetramers of hexokinase (400 kDa) bind to VDAC and prevent Bax binding by steric hindrance. Despite evidence that the MPT-pore is

not a universal mechanism for the release of apoptogenic proteins from the IMS the Cyp D inhibitor CSA prevented Bax-induced cytochrome c release from isolated mitochondria in the presence of Ca^{2+} (Marzo et al., 1998b) and not in the absence of Ca^{2+}(von Ahsen et al., 2000). In another study Bax, in the absence of Ca^{2+}, induced cytochrome c release from isolated mitochondria but did not cause mitochondrial swelling characteristic of MPT-pore opening (Jurgensmeier et al., 1998). Furthermore Bax-induced cytochrome c release was inhibited by CSA indicating that Cyp D was involved in this process since it is the only cyclophilin present in mitochondria. The dissipation of $\Delta\Psi m$ during lymphocyte apoptosis was prevented by the MPT-pore inhibitors CSA, mCSA (a non-immunosupressive analogue of CSA) and bongkrekic acid (Zamzami et al., 1996). However data obtained from apoptotic cells treated with CSA are more difficult to interpret since CSA also interacts with the other cellular cyclophilin isoforms e.g. cyclophilin A (Cyp A) which is present in the cytosol. In a neuronal cell line, the antisense suppression of Cyp A mimics the capacity of CSA to block apoptosis induced by staurosporine, NO and other stimuli (Capano et al., 2002). The inhibitory effects of CSA suggest that overexpression of Cyp D would induce apoptosis however the overexpression of Cyp D suppressed the spontaneous apoptosis observed in ANT-1 overexpressing cells (Bauer et al., 1999) and in another study it delayed apoptosis induced by staurosporine (Lin & Lechleiter, 2002). More recently, Cyp D overexpression in B50 neuronal cells was shown to promote MPT and necrosis induced by the NO donor nitroprusside but inhibited apoptosis induced by NO or staurosporine (Li et al., 2004). The inconsistencies in these results might be due to Cyp D having more than one role and one of these might be CSA sensitive while the other is not. For example, Cyp D might interact with mitochondrial peroxiredoxin in a CSA

insensitive manner. Peroxiredoxins are involved in protection against oxidative stress (Lee et al., 2001) in addition to a CSA sensitive role preventing MPT-pore opening.

Results from the present study indicate that Bax binding to VDAC-ANT was altered by the ANT ligands atractyloside (promotes apoptosis) and bongkrekic acid (inhibits apoptosis). The addition of atractyloside significantly increased the amount relative of VDAC compared to ANT that was retained by GST-Bax. The same amount of VDAC was present but there was an 80% reduction in ANT retained compared to control (no additions). Bongkrekic acid increased the amount of both VDAC (by 81%) and ANT (63%) bound to GST-Bax. These data indicated that the ANT ligands alter the composition of the VDAC-ANT complexes which interact with Bax (Figure **[7.1]**). Recently it was shown that hexokinase I containing VDAC-ANT contact sites isolated from rat kidney cortex or brain contained cytochrome c (Vyssokikh et al., 2004). The cytochrome c distribution was proposed to be located in three sub-mitochondrial compartments at the surface of the cristae, bound to the peripheral IMM and associated with the contact sites. The contact site associated cytochrome c was thought to represent a specific releasable pool in the early period of Bax action (Capano & Crompton, 2002) and the presence of cytochrome c at the contact sites was shown to be dependent on the VDAC-ANT structure. Atractyloside promotes contact site formation (Bucheler et al., 1991, Vyssokikh et al., 2001) and increased the amount of cytochrome c associated with the contact sites where as bongkrekic acid had the opposite effect. However Vyssokikh and co-workers (Vyssokikh et al., 2004) did not investigate the effects of Bax binding to contact sites in the presence of atractyloside or bongkrekic

acid and therefore what impact the Bax-VDAC-ANT interaction has on the composition of the contact sites remained unclear.

The question arises as to the role of VDAC-ANT contact sites in the Bax-induced permeabilisation of the OMM. Are the contact sites receptors for Bax localisation to mitochondria or do they or individual components participate directly in the permeabilisation of the OMM? From the results obtained in Chapters 4 and 5 it is not possible to determine if the co-immunoprecipitation of VDAC and ANT merely reflects the ability of VDAC and ANT to bind together or whether it points to the formation of a Bax-VDAC-ANT complex. Previous studies have shown that VDAC and Bax form channels when reconstituted into phospholipid membranes (Shimzu et al., 2000) and these channels are permeable to cytochrome c. However a recent study by another group found no electrophysiologically detectable interaction between VDAC isolated from mammalian mitochondria, and either monomeric or oligomeric Bax (Rostovtseva et al., 2004). Contrary to the data obtained in this investigation the authors proposed that this is consistent with other data that failed to detect Bax-VDAC interaction by immunoprecipitation or cross-linking (Mihhailov et al., 2001). Furthermore these authors demonstrated that t-Bid affects the voltage gating of VDAC by inducing channel closure. The diameter of VDAC is not wide enough to allow the passage of cytochrome c and therefore cannot directly be responsible for the permeabilisation of the OMM. Another hypothesis is based on the ability of Bax to close VDAC which results in the accumulation of small metabolites in the IMS followed by mitochondrial swelling and the loss of OMM integrity (Vander Heiden et al., 2001, Vander Heiden et al., 2000). However, a number of studies have shown the absence of mitochondrial

swelling and the maintenance of integrity of the OMM during apoptosis (Waterhouse et al., 2002).

Other data has shown that Bax is capable of direct interaction with ANT in the IMM to form a non-specific pore that is inhibited by bongkrekic acid and CSA (Marzo et al., 1998b). Other evidence obtained using a yeast two-hybrid system demonstrated that Bax interacts with amino acids 105-156 of ANT-2. Further studies have shown that Bax can also interact with ANT to prevent ATP/ADP exchange across the IMM (Belzacq et al., 2003). Following insertion into the OMM, Bax activity might be modulated by ANT in the IMM. The amino acid sequence for human ANT-1 and ANT-2 are 95% identical. Contrary to data published by Kroemer's laboratory, Bauer's group (Bauer et al., 1999) demonstrated that overexpression of ANT-1 induces apoptosis whereas ANT-2 does not. Both isoforms can exist within the same mitochondrion (Vyssokikh et al., 2001) however ANT-2 was found exclusively in the cristae and both isoforms were present in the peripheral inner membrane. In addition ANT-1 was found to form complexes with VDAC and to have a higher affinity for Cyp D than ANT-2. In the present study an anti-ANT polyclonal antibody was used to detect ANT, this recognises the C-terminal epitope YDEIKKYV which is common to both ANT isoforms. Since VDAC and ANT were detected this suggests the ANT-1 isoform was present but ANT-2 interaction with GST-Bax cannot be ruled out. Models for the role of contact sites in the Bax-induced release of proteins from the IMS are summarised in figure **[7.1]**.

The phospholipid cardiolipin is involved in Bid targeting to lipid membranes (Lutter et al., 2001, Lutter et al., 2000) and promoting the formation of large pores in membranes by tBid and monomeric Bax (Kuwana et al., 2002). Cardiolipin is found in high concentrations throughout the IMM and also at VDAC-ANT contact sites (17-20%) (Simbeni et al., 1991, Ardail et al., 1990). In the OMM cardiolipin is present at lower concentrations (0.3-4%) (De Kroon et al., 1997). The contact sites might act as receptors for Bax following translocation to mitochondria. Bax interacts with cardiolipin to induce disruption of the phospholipid bilayer resulting in the formation of transient pores through which apoptogenic proteins can pass. One of the functions of tBid, which also localises to the contact sites (Lutter et al., 2001), is to promote oligomerisation of Bax and Bak. The oligomerised form of Bax is thought to be necessary for cytochrome c release to occur (Antonsson et al., 2000). *In vitro* the oligomeric state of Bax can be altered by non-ionic detergents (Hsu & Youle, 1997). Zwitterionic detergents such as CHAPS do not promote oligomerisation. The data shown in Chapter 4 shows that GST-Bax purified in the presence of CHAPS retained VDAC and ANT from rat heart mitochondrial membrane extracts indicating that monomeric Bax binds to contact sites and oligomerisation occurs afterwards. Bax also forms larger Bax complexes consisting of thousands of Bax molecules (Nechushtan et al., 2001). In some cases it was shown the formation of the larger Bax complexes preceded cytochrome c release (De Giorgi et al., 2002) and in others it occurred much later (Capano & Crompton, 2002). A study by Kuwana and co-workers (Kuwana et al., 2002) demonstrates that Bax interaction with cardiolipin containing outer mitochondrial membrane vesicles (OMVs) is sufficient to permeabilise the OMVs and mimics many properties of apoptotic permeabilisation of the OMM. However this model does not

encompass all aspects of OMM permeabilisation, for example the IMM of mitochondria or the membrane of mitoplasts (mitochondria lacking the OMM) are not completely permeabilised by tBid/Bax despite the fact that the IMM contains large amounts of cardiolipin. Therefore other regulatory components must be present during OMM permeabilisation.

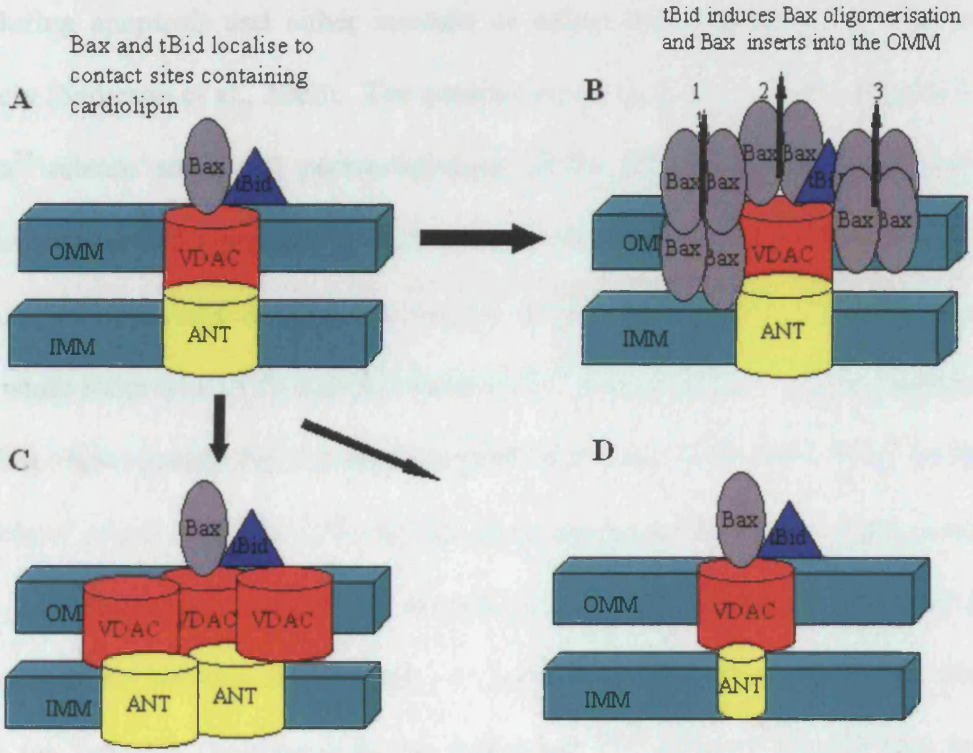

Figure [7.1] Bax interacts with VDAC and ANT: models for the role of Bax in the release of apoptogenic proteins from the IMS. **A** Bax and tBid localise to the VDAC-ANT intermembrane contact sites. **B** After tBid induced oligomerisation Bax might participate in the release of proteins from the IMS by 1 forming Bax channels that are regulated by ANT-2 interacting with VDAC to produce Bax-VDAC channels, 3 interacting with cardiolipin at the contact sites leading to the localised disruption of the lipid bilayer resulting in the formation of transient pores. **C** The ANT ligands bongkrekic acid and **D** atractyloside alters the relative amounts of VDAC and ANT that interact with Bax.

Mitochondrial apoptosis may be mediated through differential apoptotic pathways including those involving the ER (Nutt et al., 2002). In this case some apoptotic stimuli may lead to the release of Ca^{2+} from the ER stores, which in turn leads to increases in mitochondrial matrix Ca^{2+} (see section **[6.1]**), MPT, mitochondrial swelling and rupture of the OMM allowing the release of apoptogenic proteins from the IMS. Both pro-apoptotic proteins (Bax and Bak) and anti-apoptotic proteins e.g. Bcl-2 localise to the ER during apoptosis and either increase or reduce the releasable Ca^{2+} ER pool respectively (Scorrano et al., 2002). The question arises as to the relative contributions of the Ca^{2+} release and direct permeabilisation of the OMM pathways in apoptosis induced in various cell types and by different stimuli. Apoptotic messengers such as ceramide, arachidonic acid and reactive oxygen species (ROS) rely on the Ca^{2+} release pathway while other stimuli do not (Scorrano et al., 2003, Nutt et al., 2002, Nakamura et al., 2000). How exactly Bcl-2 proteins regulate the release of proteins from the IMS and the role of mitochondria in different cell types during apoptosis are active areas of research, the results from which will hopefully enhance our understanding of this process and allow for the development of novel therapies for diseases in which apoptosis (or lack of) contributes to the pathology, for example cancers and heart disease.

References

Adams, J. M. & Cory, S. The Bcl-2 protein family: arbiters of cell survival. *Science* **281,** 1322-1326 (1998)

Al Nasser, I. & Crompton, M. The reversible Ca^{2+}-induced permeabilization of rat liver mitochondria. *Biochem. J.* **239,** 19-29 (1986)

Antonsson, B., Conti, F., Ciavatta, A. M., Montesuit, S., Lewis, S., Martinou, I., Bernasconi, L., Bernard, A., Mermod, J-J., Mazzei, G., Maundrell, K., Gambale, F., Sadoul, R. & Martinou, J-C. Inhibition of Bax forming activity by Bcl-2. *Science* **277,** 370-372 (1997)

Antonsson, B., Montessuit, S., Lauper, S., Eskes, R. & Martinou, J-C. Bax oligomerisation is required for channel-forming activity in liposomes and to trigger cytochrome c release from mitochondria. *Biochem. J.* **345,** 271-278 (2000)

Antonsson, B., Montessuit, S., Sanchez, C. & Martinou, J-C. Bax is present as high molecular weight oligomer/complex in mitochondrial membranes of apoptotic cells. *J. Biol. Chem.* **267,** 11615-11623 (2001)

Anversa, P., Leri, A., Kajstura, J. & Nadal-Ginard, B. Myocyte growth and cardiac repair. *J. Mol. Cell Cardiol.* **34,** 91-105 (2002)

Appaix, F., Guerrero, K., Rampal, D., Izikki, M., Kaambre, T., Sikk, P., Brdiczka, D., Riva-Lavielle, C., Olivares, J., Longuet, M., Antonsson, B. & Saks, V. A. Bax and heart mitochondria: uncoupling and inhibition of respiration without permeability transition. *Biochim. Biophys. Acta* **1556,** 155-167 (2002)

References

Apte, S. S., Mattei, M-G. & Olsen, B. R. Mapping of human Bax gene to chromosome 19q13.3-q13.4 and isolation of a novel alternatively spliced transcript, Bax-delta. *Genomics* **26,** 592-594 (1995)

Ardail, D., Privat, J. P., Egret-Chalier, M., Levrat, C., Lerme, F. & Louisot, P. Mitochondrial contact sites, lipid composition and dynamics. *J. Biol. Chem.* **265,** 18797-18802 (1990)

Arnoult, D., Gaume, B., Karbowski, M., Sharpe, J. C., Cecconi, J. C. & Youle, R. J. Mitochondrial release of AIF and Endo G requires caspase activation downstream of Bax/Bak-mediated permeabilisation. *EMBO J.***22,** 4385-4399 (2003)

Arnoult, D., Parone, P., Martinou, J-C., Antonsson, B., Estaquier, J. & Ameisen, J. C. Mitochondrial release of apoptosis-inducing factor occurs downstream of cytochrome c release in response to several pro-apoptotic stimuli. *J. Cell Biol.* **156,** 923-929 (2002)

Asoh, S., Nishhimaki, K., Nanbu-Wakao, R. & Ohta, S. A trace amount of the human pro-apoptotic factor Bax induces bacterial death accompanied by damage of DNA. *J. Biol. Chem.* **273,** 11384-11391 (1998)

Basanez, G., Sharpe, J.C., Galanis, J., Brandt, T.B., Hardwick, J.M. & Zimmerberg, J. Bax-type apoptotic proteins porate pure lipid bilayers through a mechanism sensitive to intrinsic monolayer curvature. *J. Biol. Chem.* **277,** 49360-49356 (2002)

Bauer, M. K. A., Schubert, A., Rocks, O. & Grimm, S. Adenine Nucleotide Translocase-1, a Component of the Permeability Transition Pore, Can Dominantly Induce Apoptosis. *J. Cell Biol.* **147,** 1493-1501 (1999)

References

Becker, L., B., Vanden Hoek, T. L., Shao, S. H., Li, C., Q. & Schumacker, P. T. Generation of superoxide in cardiomyocytes during ischaemia before reperfusion. *Am. J. Physiol.* **277,** H2240-H2246 (1999)

Belzacq, A-S., Vieira, F. V., Vandecasteele, G., Cohen, I., Prevost, M-C., Larquet, E., Pariselli, F., Petit, P. X., Kahn, A., Rizzuto, R., Brenner, C. & Kroemer, G. Bcl-2 and Bax modulate Adenine Nucleotide Translocase Activity. *Cancer Res.* **63,** 541-546 (2003)

Bergsma, D. J., Eder, C., Gross, M., Kerstern, H., Sylvester, D., Appelbaum, E., Cusimaro, D., Livi, G. P., McLaughlin, M. M. & Kasyan K. et al., The cyclophilin multigene family of peptidyl-prolyl isomerases. Characterisation of three separate human isoforms. *J. Biol. Chem.* **266,** 23204-23214 (1991)

Bernardi, P. Mitochondrial transport of cations: channels, exchangers, and permeability transition. *Physiol. Rev.* **79,** 1127-1155 (1999)

Berridge, M., J., Lipp, P. & Bootman, M., D. The versatility and universality of calcium signalling. *Nat. Rev. Mol. Cell. Biol.* **1,** 11-12 (2000)

Bialik, S., Cryns, V. L., Drincic, A., Miyata, S., Wollowick, A. L., Srinvasan, A. & Kitsis, R. N. The mitochondrial apoptotic pathway is activated by serum and glucose deprivation in cardiac myocytes. *Circ. Res.* **85,** 403-414 (1999)

Blachly-Dyson, E., Zambronicz, E. B., Yu, W. H., Adam, V., McCarbe, E. R., Adelman, J., Colombini, M. & Forte, M. Cloning and functional expression in yeast of two human isoforms of the outer mitochondrial membrane channel, the voltage dependent anion channel. *J. Biol. Chem.* **268,** 1835-1841 (1993)

References

Boise, L. H., Gonzalez-Garcia, M., Postema, C. E., Ding, L., Lindesten, T., Turka, L. A., Mao, X., Nunez, G. & Thompson, C. B. Bcl-X_L, a bcl-2 related gene that functions as a dominant regulator of apoptotic cell death. *Cell* **74,** 597-608 (1993)

Borutaite, V., Jekabsone, A., Morkuniene, R. & Brown, G. C. Inhibition of mitochondrial permeability transition prevents mitochondrial dysfunction, cytochrome c release and apoptosis induced by heart ischaemia. *J. Mol. Cell. Cardiol.* **35,** 357-366 (2003)

Bossy-Wetzel, E., Newmeyer, D. D. & Green, D. R. Mitochondrial cytochrome c release in apoptosis occurs downstream of DEVD-specific caspase activation and independently of mitochondrial depolarisation. *EMBO J.* **17,** 37-49 (1998)

Boyer, C. S., Neve, E. P., Moore, G. A. & Moldens, P. Effects of mitochondrial protein concentration on the efficiency of the outer membrane removal by the cholesterol-selective detergent digitononin. *Biochim. Biophys. Acta.* **1190,** 304-308 (1994)

Brandolin, G., Le-Saux, A., Trezeguet, V., Lauquinn & Vignais, P. V. Chemical, immunological, enzymatic, and genetic approaches to studying the arrangement of the peptide chain of the ADP/ATP carrier in the mitochondrial membrane. *J. Bioenerg. Biomembr.***25,** 493-501 (1993)

Breckenridge, D. G., Stojanovic, M., Marcellus, R. C. & Shore, G. C. Caspase cleavage product of BAP31 induces mitochondrial fission through endoplasmic reticulum calcium signals, enhancing cytochrome c release to the cytosol. *J. Cell Biol.* **160,** 1115-1127 (2003)

Brdiczka, D., Beutner, G., Ruck, A., Dolder, M. & Wallimann, T. The molecular structure of contact sites. Their role in regulation of energy metabolism and permeability transition. *BioFactors* **8,** 235-242 (1998)

References

Brdiczka, D. Contact sites between mitochondrial envelope membranes *Biochim. Biophys. Acta* **1071,** 291-312 (1991)

Brenner, C., Cadiou, H., Viera, H. L. A., Zamzami, N., Marzo, I., Z., Leber, B., Andrews, D., Duchlohier, H., Reed, J. C. & Kroemer, G. Bcl-2 and Bax regulate the channel activity of the mitochondrial adenine nucleotide translocator. *Oncogene* **19,** 329-336 (2000)

Brustovetsky, N., Brustovetsky, T., Jemmerson, R. & Dubinsky, J. M. Calcium-induced cytochrome c release from CNS mitochondria is associated with permeability transition and rupture of the outer membrane. *J. Neurochemistry* **80,** 207-218 (2002)

Brustovetsky, N. & Klingenberg, M. The mitochondrial ADP/ATP carrier can be reversibly converted into a large channel by Ca^{2+}. *Biochemistry* **35,** 8483-8488 (1996)

Bucheler, K., Adams, V. & Brdiczka, D. Localisation of the ATP/ADP translocator in the inner membrane and regulation of contact sites between mitochondrial membranes by ADP. A study on freeze-fractured isolated mitochondria. *Biochim. Biophys. Acta.* **1056,** 233-242 (1991)

Buendia, B., Santa-Maria, A. & Courvalin, J. C. Caspase-dependent proteolysis of integral and peripheral proteins of nuclear membranes and nuclear pore complex proteins during apoptosis. *J. Cell Sci.* **112,** 1743-1753 (1999)

Cain, K., Bratton, S. B., Langlais, C., Walker, G., Brown, D. G., Sun, X. M. & Cohen, G. M. Apaf-1 oligomerises into biologically active approximately 700 kDa and inactive approximately 1.4 MDa apoptosome complexes. *J. Biol. Chem.* **275,** 6067-6070 (2000)

References

Cain, K., Brown, D. G., Langlais, C. & Cohen, G. M. Caspase action involves the formation of the apoptosome, a large (700 kDa) caspase-activating complex. *J. Biol. Chem.* **274,** 22686-22699 (1999)

Cao, G., Minami, M., Pei, W., Yan, C., Chen, D., O'Horo, Graham, S. H. & Chen, J. Intracellular Bax translocation after transient cerebral Ischemia: Implications for a role of mitochondrial apoptotic signaling pathway in ischemic neuronal death. *J. Cerebral Blood Flow and Metabolism* **21,** 321-333 (2001)

Capano, M. & Crompton, M. Biphasic translocation of Bax to mitochondria. *Biochem. J.* **367,** 169-178 (2002)

Capano, M., Virji, S. & Crompton, M. Cyclophilin-A is involved in excitotoxin-induced caspase activation in rat neuronal B50 cells. *Biochem. J.* **363,** 29-36 (2002)

Cartron, P-F., Moreau, C., Oliver, L., Mayat, E., Meflah, K. & Vallette, F. M. Involvement of the N-terminus of Bax in its intracellular localization and function *FEBS. Letts.* **512,** 95-100 (2002)

Cartron, P-F., Oliver, L., Martin, S., Moreau, C., LeCabellec, M-T., Jezequel, P., Meflah, K. & Vallette, F. M. The expression of a new variant of the pro-apoptotic molecule Bax , Bax-psi, is correlated with an increased survival of glioblastoma multiforme patients. *Hum. Molec. Genet.* **11,** 675-687 (2002)

Cartron, P. F., Priault, M., Oliver, L., Meflah, K., Manon, S. & Vallette, F. M. The N-terminal end of Bax contains the mitochondrial-targeting signal. *J. Biol. Chem.* **278,** 11633-11641 (2003)

Cheng, E. H., Sheiko, T. V., Fisher, J. K., Craigen, W. J. & Korsmeyer, S. J. VDAC2 inhibits BAK activation and mitochondrial apoptosis. *Science* **301,** 513-517 (2003)

References

Clarke, S. J., McStay, G. & Halestrap, A. P. Sanglifehrin A acts as a potent inhibitor of mitochondrial permeability transition and reperfusion injury of the heart by binding to Cyclophilin-D at a different site from Cyclosporin A. *J. Biol. Chem.* **277,** 34793-34799 (2002)

Clerk, A., Cole, S. M., Cullingford, T. E., Harrison, J. G., Jormakka, M. & Valks, D. M. Regulation of cardiac myocyte cell death. *Pharmocology & Therapeutics* **97,** 223-261 (2003)

Connern, C. P & Halestrap, A. P. Purification and N-terminal sequencing of peptidyl-prolyl cis-trans isomerase from rat liver mitochondrial matrix reveals the existence of a distinct mitochondrial cyclophilin. *Biochem. J.* **284,** 381-385 (1992)

Crompton, M. The mitochondrial permeability transition pore and its role in cell death. *Biochem. J.* **341,** 233-249 (1999)

Crompton, M., Capano, M. & Carafoli, E. Respiration-dependent efflux of magnesium ions from heart mitochondria. *Biochem. J.* **154,** 735-742 (1976)

Crompton M., Virji, S. & Ward, J. Cyclophilin-D strongly binds to complexes of the Voltage Dependent Anion Channel and the Adenine Nucleotide Translocase to form the Permeability Transition Pore. *Eur. J. Biochem.* **258,** 729-735 (1998)

Crompton, M. & Andreeva, L. On the interaction of $Ca^{2+}$and cyclosporin A with a mitochondrial inner membrane pore: a study using cobaltammine complex inhibitors of the Ca^{2+} uniporter. *Biochem. J.* **302,** 181-185 (1994)

Crompton, M. & Costi, A. Kinetic evidence for a heart mitochondrial pore activated by Ca^{2+}, inorganic phosphate and oxidative stress. A potential mechanism for mitochondrial dysfunction during cellular Ca^{2+} overload. *Eur. J. Biochem.* **178,** 489-501 (1988)

References

Crompton, M., Ellinger, H. & Costi, A. Inhibition by cyclosporin A of a Ca^{2+}-dependent pore in heart mitochondria activated by inorganic phosphate and oxidative stress. *Biochem. J.* **255,** 357-360 (1988)

Crompton, M., Barksby, E., Johnson, N. & Capano, M. Mitochondrial Intermembrane junctional complexes and their involvement in cell death. *Biochimie.* **10,** 1473-1484 (2002)

Daugas, E., Nochy, D., Ravagnan, L., Loeffler, M., Susin, S. A., Zamzami, N. & Kroemer, G. Apoptosis-inducing factor (AIF): a ubiquitous mitochondrial oxidoreductase involved in apoptosis. *FEBS Letts.* **476,** 118-123 (2000)

Deckwerth, T. L. & Johnson, E. M. Temporal analysis of events associated with programmed cell death (apoptosis) of sympathetic neurons deprived of nerve growth factor. *J. Cell Biol.* **123,** 1207-1222 (1993)

De Giorgi, F., Lartigue, L., Bauer, M. K., Schubert, A., Grimm, S., Hanson, G. T., Remington, S. J., Youle, R. J. & Ichas, F. The permeability transition pore signals apoptosis by directing Bax translocation and multimerization. *FASEB J.* **10,** 607-610 (2002)

De Jong, D., Prins, F. A., Mason, D. Y., Reed, J. C., Van Ommen, G. B. & Kluin, P. M. Subcellular localisation of the bcl-2 protein in malignant and normal lymphoid cells. *Cancer Res.* **54,** 256-260 (1994)

De Kroon, A. I., Dolis, D., Mayer, A., Lill, R. & De Kruijff, B. Phospholipid composition of highly purified mitochondrial outer membranes of rat liver and *Neurospora crassa*. Is cardiolipin present in the mitochondrial outer membrane? *Biochim. Biophys. Acta.* **1325,** 108-116 (1997)

References

De Luca, H. F. & Engstrom, G. W. Calcium uptake by rat kidney mitochondria. *Proc. Natl. Acad. Sci. USA.* **47,** 1744-1750 (1961)

De Maria, R., Lenti, L., Malisan, F., d'Agostino, F., Tomassino, B., Rippo, M. R. & Testi, R. Requirement for GD3 ganglioside in CD95 and ceramide induced apoptosis. *Science* **272,** 1652-1655 (1997)

Desagher, S., Osend-Sand, A., Nichols, A., Eskes, R., Montessuit, S., Lauper, S., Maundrell, K., Antonsson, B. & Martinou, J-C. Bid induced conformational change of Bax is responsible for mitochondrial cytochrome c release during apoptosis. *J. Cell Biol.* **144,** 891-901 (1999)

Deverman, B. E., Cook, B. L., Manson, S. R., Niederhoff, R. A., Langer, E. M., Rosova, I., Kulans, L. A., Fu, X., Weinberg, J. S., Heinecke, J. W., Roth, K. A. & Weintraub, S. J. Bcl-XL deamidation is a critical switch in the regulation of the response to DNA damage. *Cell* **111,** 51-62 (2002)

Dianoux, A. C., Noel, F., Fiore, C., Trezeguet, V., Kieffer, S., Jaquinod, M., Lauquin, G. J. & Brandolin, G. Two distinct regions of the yeast mitochondrial ADP/ATP carrier are photolabelled by a new ADP analogue: 2-azido-3'-O-naphthoyl-[beta-32P]ADP. Identification of the binding segments by mass spectrometry. *Biochemistry* **39,** 11477-11487 (2000)

Distolhorst, C. W., Lam, M., & Mc Cormack, T. S. Bcl-2 inhibits hydrogen peroxide-induced ER Ca^{2+} pool depletion. *Oncogene* **10,** 2051-2055 (1996)

Doran, E. & Halestrap, P. Cytochrome c release from isolated rat liver mitochondria can occur independently of outer-membrane rupture: possible role of contact sites. *Biochem. J.* **348,** 343-350 (2000)

References

Dorner, A., Olesch, M., Giessen, S., Pauschinger, M. & Schultheiss H-P. Transcription of the adenine nucleotide translocase isoforms in varios types of tissues in the rat. *Biochim. Biophys. Acta* **1417,** 16-24 (1999)

Dorner, A., Pauschinger, M., Badorff, A,. Noutsais, M., Giessen, S., Schulze, K. et al., Tissue specific transcription pattern of the Adenine Nucleotide Translocase isoforms in humans, *FEBS Letts.* **414,** 258-262 (1997)

Doyle, V., Virji, S. & Crompton, M. Evidence that cyclophilin-A protects cells against oxidative stress. *Biochem. J.* **341,** 127-132 (1999)

Du, C., Fang, M., Li, L. & Wang, X. Smac, a mitochondrial protein that promotes cytochrome c-dependent caspase activation by eliminating IAP inhibition. *Cell* **102,** 33-42 (2000)

Duilio, C., Ambrosio, G., Kuppusamy, P., Dipaula, A., Becker, L. C. & Zweier, J. L. Neutrophils are primary sources of O_2 radicals during reperfusion after prolonged myocardial ischaemia. *Am. J. Physiol.* **280,** H2649-H2657 (2001)

Earnshaw, W. C., Martins, L. M. & Kaufmann, S. H. Mammalian caspases: structure, activation, substrates, and functions during apoptosis. *Annu. Rev. Biochem.* **68,** 383-424 (1999)

Eberstadt, M., Huang, B., Chen, Z., Meadows, R. P, Ng, S. C., Zheng, C., Leonardo, M. J. & Fesik, S. W. NMR structure and mutagenesis of the FADD (Mort 1) death effector domain. *Nature* **392,** 941-945 (1998)

References

Ellerby, H. M., Martin, S. J., Ellerby, L. M., Naiem, S. S., Rabizadeh, S., Salvesen, G. S., Casiano, C. A., Cashman, N. R., Green, D. R. & Bredesen, D. E. Establishment of a cell-free system of neuronal apoptosis: Comparison of premitochondrial, mitochondrial, and postmitochondrial phases *J. Neurosci.* **17,** 6165-6178 (1997)

Enari, M., Sakahira, H., Yokoyama, H., Okawa, K., Iwamatsu, A. & Nagata, S. A caspase-activated Dnase that degrades DNA during apoptosis and its inhibitor ICAD. *Nature* **391,** 43-50 (1998)

Eskes, R., Antonsson, B., Osen-Sand, A., Montessuit, S., Richter, C., Sadoul, R., Mazzei, G., Nichols, A. & Martinou, J-C. Bax induced cytochrome c release from mitochondria is independent of the permeability transition pore but highly dependent on Mg ions. *J. Cell Biol.* **143,** 217-224 (1998)

Ferrari, R., Agnoletti, L., Comini, L., Gaia, G., Bachetti, T., Cacgnoni, A., Ceconi, C., Curello, S.,& Visioli, O. Oxidative stress during myocardial ischaemia and heart failure. *Eur. Heart J.* **19,** (suppl. B) B2-B11 (1998)

Ferri, K. F. & Kroemer, G. Organelle-specific initiation of cell death pathways. *Nat. Cell. Biol.* **3,** E255-E263 (2001)

Fiore, C., Trezeguet, V., Le Saux, A., Roux, P., Schwimmer, C., Dianoux, A.C., Noel, F., Lauquin GJ-M., Brandolin G. & Vignais, P. V. The mitochondrial ADP/ATP carrier: Structure, physiological and pathological aspects. *Biochimie* **80,** 137-150 (1998)

Fliss, H. & Gattinger, D. Apoptosis in ischaemic and reperfused rat myocardium. *Circ. Res.* **79,** 949-956 (1996)

References

Foyouzi-Youssefi, R., Arnaudeau, S., Borner, C., Kelly, W. L., Tschopp, J., Lew, D. P., Demaurex, N. & Krause, K. H. Bcl-2 decreases the free Ca^{2+} concentration within the endoplasmic reticulum. *Pro. Acad. Sci. USA.* **11,** 5723-5728 (2000)

Frank, S., Gaume, B., Bergmann-Leitner, E. S., Leitner, W. W., Robert, E. G., Smith, C. L. & Youle, R. J. The role of dynamin-related protein 1, a mediator of mitochondrial fission in apoptosis. *Dev. Cell.* **1,** 515-525 (2001)

Fritz, S., Rapaport, D., Klanner, E., Neupert, W. & Westermann, B. Connection of the mitochondrial outer and inner membranes by Fzo 1 is critical for organellar fusion. *J. Cell Biol.* **152,** 683-692 (2001)

Gallitelli, M. F., Schultz, M., Isenberg, G. & Rudolf, I. Twitch-potential increases calcium in peripheral more than in central mitochondria of guinea pig ventricular myocytes. *J. Physiol.* **518,** 433-447 (1999)

Gavreili, Y., Sherman, Y. & Ben-Sasson, S. A. Idnetification of programmed cell death in situ via specific labelling of nuclear DNA fragmentation. *J. Cell. Biol.* **119,** 493-501 (1999)

Goldstein, J. C., Waterhouse, W. J., Juin, P., Evan, G.I. & Green, D. R. The coordinate release of cytochrome c during apoptosis is rapid complete and kinetically invariant. *Nat. Cell. Biol.* **3,** 156-162 (2000)

Goldstone, G. P., Roos, I. & Crompton, M. Effects of Adrenergic Agonists and Mitochondrial Energy State on the Ca^{2+} Transport Systems of Mitochondria. *Biochemistry* **26,** 246-254 (1987)

References

Gonzalez-Garcia, M., Perez-Ballestero, R., Ding, L., Duan, L., Boise, L. H., Thompson, C. B. & Nunez, G. Bcl-X_L is the major bcl-xl mRNA form expressed during murine development and its product localises to mitochondria. *Development* **120,** 3033-3042 (1994)

Goping, I. S., Gross, A., Lavoie, N., Nguyen, M., Jemmerson, R., Roth, K., Korsmeyer, S. J. & Shore, G. C. Regulated targeting of Bax to mitochondria. *J. Cell. Biol.* **143,** 207-215 (1998)

Granville, D. J. & Gottlieb, R. A. The mitochondrial voltage-dependent anion channel (VDAC) as a therapeutic target for initiating cell death. *Curr. Med. Chem.* **10,** 1527-1533 (2003)

Griffiths, E. J. & Halestrap, A. P. Mitochondrial non-specific pores remain closed during cardiac ischaemia, but open upon reperfusion. *Biochem. J.* **307,** 93-98 (1995)

Griffiths, E. J. & Halestrap, A. P. Protection by cyclosporin A of ischaemia/reperfusion-induced damage in isolated rat hearts. *J. Mol. Cell. Cardiol.* **25,** 1461-1469 (1993)

Gross, A., Jockel, J., Wei, M. C. & Korsmeyer, S. J. Enforced dimerization of Bax results in its translocation, mitochondrial dysfunction, and apoptosis *EMBO J.* **17,** 3878-3885 (1998)

Grubb, D. R., Ly, J. D., Vaillant , F., Johnson, K. L. & Lawen. Mitochondrial cytochrome c release is caspase-dependent and does not involve mitochondrial permeability transition in didemnin B-induced apoptosis. *Oncogene* **20,** 4085-4094 (2001)

Gunter, K. K & Gunter, T. E. Transport of calcium by mitochondria. *J. Bioerg. Biomembr.***5,** 471-485 (1994)

References

Gunter, T. E. & Pfeiffer, D. R. Mechanisms by which mitochondria transport calcium. *Am. J. Physiol.* **258,** C753-C786 (1990)

Hackenbrock, C. R. Chemical and physical fixation of isolated mitochondria in low energy and high energy states. *Pro. Natl. Acad. Sci. USA.* **61,** 598-605 (1968)

Hajnoczky, G., Davies, E. & Madesh, M. Calcium signalling and apoptosis. *Biochem. Biophys. Commun.* **304,** 445-454 (2003)

Hajnoczky, G., Robb-Gaspers, L. D., Seitz, M. B. & Thomas, A. P. Decoding of cytosolic calcium oscillations in the mitochondria. *Cell* **82,** 415-424 (1995)

Halestrap, A. P., Clarke, S. J. & Javadov, S. A. Mitochondrial permeability transition pore opening during myocardial reperfusion –a target for cardioprotection. *Cardiovasc. Res.* **61,** 372-385 (2004)

Halestrap, A. P. & Davidson, A. M. Inhibition of Ca^{2+} induced mitochondrial swelling by cyclosporin A is probably caused by the by the inhibitor binding to peptidyl-prolyl cis-trans-isomerase and preventing its interaction with the adenine nucleotide translocase. *Biochem. J.* **268,** 153-160 (1990)

Halestrap, A. P., Woodfield, K-Y. & Connern, C. P. Oxidative stress, thiol reagents, and membrane potential modulate the mitochondrial permeability transition by affecting nucleotide binding to the adenine nucleotide translocase. *J. Biol. Chem.* **272,** 3346-3354 (1997)

Hansford, R. G. Dehydrogenase activation by Ca^{2+} in cells and tissues. *Bioenerg. Biomembr.* **6,** 823-854 (1991)

References

Haunstetter, A. & Izumo, S. Apoptosis: basic mechanisms and implications for cardiovascular disease. *Circ. Res.* **82,** 371-376 (1998)

Hegde, R., Srinivasula, S. M., Zhang, Z., Wassell, R., Mukattash, R., Cilenti, L., DuBois, G., Lazebnik, Y., Zervos, A. S., Fernandes-Alnemri, T., Alnemri, E. S. Identification of Omi/HtrA2 as a mitochondrial apoptotic serine protease that disrupts inhibitor of apoptosis protein-caspase interaction. *J. Biol. Chem.* **277,** 432-438 (2002)

Heimlich, G., McKinnon, A. D., Bernardo, K., Brdiczka, D., Reed, J. C., Kain, R., Kronke M. & Jurgensmeier, J. M. Bax-induced cytochrome c release from mitochondria depends on α-helices-5 and –6. *Biochem. J.* **378,** 247-255 (2004)

Hengartner, M. O. The biochemistry of apoptosis. *Nature* **407,** 770-776 (2000)

Hermann, C., Assmus, B., Urbich, C., Zeiher, A. M. & Dimmeler, S. Insulin-mediated stimulation of protein kinase Akt: A potent survival signaling cascade for endothelial cells. *Arterioscler. Thromb. Vasc. Biol.* **20,** 402-409 (2000)

Hirata, H., Takahashi, A., Kohayashi, S., Yonehara, S., Sawai, H., Okazaki, T., Yamamoto, K., & Sasada, M. Caspases are activated in a branched protease cascade and control distinct downsream processes in Fas-induced apoptosis. *J. Exp. Med.* **187,** 587-600 (1998)

Hofmann, K. The molecular nature of apoptogenic signalling proteins. *Cell Mol. Life Sci.* **55,** 1113-1128 (1999)

Hsu, Y. T. & Youle, R. J. Bax in murine thymus is a soluble monomeric protein that displays differential detergent –induced conformations. *J. Biol. Chem.* **272,** 10777-10787 (1998)

References

Hsu, Y. T. & Youle, R. J. Nonionic detergents induce dimerization among members of the Bcl-2 family. *J. Biol. Chem.* **272,** 13829-13834 (1997)

Huang, B., Eberstadt, M., Oejniczak, E. T., Meadows, R. P. & Fesik, S. W NMR structure and mutagenesis of the Fas (Apo-1/CD95) death domain. *Nature* **384,** 638-641 (1996)

Hunter, P. R. & Haworth, R. A. The Ca^{2+} induced membrane transition in mitochondria III. Transitional Ca^{2+} release. *Arch. Biochem. Biophys.* **195,** 468-477 (1979)

Ishihara, N., Jofuku, A., Eura, Y. & Mihara, K. Regulation of mitochondrial morphology by membrane potential, and DRP1-dependent division and FZO-1 dependent fusion reaction in mammalian cells. *Biochem. Biophys. Res. Commun.* **301,** 891-898 (2003)

Jacotot, E., Ferri, K., Hamel, C., Brenner, C., Druillenec, S., Hoekeke, J., Rustin, P., Metiver, D., Lenoir, C., Geuskens, M., Vieira, H. L. A., Loeffler, M., Belzacq, A-S., Briand, J-P., Zamzami, N., Edelman, L., Xie, Z. H., Reed, J. C., Roques, B. P. & Kroemer, G. Control of mitochondrial membrane permeabilisation by adenine nucleotide translocator interacting with HIV-1 Vpr and Bcl-2. *J. Exp. Med.* **193,** 509-520 (2001)

Janicke, R. U., Ng, P., Spengart, M. L. & Porter, A. G. Caspase-3 is required for α-fodrin cleavage but dispensible for cleavage of other death substrates in apoptosis. *J. Biol. Chem.* **273,** 15540-15545 (1998)

Jiang, X. & Wang, X. Cytochrome c promotes caspase-9 activation by inducing nucleotide binding to Apaf-1. *J. Biol. Chem.* **275,** 31199-31203 (2000)

References

Jin, K. L., Graham, S. H., Mao, X. O., He, X., Nagayama, T., Simon, R. P. & Greenberg, D. A. Bax κ, a novel splice variant from rat brain lacking an ART domain, promotes neuronal cell death. *J. Neurochem.* **77,** 1508-1519 (2001)

Johnson, N., Khan, A., Virji, S., Ward, J. M. & Crompton, M. Import and processing of heart mitochondrial cyclophilin D. *Eur. J. Biochem.* **263,** 353-359 (1999)

Joseph-Liauzun, E., Delmos, P., Shine, D. & Ferrara, P. Topological analysis of the peripheral benzodiazepine receptor in yeast mitochondrial membranes support a five transmembrane structure. *J. Biol. Chem.* **273,** 2146-2152 (1998)

Jung, F., Weiland, U., Johns, R. A., Ihling, C. & Dimmeler, S. Chronic hypoxia induces apoptosis in cardiac myocytes: A possible role for Bcl-2-like proteins. *Biochem. Biophys. Res. Commun.* **286,** 419-425 (2001)

Jurgensmeier, J. M., Xie, S., Deveraux, Q., Ellerby, L., Bredesen, D. & Reed, J. C. Bax directly induces release of cytochrome c from isolated mitochondria. *Proc. Natl. Acad. Sci. USA* **95,** 4997-5002 (1998)

Kajstura, J., Cheng, W., Reiss, K., Clark, W., Sonnenblick, E. H., Krajewski, S. Reed, J. C., Olivetti, G. & Anversa, P. Apoptotic and necrotic myocyte cell death are independent contributing variables of infarct size in rats. *Lab. Invest.* **74,** 86-107 (1996)

Karbowski, M., Arnoult, D., Chen, H., Chan, D. C., Smith, C. L. & Youle, R. J. Quantitation of mitochondrial dynamics by photolabelling of individual organelles shows that mitochondrial fusion is blocked during the Bax activation phase of apoptosis. *J. Cell Biol.* **164,** 493-499 (2004)

Karbowski, M. & Youle, R. J. The dynamics of mitochondrial morphology in healthy cell and during apoptosis. *Cell Death Diff.* **10,** 870-880 (2003)

References

Kerr, J. F., Wyllie, A. H. & Currie, A. R. Apoptosis: a basic biological phenomenon with wide-ranging implications in tissue kinetics. *Br. J. Cancer* **26,** 239-257 (1972)

Kirichok, Y., Krapivinsky, G. & Clapham, D. E. The mitochondrial calcium uniporter is a highly selective ion channel. *Nature* **427,** 360-364 (2004)

Kluck, R. M., Bossy-Wetzel, E., Green, D. R. & Newmeyer, D.D. The release of cytochrome c from mitochondria: a primary site for Bcl-2 regulation of apoptosis. *Science* **275,** 1132-1136 (1997)

Kluck, R. M., Degli Esposti, M., Perkins, G., Kuwana, T., Bossy-Wetzel, E., Goldberg, M., Allen, T., Barker, M.J., Green, D. R. & Newmeyer, D. D. The proapoptotic proteins Bid and Bax cause a limited permeabilization of the mitochondrial outer membrane that is enhanced by cytosol. *J. Biol. Chem.* **47,** 809-822 (1999)

Kottke, M., Adam, M. & Reisinger, I. Mitochondrial boundary membrane sites in brain: points of hexokinase and creatine kinase location, and control of Ca^{2+} transport. *Biochim. Biophys. Acta.* **935,** 87-102 (1988)

Krajewski, S., Tanaka, S., Takayama, S., Schibler, M. J. Fenton, W. & Reed, J. C. Investigation of the subcellular distribution of the bcl-2 oncoprotein: residence in the nuclear envelope, endoplasmic reticulum, and the outer mitochondrial membranes. *Cancer Res.* **53,** 4701-4714 (1993)

Kroger, A. & Klingenberg, M. On the role of ubiquinone in mitochondria II redox reactions of ubiquinone under the control of oxidative phosphorylation. *Biochem Z.* **344,** 317-336 (1966)

Kuwana, T. & Newmeyer, D.D. Bcl-2 family proteins and the role of mitochondria in apoptosis.*Curr. Opin. Cell Biol.* **15,** 691-699 (2003)

References

Kuwana, T., Mackey, M. R., Perkins, G., Ellison, M. H., Latterich, M., Scheiter, R., Green, D. R. & Newmeyer, D. D. Bid, Bax and lipids cooperate to form supramolecular openings in the outer mitochondrial membrane. *Cell* **111,** 331-342 (2002)

Kuwana, T., Smith, J. J., Muzio, M., Dixit, V., Newmeyer, D. D. & Kornbluth S. Apoptosis induction by caspase-8 is amplified through the mitochondrial release of cytochrome c. *J. Biol. Chem.* **273,** 16589-16594 (1998)

Lee, S. P., Huang, Y. S., Kim, Y. J., Kuon, K. S., Kim, H. J., Kim, K. & Chae, H. Z. Cyclophilin A binds to peroxiredoxins and activates its peroxidase activity. *J. Biol. Chem.* **276,** 29826-29832 (2001)

Leist, M. & Jaattela, M. Four deaths and a funeral: from caspases to alternative mechanisms. *Nat. Rev. Mol. Cell. Biol.* **2,** 589-598 (2001)

Leist, M., Single, B., Castaldi, A. F., Kuhnle, S. & Nicotera, P. Intracellular adenosine triphosphate concentration: a switch in the decision between apoptosis and necrosis. *J. Exp. Med.* **185,** 1481-1486 (1997)

Lewis, S., Bethell, S. S., Patel, S., Martinou, J-C. & Antonsson, B. Purification and Biochemical Properties of Soluble Recombinant Human Bax. *Protein Expression and Purification* **13,** 120-126 (1998)

Li, H., Zhu, H., Xu, C. J. & Yuan, J. Cleavage of Bid by caspase-8 mediates mitochondrial damage in the Fas pathway of apoptosis. *Cell* **94,** 491-501 (1998)

Li, L. Y., Luo, X. & Wang, X. Endonuclease G is an apoptotic DNase when released from mitochondria. *Nature* **412,** 95-99 (2001)

References

Li, Y., Johnson, N., Capano, M., Edwards, M. & Crompton, M. Cyclophilin-D promotes the mitochondrial permeability transition but has the opposite effects on necrosis and apoptosis. *Biochem. J.* **383,** 101-109 (2004)

Lin, D. T. & Lechleiter, J. D. Mitochondrial targeted cyclophilin D protects cells from cell death by peptidyl prolyl isomerisation. *J. Biol. Chem.* **277,** 31134-31141 (2002)

Lithgow, T., van Driel, R., Bertram, J.F. & Strasser, A. The protein product of the oncogene bcl-2 is a component of the nuclear envelope, the endoplasmic reticulum, and the outer mitochondrial membrane. *Cell. Growth. Diff.* **5,** 411-417 (1994)

Locksley, R. M., Killeen, N. & Lenardo, M. J. The TNF and TNF receptor superfamilies: integrating mammalian biology. *Cell* **104,** 487-501 (2001)

Loeffler, M. & Kroemer, G. The mitochondria in cell death: certainties & incognita. *Exp. Cell Res.* **256,** 19-26 (2000)

Lovat, P. E., Ranalli, M., Annichiarrico-Petruzzelli, M., Bernassola, F., Piacentini, M., Malcolm, A. J., Pearson, A. D. J., Melino, G. & Redfern, C. P. F. Effector Mechanisms of Fenretinide-induced Apoptosis in Neuroblastoma. *Exp. Cell Res.* **260,** 50-60 (2000)

Lui, X., Kim, N., Yang, J., Jemmerson, R. & Wang, X. Induction of apoptotic program in cell-free extracts: requirement for dATP and cytochrome c. *Cell* **86,** 147-151 (1996)

Lui, X., Zou, H., Slaughter, C. & Wang, X. DFF, a heterodimeric protein that functions downstream of caspase-3 to trigger DNA fragmentation during apoptosis. *Cell* **89,** 175-184 (1997)

References

Luo, X., Budihardjo, I., Zou, N., Slaughter, C. & Wang, X. Bid, a bcl-2 interacting protein, mediates cytochrome c release from mitochondria in response to activation cell surface death receptors. *Cell* **94,** 481-490 (1998)

Lutter, M., Fang, M., Luo, X., Nishijima, M., Xie, X. & Wang, X. Cardiolipin provides specificity for targeting of tBid to mitochondria. *Nat. Cell. Biol.* **10,** 754-761 (2000)

Lutter, M., Perkins, G. A. & Wang, X. The pro-apoptotic Bcl-2 family member tBid localises to mitochondrial contact sites. *BMC. Cell Biol.* **2,** 22 (2001)

MacLellan, W. R. & Schneider, M. D. Death by design. *Circ. Res.* **81,** 137-144 (1997)

Malhotra, R. & Brosius, F. C. III Glucose uptake and glycolysis reduce hypoxia-induced apoptosis in cultured neonatal rat cardiac myocytes. *J. Biol. Chem.* **274,** 12567-12575 (1999)

Manella, C. A., Forte, M. & Colombini, M. Towards the molecular structure of the mitochondrial channel, VDAC. *J. Bioenerg. Biomembr.* **24,** 7-19 (1992)

Marchetti, P., Castedo, M., Susin, S.A., Zamzami, N., Hirsch, T., Macho, A., Haeffner, A., Hirsch, F., Geuskens, M. & Kroemer, G. Mitochondrial permeability transition is a central coordinating event of apoptosis. *J. Exp. Med.* **184,** 1155-1166 (1996)

Marzo, I., Brenner, C., Zamzami, N., Jurgensmeier, J. M., Susin, S. A., Vieira, H. L. E., Prevost, M. C., Xie, Z., Matsuyama, S., Reed, J. C. & Kroemer, G. Bax and the adenine nucleotide translocase cooperate in the mitochondrial control of apoptosis. *Science* **281,** 2027-2035 (1998)b

References

Marzo, I., Brenner, C., Zamzami, N., Susin, S. A., Beutner, D., Brdiczka, D., Remy, R., Xie, Z-H., Reed, J. C. & Kroemer, G. The permeability transition pore complex: a target for apoptosis regulation by caspases and Bcl-2 related proteins. *J. Exp. Med.* **187,** 1261-1271 (1998)a

Matsui, T., Li, L., Del Monte, R., Fukui, Y., Franke, T. F., Hajjar, R. J. & Rosenzweig, A. Adenoviral gene transfer of activated phosphatidylinositol 3' –kinase and Akt inhibits apoptosis of hypoxic cardiomyocytes *in vitro. Circulation* **100,** 2373-2379 (1999)

McCormack, J. G. & Denton, R. M. Ca^{2+} as a second messenger within the mitochondria of the heart and other tissues. *Annu. Rev. Physiol.* **52,** 451-466 (1990)

McCormack, J. G. & Denton, R. M. Role of Ca^{2+} ions in the regulation of intramitochondrial metabolism in rat heart. *Biochem. J.* **218,** 235-247 (1984)

McEnery, M. W., Snowman, A. M., Trifiletti, R. R. & Snyder, S. H. Isolation of the mitochondrial benzodiazepine receptor: association with the voltage dependent anion channel and the adenine nucleotide carrier *Proc. Natl. Acad. Sci. USA.* **89,** 3170-3174 (1992)

Mikhailov, V., Mikhailov, M., Pulkrabek, D. J., Dong, Z., Venkatachalam, M. A. & Saikumar, P. Bcl-2 prevents Bax oligomerisation in the outer mitochondrial membrane. *J. Biol. Chem.* **276,** 18361-18374 (2001)

Minn, A. J., Kettlun, C. S., Liang, H., Kelekar, A., Vander Heiden, M. G., Chang, B. S., Fesik, S. W., Fill, M. & Thompson, C. B. Bcl-X_L regulates apoptosis by heterodimerisation-dependent and –independent mechanisms. *EMBO J.* **18,** 632-643 (1999)

References

Minn, A. J., Velez, P., Schendel, S. L., Liang, H., Muchmore, S. W., Fesik, S. W., Fill, M. & Thompson, C. B. Bcl-X_L forms an ion channel in synthetic lipid membranes. *Nature* **385,** 353-357 (1997)

Mironova, G. D., Baumann, M., Kolomytkin, O., Krasichkova, Z., Berdimurator, A., Sirota, T., Virtanen, I. & Saris, N. E. Purification of the channel component of the mitochondrial calcium uniporter and its reconstitution into planar lipids. *J. Bioenerg. Biomembr.* **2,** 231-238 (1994)

Miyashita, T. & Reed, J. C. Tumour suppressor p53 is a direct transcriptional activator of the human bax gene. *Cell* **80,** 293-299 (1995)

Montero, M., Alsono, M. T, Carnicero, E., Cuchillo-Ibanez, I., Albillos, A., Garcia, A. G., Garcia-Sancio, J. & Alvarez, J. Chromaffin-cell stimulation triggers fast millimolar mitochondrial Ca^{2+} transients that modulate secretion. *Nat. Cell. Biol.* **2,** 57-61 (2000)

Montessuit, S., Mazzei, G., Magnenat, E. & Antonsson, B. Expression and purification of full-length human Bax. *Protein Expression and Purification* **15,** 202-206 (1999)

Moore, C. L. Specific inhibition of mitochondrial Ca^{2+}transport by ruthenium red. *Biochem. Biophys. Res. Commun.* **42,** 298-304 (1971)

Mozdy, A. D. & Shaw, J. M. A fuzzy mitochondrial fusion apparatus comes into focus. *Nat. Rev. Cell Biol.* **4,** 468-478 (2003)

References

Muchmore, S. W., Sattler, M., Liang, H., Meadows, R. P., Harlan, J. E., Yoon, H. S., Nettesheim, D., Chang, B. S., Thompson, C. B., Wong, S. L., Ng, S. L. & Fesik, S. W. X-ray and NMR structure of human Bcl-X_L, an inhibitor of programmed death. *Nature* **381,** 335-341 (1996)

Muller, V., Basset, G., Nelson, D. R. & Klingenberg, M. Probing the role of positive residues in the ADP/ATP carrier from yeast. The effect of six arginine mutations of the oxidative phosphorylation and AAC expression. *Biochemistry* **35,** 16132-16143 (1996)

Muzio, M., Stockwell, B. R., Salvesen, G. S. & Dixit, V. M. An induced proximity model for caspase-8 activation. *J. Biol. Chem.* **273,** 2926-2930 (1998)

Nagata, S. Apoptosis DNA fragmentation. *Exp. Cell Res.* **256,** 12-18 (2000)

Nakamura, K., Bossy-Wetzel, E., Burns, K., Fadel, M. P., Lozyk, M., Goping, I. S., Opas, M., Bleackley, R. C., Green, D. R. & Michalak, M. Changes in endoplasmic reticulum luminal environment affects cell sensitivity to apoptosis. *J. Cell Biol.* **150,** 731-740 (2000)

Narita, M., Shimizu, S., Ito, T., Chittenden, T., Lutz, R., Matsuda, H. & Tsujimoto, Y. Bax interacts with the permeability transition pore to induce the permeability transition and cytochrome c release in isolated mitochondria. *Proc. Natl. Acad. Sci. USA.* **95,** 14681-14686 (1998)

Nazareth, W., Yafei, N. & Crompton, M. Inhibition of anoxia-induced injury in heart myocytes by cyclosporin A. *J. Mol. Cell. Cardiol.* **23,** 1351-1354 (1991)

Nechushtan, A., Smith, C. L., Hsu, Y. T. & Youle, R.J. Conformation of the Bax C-terminal region regulates subcellular location and cell death. *EMBO J.* **18,** 2330-2341 (1999)

References

Nechushtan, A., Smith, C. L., Lamensdorf, I., Yoon, S-H. & Youle, R. J. Bax and Bak Coalesce into Novel Mitochondrial-associated Clusters during Apoptosis. *J. Cell. Biol.* **3,** 1265-1276 (2001)

Nehr, E. Vesicle pools and Ca^{2+} microdomains: new tools for understanding their roles in neurotransmitter release. *Neuron* **20,** 389-399 (1998)

Newmeyer, D. D., Farschon, D. M. & Reed J. C. Cell free apoptosis in Xenopus egg extracts: inhibition by bcl-2 and requirement for an organelle fraction enriched in mitochondria. *Cell* **79,** 353-364 (1994)

Nicotera, P., Leist, M., Ferrando-May, E. Intracellular ATP, a switch in the decision between apoptosis and necrosis. *Toxicol. Lett.* **103,** 139-142 (1998)

Nieminen, A. L, Byrne, A. M., Herman, B. & Lemasters J. J. Mitochondrial permeability transition in hepatocytes induced by t-BuOOH: NAD(P)H and reactive oxygen species. *Am J Physiol.* **272,** C1286-1294 (1997)

Nieminen, A. L., Saylor, A. K., Tesfai, S. A., Herman, B. & Lemasters, J. J. Contribution of the mitochondrial permeability transition to lethal cell injury after exposure of hepatocytes to t-butylhydroperoxide. *Biochem. J.* **307,** 99-106 (1995)

Nutt, L. K, Pataer, A., Pahler, J., Fang, B., Roth, J., Mc Conkey, D. J. & Swisher, S. G. Bax and Bak promote apoptosis by modulating endoplasmic reticular and mitochondrial Ca^{2+} stores. *J. Biol. Chem.* **277,** 9219-9225 (2002)

Oakes, S. A., Opferman, J. T., Pozzan, T., Korsmeyer, S. J. & Scorrano, L. Regulation of endoplasmic reticulum Ca^{2+} dynamics by proapoptotic Bcl-2 family members. *Biochemical Pharmacology* **66,** 1335-1340 (2003)

References

Oliver, L., Priault, M., Tremblais, K., Le Cabellec, M., Meflah, K., Manon, S. & Vallete, F. M. The substitution of the C-terminus of Bax by Bcl-X_L does not affect its subcellular localisation but abrogates its pro-apoptotic function. *FEBS. Letts.* **487,** 161-165 (2000)

Oltvai, Z. N., Milliman, C. L. & Korsmeyer, S. J. Bcl-2 heterodimerizes in vivo with a conserved homolog, Bax that accelerates programmed cell death *Cell* **74,** 609-619 (1993)

Oyadomari, S., Araki, E. & Mori, M. Endoplasmic reticulum stress-mediated apoptosis in pancreatic beta-cells. *Apoptosis* **7,** 335-345 (2002)

Pan, Z., Bhat, M. B., Nieminen, A-L. & Ma, J. Synergistic movement of Ca^{2+} and Bax in cells undergoing apoptosis. *J. Biol. Chem.* **276,** 32257-32263 (2001)

Papadopoulos, V., Dharmarajan, A. M., Li, H., Culty, M., Lemay, M. & Sridaran, R. Mitochondrial peripheral type benzodiazepine receptor type expression *Biochem. Pharm.* **58,** 1389-1393 (1999)

Pastorino, J. G. & Hoek, J. B. The Integration of Energy Metabolism and Control of Apoptosis. *Curr. Med. Chem.* **10,** 1535-1551 (2003)

Pastorino, J. G., Chen, S-T., Tafani, M., Snyder, J. W. & Farber, J. L. The overexpression of Bax produces cell death upon induction of the mitochondrial permeability transition. *J. Biol. Chem.* **273,** 7770-7775 (1998)

Pastorino, J. G., Shulga, N. & Hoek, J. B. Mitochondrial Binding of Hexokinase II Inhibits Bax-induced Cytochrome c Release and Apoptosis. *J. Biol. Chem.* **277,** 7610-7618 (2002)

References

Pastorino, J. G., Synder, J. W., Serroni, A., Hoek, J. B. & Farber, J. L. Cyclosporin and carnitine prevent anoxic death of cultured hepatocytes by inhibiting the mitochondrial permeability transition. *J. Biol. Chem.* **268,** 13791-13798 (1993)

Pastorino, J. G., Tafani, M., Rothman, R. J., Marcineviciute, A., Hoek, J. B. & Farber, J. L. Functional Consequences of the Sustained or Transient Activation by Bax of the Mitochondrial Permeability Transition Pore. *J. Biol. Chem.* **44,** 31734-31739 (1999)

Pavlov, E. V., Priault, M., Pietkiewicz, D., Cheng, E., Antonsson, B., Manon, S., Korsmeyer, S. J., Manella, C. A. & Kinnally, K. W. A high conductance channel of mitochondria linked to apoptosis in mammalian cells and Bax expression in yeast. *J. Cell Biol.* **155,** 725-732 (2001)

Petit, P. X., LeCoeur, H., Zorn, E., Dauguet, C., Mignotte, B. & Gougeon, M. L. Alterations of mitochondrial structure and function are early events of dexamethasone-induced thymocyte apoptosis. *J. Cell Biol.* **130,** 157-167 (1995)

Pfeiffer, D, R., Gudz, T. I., Novgorodov, S.A. & Erdahl, W. L. The peptide mastoparan is a potent facilitator of the mitochondrial permeability transition. *J. Biol. Chem.* **270,** 4923-4932 (1995)

Pinton, P., Ferrari, D., Megalhaes, P., Schulze-Osthoff, K., Di Virgilio, F., Pozzan, T. & Rizzuto, R. Reduced loading of intracellular Ca^{2+} stores and downregulation of capacitative Ca^{2+}influx in Bcl-2 overexpressing cells. *J. Cell Biol.* **148,** 857-862 (2000)

Pinton, P., Ferrari, D., Rapizzi, E., Di Virgilo, F., Pozzan, T., Rizzuto, R. The calcium concentration of the endoplasmic reticulum is a key determinant of ceramide-induced apoptosis: significance for the molecular mechanism of Bcl-2. *EMBO J.* **11,** 2690-2701 (2001)

References

Porath, J., Carlsson, J., Olsson, I. & Belfrage, G. Metal chelate chromatography, a new approach to protein fractionation. *Nature* **258,** 598-9 (1975)

Pozzan, T., Rizzuto, R., Volpe, P. Meldolesi, J. Molecular and cellular physiology of intracellular Ca^{2+} stores. *Physiol. Rev.* **74,** 595-636 (1994)

Priault, M., Camougrand, N., Chandhuri, B. & Manon, S. Role of the C-terminal domain of Bax and Bcl-X_L in their localisation and function in yeast. *FEBS. Letts.* **443,** 225-228 (1999)

Qin, F., Shite, J., Mao, W. & Liang, C. Selegiline attenuates cardiac oxidative stress and apoptosis in heart failure: association with improvement in cardiac function. *Eur. J. Pharmacol.* **461,** 149-158 (2003)

Rao, L., Perez, D. & White, E. Lamin proteolysis facilitates nuclear events during apoptosis. *J. Cell Biol.* **135,** 1441-1455 (1996)

Reed, J. C. Cytochrome c can't live with it, can't live without it *Cell* **91,** 559-562 (1997)

Reed, J. C., Stein, C., Subasinghe, C., Haldar, S., Croce, C. M., Yum, S. & Cohen, J. Antisense-mediated inhibition of Bcl-2 protooncogene expression and leukemic cell growth and survival: comparisons of phosphodiester and phosphorothioate oligodeoxynucleotides. *Cancer Res.* 6565-6570 (1990)

Reed, J. C., Zhihua, X., Shinichi, K., Zapata, J. M., Qunli, X., Schendel, S., Krajewska, M. & Krajewski, S. Methods of measuring Bcl-2 proteins and their function. *Apoptosis. A practical approach.* **9,** 197 (1999)

Reed, K. C. & Bygrave, F. L. A low molecular weight ruthenium complex inhibitory to Ca^{2+} transport. *FEBS. Letts.* **46,** 109-114 (1972)

References

Reichert, A. S. & Neupert, W. Contact sites between the outer and inner membrane of mitochondria in protein transport. *Biochim. Biophys. Acta.* **1592,** 41-49 (2002)

Rizzuto, R., Bernardi, P. & Pozzan, T. Mitochondria as all-round players in the calcium game. *J. Physiol.* **529,** 37-47 (2000)

Rizzuto, R., Brini, M., Murgia, M. & Pozzan, T. Microdomains with high Ca^{2+} close to IP_3-sensitive channels that are sensed by neighbouring mitochondria. *Science* **262,** 744-747 (1993)

Rizzuto, R., Pinton, P., Carrington, W., Fay, F. S., Fogarty, K. E., Lifshitz, L. M., Tuft, R. A. & Pozzan, T. Close contact with the endoplasmic reticulum as determinants of mitochondrial Ca^{2+} responses. *Science* **280,** 1763-1766 (1998)

Rodriguez, J. & Lazebnik, Y. Caspase-9 and APAF-1 form an active holoenzyme. *Genes Dev.* **13,** 3179-3184 (1999)

Rostovtseva, T. K, Antonsson, B., Suzuki, M., Youle, R., Colombini, M. & Bezrukov, S. M. Bid but not Bax regulates VDAC channels. *J. Biol. Chem.* **279,** 13575-13583 (2004)

Saito, M., Korsmeyer, S.J. & Schlesinger, P.H Bax-dependent transport of cytochrome c reconstituted in pure liposomes. *Nat. Cell. Biol.* **2,** 553-555 (2000)

Santel, A. & Fuller, M. T. Control of mitochondrial morphology by human mitocfusin. *J. Cell Sci.* **114,** 867-874 (2001)

Sakahira, H., Enari, M. & Nagata, S. Cleavage of CAD inhibitor in CAD activation and DNA degradation during apoptosis. *Nature* **391,** 43-50 (1998)

References

Scaffidi, C. Schmitz, I., Zha, J., Korsmeyer, S. J., Krammer, P. H. & Peter M. E. Differential modulation of apoptosis sensitivity in CD95 type I and type II cells. *J. Biol. Chem.* **274,** 22532-22538 (1999)

Scaffidi, C., Fulda, S., Srinivasan, A., Friesen, C., Li, F., Tomaselli, K. G., Debatin, K. M., Krammer, P. H. & Peter, M. E. Two CD95 (Apo/Fas) signalling pathways. *EMBO J.* **17,** 1675-1687 (1998)

Schendel, S. L., Xie, Z., Montal, M.O., Matsuyama, S., Montal, M. & Reed, J. C. Channel formation by antiapoptotic protein Bcl-2. *Proc. Natl. Acad. Sci. USA.* **94,** 11357-11362 (1997)

Schlesinger, P. H., Gross, A., Yin, X-M., Yamamoto, K., Siato, M., Waksman, G. & Korsmeyer, S. J. Comparisons of the ion channel characteristics of proapoptotic Bax and antiapoptotic Bcl-2. *Proc. Natl. Acad. Sci. USA.* **94,** 11357-11362 (1997)

Schein, C. H. Optimizing protein folding to the native state in bacteria *Curr. Opin. Biotechnol.* **5,** 746-750 (1991)

Schein, S. J., Colombini, M. & Finkelstein, A. Reconstitution in planar lipid bilayers of a voltage dependent anion-selective channel obtained from paramecium mitochondria. *J. Membr. Biol.* **30,** 99-120 (1976)

Scorrano, L., Ashiya, M., Buttle, K., Weiler, S., Oakes, S. A., Mannella, C. A. & Korsmeyer, S. J. A distinct pathway remodels mitochondrial cristae and mobilises cytochrome c during apoptosis. *Dev. Cell.* **2,** 55-67 (2002)

Scorrano, L., Oakes, S. A., Opferman, J. T., Cheng, E. H., Sorcinelli, M. D., Pozzan, T. & Korsmeyer, S. J. Bax and Bak regulation of the endoplasmic reticulum Ca^{2+} : a control point for apoptosis. *Science* **300,** 135-139 (2003)

References

Scorrano, L., Petonilli, B., Di Lisa, F. & Bernardi, P. Commitment to apoptosis by GD3 ganglioside depends on opening of the permeability transition pore. *J. Biol. Chem.* **274,** 22581-22585 (1999)

Scott, S. V., Cassidy-Stone, A., Meeusen, S. L. & Nunnari, J. Staying in aerobic shape: how the structural integrity of mitochondria and mitochondrial DNA is maintained. *Curr. Opin. Cell Biol.* **15,** 482-488 (2003)

Sedlak, T. W., Oltvai, Z. N., Yang, E., Wang, K., Boise, L. H., Thompson, C. B. & Korsmeyer, S. J. Multiple Bcl-2 family members demonstrate selective dimerisation with Bax. *Pro. Natl. Acad. Sci. USA.* **92,** 7834-7838 (1995)

Shimizu, S., Ide, T. & Tsujimoto, Y. Electrophysiological study of a novel large pore formed by Bax and VDAC, which is permeable to cytochrome c *J. Biol. Chem.* **275,** 12321-12325 (2000)

Shimizu, S., Konishi, A., Kodama, T. & Tsujimoto, Y. BH4 domain anti-apoptotic Bcl-2 family members closes VDAC, and inhibits apoptotic mitochondrial changes and cell death *Proc. Natl. Acad. Sci. USA* **97,** 3100-3105 (1999)

Shimizu, S., Narita, M. & Tsujimoto, Y. Bcl-2 family proteins regulate the release of apoptogenic cytochrome c by the mitochondrial channel VDAC. *Nature* **399,** 483-487 (1999)

Shiraishi, J., Tatsumi, T., Keira, N., Alashi, K., Mano, A., Yamanaka, S., Matoba, S., Asayama, J., Yaoi, T., Fushiki, S., Fliss, H. & Nakagama, M. *Am. J. Physiol. Heart Circ. Physiol.* **281,** H1637-H1647 (2001)

References

Simbini, R., Pon, L., Zinser, E., Paltauf, F. & Daum, G. Mitochondrial membrane contact sites of yeast. Characterisation of lipid components and possible involvement in intra-mitochondrial translocation of phospholipids. *J Biol. Chem.* **266,** 10047-10049 (1991)

Slee, E. A., Harte, M. T., Kluck, R. M., Wolf, B. B., Casiano, C. A., Newmeyer, D. D., Wang, H-G., Reed, J. C., Nicholson, D. W., Alnemri, E. S., Green, D. R. & Martin, S. J. Ordering the cytochrome c initiated caspase cascade: hierarchical activation of caspases-2, -3, -6, -7, -8 and –10 in a caspase-9 dependent manner. *Cell. J. Biol.* **144,** 281-292 (1999)

Slee, E., Adrain, C. & Martin, S. J. Executioner caspase-3, -6, and -7 perform distinct non-redundant roles during the demolition phase of apoptosis *J. Biol. Chem.* **276,** 7320-7326 (2001)

Smironova, E., Shurland, D. L., Ryazantsev, S. W. & van der Bliek, A. M. A human dynamin-related protein controls the distribution of mitochondria. *J. Cell Biol.* **143,** 351-358 (1998)

Smith, D. & Johnson, K. S. Single-step purification of polypeptides expressed in Escherichia coli as fusion with glutathione S-transferase *Gene* **67,** 31-40 (1988)

Sparagna, G. C., Gunter, K. K. & Gunter, T. E. A system for producing and monitoring *in vitro* calcium pulses similar to those *in vivo*. *Anal. Biochem.* **219,** 96-103 (1994)

Sparagna, G. C., Gunter, K. K., Sheu, S. S. & Gunter, T. E. Mitochondrial calcium uptake from physiological-type pulses of calcium. A description of the rapid uptake mode. *J. Biol. Chem.* **270,** 27510-27515 (1995)

References

Srinivasula, S. M., Datta, P., Fan, X. J., Fernandes-Alnermri, T., Huang, Z. & Alnermri, R. S. Molecular determinants of the caspase-promoting activity of smac/Diablo and its role in the death receptor pathway. *J. Biol. Chem.* **275,** 36152-36157 (2000)

Susin, S. A., Lorenzo, H. K., Zamzami, N., Marzo, I., Brenner, C., Larochette, N., Prevost, M. C., Alzari, P. & Kroemer, G. Mitochondrial release of caspase-2 and –9 during the apoptotic process. *J. Exp. Med.* **189,** 381-394 (1999)a

Susin, S.A., Lorenzo, H. K., Zamzami, N., Marzo, I., Snow, B. E., Brothers, G. M., Mangion, J., Jacotot, E., Costantini, P., Loeffler, M., Larochette, N. Goodlett, D. R., Abersold, R., Siderovski, D. P., Penninger, J. M. & Kroemer, G. Molecular characterisation of mitochondrial apoptosis-inducing factor. *Nature* **397,** 441-448 (1999)b

Suzuki, Y., Imai, Y., Nakayama, H., Takahashi, K., Takio, K. & Takahashi, R. A serine protease Htr A2 is released from the mitochondria and interacts with XIAP, inducing cell death. *Mol. Cell* **8,** 613-621 (2001)

Suzuki, M., Youle, R. J. & Tjandra, N. Structure of Bax: coregulation of dimer formation and intracellular localisation *Cell* **103,** 645-654 (2000)

Szalai, G., Krishnamurthy, R. & Hajnoczky, G. Apoptosis driven by IP_3-linked mitochondrial calcium signals. *EMBO J.* **22,** 6349-6361 (1999)

Takahashi, H., Nakamura, S., Asano, K., Kinouchi, M., Ishida-Yamamoto, A. & Izuka, H. Fas antigen modulates ultraviolet B-induced apoptosis of SVHK cells: sequential activation of caspase 8, 3 and 1 in the apoptotic process. *Exp. Cell Res.* **249,** 291-289 (1999)

References

Tanaka, M., Ito, H., Adachi, S., Akimoto, H., Nishikawa, T., Kasajima, T., Marumo, F. & Hiroe, M. Hypoxia induces apoptosis with enhanced expression of Fas antigen messenger RNA in cultured neonatal rat cardiomyocytes. *Circ. Res.* **75,** 426-433 (1994)

Tatsumi, T., Shiraishi, J., Keira, N., Akashi, K., Mano, A., Yamanaka, S., Matoba, S., Fushiki, S., Fliss, H. & Nakagawa, M. Intracellular ATP is required for mitochondrial apoptotic pathways in isolated hypoxic rat cardiac myocytes. *Cardiovasular Res.* **59,** 428-440 (2003)

Tremblais, K., Oliver, L., Juin, P., LeCabellec, T. M., Meflah, K. & Vallete, F. M. The C-terminus of Bax is not a membrane/anchoring signal. *Bichem .Biopyhs. Res. Commun.* **260,** 582-591 (1999)

Tsujimoto, Y., Cossman, J., Jaffe, E. & Croce, C. M. Involvement of bcl-2 gene in human follicular lymphoma. *Science* **228,** 1440-1443 (1985)

Vanden Hoek, T. L., Li, C., Shao, Z., Schumacker, P. T. & Becker, L.B. Significant levels of oxidants are generated by isolated cardiomyocytes during ischaemia prior to reperfusion. *J. Mol. Cardiol.* **29,** 2571-2583 (1997)

Vander Heiden, M. G., Chandel, N. S. Li, X. X. Schumacker, P. T., Colombini, M. & Thompson, C. B. Outer mitochondrial membrane permeability can regulate coupled respiration and cell survival. *Pro. Natl. Acad. Sci. USA.* **9,** 4666-4671 (2000)

Vander Heiden, M. G., Chandel, N. S., Schumacker, P. T. & Thompson, C. B. Bcl-X_L prevents cell death following growth factor withdrawal by facilitating mitochondrial ATP/ADP exchange. *Mol. Cell.* **2,** 159-167 (1999)

Vander Heiden, M. G., Chandel, N. S., Williamson, E. K., Schumacker, P. T. & Thompson, C. B. Bcl-X_L regulates the membrane potential and volume homeostasis of mitochondria. *Cell* **91,** 627-637 (1997)

References

Vander Heiden, M. G., Li, X. X., Gottlieb, E., Hill, R. H., Thompson, C. B. & Colombini, M. Bcl-X_L promotes the open conformation of the voltage-dependent anion channel and metabolic passage through the outer mitochondrial membrane. *J. Biol. Chem.* **276,** 1941-1949 (2001)

Van Engeland, M., Nieland, L. J., Ramaekers, F. C., Schutte, B. & Reutelingsperger. C. P. Annexin V-affinity assay: a review on an apoptosis detection system based on phosphatidylserine exposure. *Cytometry* **31,** 1-9 (1998)

Vasington, F. D., Gazzotti, P., Tiozzo, R. & Carafoli, E. The effect of ruthenium red on Ca^{2+} transport and respiration in rat liver mitochondria. *Biochim. Biophys. Acta.* **256,** 25643-25654 (1972)

Vayssiere, J-L., Petit, P. X., Risler, Y. & Mignotte, B. Commitment to apoptosis is associated with changes in mitochondrial biogenesis and activity in cell lines conditionally immortalised with simian virus 40. *Proc. Natl. Acad. Sci. USA.* **91,** 11752-11756 (1994)

Veinot, J. P., Gattinger, P. A. & Fliss, H. Early apoptosis in human myocardial infarcts. *Human Pathology* **28,** 485-495 (1997)

Verhagen, A. M., Ekert, P.G., Pakusch, M., Silke, J., Connolly, L. M., Reid, G.E., Moritz, R. L., Simpson, R. J. & Vaux, D. L. Identification of DIABLO, a mammalian protein that promotes apoptosis by binding to and antagonizing IAP proteins. *Cell* **102,** 43-53 (2000)

References

Verhagen, A. M., Silke, J., Ekert, P.G., Pacusch, M., Kauffmann, H., Burke, R., Wrobel, C., Moritz, R. L., Simpson, R. J. & Vaux, D. L. HtrA2 promotes cell death through its ability to antagonise inhibitor of apoptosis proteins. *J. Biol. Chem.* **277,** 445-454 (2002)

Von Ashen, O., Renkin, C., Perkins, G., Kluck, R. M., Bossy-Wetzel, E. & Newmeyer, D. D. Preservation of mitochondrial structure and function after Bid- or Bax –mediated cytochrome c release. *J. Cell. Biol.* **150,** 1027-1036 (2000)

Vyssokikh, M. Y., Katz, A., Rueck, A., Wuensch, C. & Dorner, A. Adenine nucleotide translocator isoforms 1 and 2 are differently distributed in the mitochondrial inner membrane and have distinct affinities for cyclophilin D. *Biochem. J.* **258,** 349-358 (2001)

Vyssokikh, M., Zorova, L., Zorov, D., Heimlich, G., Jurgenmeier, J., Schreiner, D. & Brdiczka, D. The intra-mitochondrial cytochrome c distribution varies correlated to the formation of a complex between VDAC and the adenine nucleotide translocase: this affects Bax-independent cytochrome c release. *Biochim. Biophys.* **1644,** 27-36 (2004)

Wang, K., Gross, A., Waksman, G. & Korsmeyer, S. J. Mutagenesis of the BH3 domain of Bax identifies residues critical for dimerisation and killing. *Mol. Cell. Biol.* **18,** 6083-6089 (1998)

Wang, J. & Lenardo, M., J. Roles of caspases in apoptosis, development, and cytokine maturation revealed by homozygous gene deficiencies. *J. Cell. Sci.* **113,** 753-757 (2000)

References

Waterhouse, N. J. Ricci, J. E. & Green, D. R. And all of a sudden it's over: mitochondrial outer membrane permeabilisation in apoptosis. *Biochimie* **84,** 113-114 (2002)

Webster, K. A., Discher, D. J., Kaiser, S., Hernandez, O., Sato, B., Bishopric, N. H. Hypoxia –activated apoptosis of cardiomyocytes requires reoxygenation or a pH shift and is independent of p53. *J. Clin. Invest.* **104,** 239-252 (1999)

Wei, M. C., Lindsten, T., Mootha, V. K., Weiler, S., Gross, A., Ashiya, M., Thompson, C. B. & Korsmeyer, S. J. t-Bid, a membrane targeted death ligand oligomerises Bak to release cytochrome c. *Gene Dev.* **16,** 2060-2071 (2000)

Wei, M. C., Zong, W-X., Cheng, E. H-Y., Lindsten, T., Panoutsakopoulou, V., Ross, A. J., Roth, K. A., MacGregor, G. R., Thompson, C. B. & Korsmeyer, S. J. Proapoptotic Bax or Bak : a requisite gateway to mitochondrial dysfunction and death *Science* **292,** 727-730 (2001)

Weinmann, M., Jendrossek, V., Handrick, R., Guner, D., Groecke, B. & Belka, C. Molecular ordering of hypoxia-induced apoptosis: critical involvement of the mitochondrial death pathway in a FADD/caspase-8 independent manner. *Oncogene* **23,** 3757-3769(2004)

West, L. A., Horvat, R. D., Roess, D. A. Barisas, G., Juenfel, J. L. & Niswender, G. D. Steriodogenic acute regulatory protein and peripheral-type benzodiazapene receptor associate at the mitochondrial membrane *Endocrinology* **42,** 502-505 (2001)

Wieckowski, M. R., Vyssokikh, M., Dymkowska, D., Antonsson, B., Brdiczka, D. & Wojtazak, L. Oligomeric C-terminal truncated Bax preferentially releases cytochrome c but not adenylate kinase from mitochondria, outer membrane vesicles and proteoliposomes. *FEBS. Letts.* **505,** 453-459 (2001)

References

Widlak, P., Li, L. Y., Wang, X. & Garrard, W. T. Action of recombinant human apoptotic endonuclease G on naked DNA and chromatin substrates: cooperation with exonuclease ans DNase I. *J. Biol. Chem.* **276,** 48404-48409 (2001)

Wolf, B. B. & Green, D. R. Suicidal tendencies: apoptotic cell death by caspase family proteinases. *J. Biol. Chem.* **274,** 20049-20052 (1999)

Wolter, K. G., Hsu, Y-T., Smith, C. L., Nechushtan, A. & Xu-Guang, X. Movement of Bax from the Cytosol to Mitochondria during Apoptosis. *J. of Cell Biol.* **139,** 1281-1292 (1997)

Woodfield, K., Ruck, A., Brdiczka, D. & Halestrap A. Direct demonstration of specific interactions between cyclophilin D and the Adenine Nucleotide Translocase confirm their role in the Mitochondrial Permeability Transition, *Biochem. J.* **336,** 287-290 (1998)

Wyllie, A. H., Kerr, J. F. & Currie, A. R. Cell death: the significance of apoptosis. *Int. Rev. Cytol.* **68,** 251-306 (1980)

Xie, G. & Wilson, J. E. Tetramic structure of mitochondrially bound rat brain hexokinase: a cross-linking study. *Arch. Biochem. Biophys.* **276,** 285-293 (1990)

Yang, J., Lui, X., Bhalla, K., Kim, C. N., Ibrado, A. M., Cai, J., Peng, T. I., Jones, D. P. & Wang, X. Prevention of apoptosis by Bcl-2: release of cytochrome c from mitochondria blocked. *Science* **275,** 1129-1132 (1997)

Ying, W-L., Emerson, J., Clarke, M. J. & Sanadi, R. D. Inhibition of mitochondrial calcium ion transport by an oxo-bridged dinuclear ruthenium ammine complex. *Biochemistry* **30,** 4949-4952 (1991)

References

Zamzami, N., Brenner, C., Marzo, I., Susin, S. A. & Kroemer, G. Subcellular and submitochondrial mode of action of Bcl-2-like onocoproteins. *Oncogene* **16,** 2265-2282 (1998)

Zamzami, N., Marchetti, P., Castedo, M., Zanin, C., Vayssiere, J-L., Petit, P.X. & Kroemer, G. Reduction in mitochondrial potential constitutes an early irreversible step of programmed lymphocyte death in vivo. *J. Exp. Med.* **181,** 1661-1672 (1995)

Zamzami, N., Susin, S. A., Marchetti, P., Hirsch, T. M., Gomez-Monterrey, I., Castedo, M. Kroemer, G. Mitochondrial control of nuclear apoptosis *J. Exp. Med.* **183,** 1533-1542 (1996)

Zazueta, C., Masso, F., Paez, A., Bravo, C., Vega, A., Montano, L., Vaquez, M., Ramirez, J. & Chavez, E Identification of a 20 kDa protein with calcium uptake transport activity. Reconstitution in a membrane model. *J. Bioenerg. Biomembr.* **26,** 555-562 (1994)

Zazueta, C., Zafra, G., Vera, G., Sanchez, C. & Chavez, E. Advances in the Purification of the Mitochondrial Ca^{2+} Uniporter using the labelled inhibitor ^{103}Ru 360 *J. of Bioenergetics and Biomembranes* **30,** 489-498 (1998)

Zazueta, C., Ramirez, J., Garcia, N., Bazza, J. & Charvez, E. Cardiolipin regulates the activity of the reconstituted mitochondrial calcium uniporter by modifying the structure of the liposome bilayer. *J. membr. Biol.* **191,** 113-122 (2003)

Zha, H., Fisk, H. A., Yaffe, M. P., Mahajan, N., Herman, B. & Reed, J. C. Structure-function comparisons of the pro-apoptotic protein Bax in yeast and mammalian cells. *Mol. Cell. Biol.* **11,** 6494-6508 (1996)

References

Zhang, H., Heim, J. & Meyhack, B. Redistribution of Bax from cytosol to membranes is induced by apoptotic stimuli and is an early step in the apoptotic pathway. *Biochem. Biophys. Res. Commun.* **251,** 454-459 (1998)

Zhou, M., Demo, McClure, T. N., Crea, R. & Bitler, C.M. A novel splice variant of the Cell Death-promoting Protein Bax. *J. Biol. Chem.* **273,** 11930-11936 (1998)

Zoratti, M. & Szabo, I. The mitochondrial permeability transition. *Biochem. Biophys. Acta. Rev. Biomembranes* **1241,** 139-176 (1995)

Zou, H., Li, Y., Liu, X. & Wang, X. An Apaf-1-cytochrome c multimeric complex is a functional apoptosome that activates procaspase-9. *J. Biol. Chem.* **274,** 11549-11556 (1999)